doi:10.1038/nature13621

Table of Contents

Radiocarbon dating and chemical pretreatment methods

Bone samples were prepared for dating using methods applied at the ORAU, University of Oxford, UK. The methods are outlined elsewhere[1]. Radiocarbon dating of charcoal was undertaken either using an ABOx-SC pretreatment method or the less rigorous ABA technique[2,3,4,5]. Shell carbonates were dated using the CarDS method with a high precision XRD method applied to each dated biomineral ensure <0.2% calcite remained[6]. This is known to be the form of the two calcium carbonate polymorphs that indicates contaminating carbonate. 'Known-age' standards were used alongside all 'unknown' samples (i.e. archaeological samples)[1].

The collagen from each bone dated was prepared using a final ultrafiltration step[7,8], which has been shown to improve the reliability of the ages obtained due to the more effective removal of low molecular weight contaminants. A bone-specific background correction was applied to all bone collagen determinations[9], down to ~5 mg collagen. A suite of analytical methods was applied to assess the quality of the bone collagen extracts. These include C:N atomic ratios, %weight collagen, %C on combustion, %N and stable isotopic ratios of C and N. Other, similar analytical methods were used for different sample types (for charcoal %C and $\delta^{13}C$, and for carbonates $\delta^{13}C$, $\delta^{18}O$ and the calcite:aragonite ratio). Radiocarbon ages are given as conventional ages BP[10]. All of the samples dated in our study were obtained from collections or archaeological sites that are listed below and all necessary permits were granted prior to sampling.

Throughout this Supplementary Methods document previous determinations will be given periodically, usually to demonstrate their unreliability compared to the new dataset presented here, where this is apparent. These are for illustrative purposes only, as a comprehensive list of all previous dates obtained is simply too large to present. In each site we analysed only radiocarbon determinations obtained using the most rigorous current techniques or analysed material from dated samples measured in other radiocarbon facilities that are probably reliable. It is now clear that the majority of the previously determined radiocarbon ages obtained from Mousterian contexts are erroneously young. The Stage Three Database, for instance, contains ~1900 radioisotopic or trapped charge determinations of which 431 are from Mousterian or related contexts: (http://www.esc.cam.ac.uk/research/research-groups/oistage3/stage-three-project-database-downloads). Of these, 240 are radiocarbon determinations, of which 104 (43%) are younger than 36,000 BP, an adequate estimate of the *terminus ante quem* (*TAQ*) for the Mousterian as determined

by the present study. Unfortunately, this does not mean that the 136 determinations in the database that are older than 36,000 BP are accurate. Several of these determinations come from much older material, beyond the radiocarbon limit, and therefore should be considered minimum ages only. Most of them were obtained using less refined cleaning methods and are dates from materials such as burnt bone, soil humus, peat extracts, 'resin' or humic acids, none of which can provide reliable ages and which would be classified by us as dubious.

Bayesian modelling

The radiocarbon determinations obtained were used to construct individual site models using Bayesian software (OxCal 4.2[11]) and the INTCAL13 curve[12]. The determinations were input as values in fraction modern (fM) plus or minor fM errors at 1σ (`R_F14C` in OxCal), or as radiocarbon ages where this was not known (for example when older dates from other labs were included), with `resolution` of 20 with some exceptions where the models were slow to converge or run. (In OxCal, commands or parameters are written in a C++ CQL (Command Query Language) format and terms and commands are shown here always in `Lucida Console` font).
It is important to note that;

1) it is not possible to interpret radiocarbon ages reliably without calibration, due to variation in the concentration of radiocarbon through time. All calibrated dates presented here are expressed in calibrated years (cal BP);

2) the calibration curve is an interim and potentially changing curve that is updated regularly by the INTCAL group. For this reason it is important to use the most recent curve and check for updates.

This latter point is particularly relevant for the >25 ka BP sections of the current curve. Recent work, for example by Muscheler et al.[13] suggests a possible problem in INTCAL13 in the period 40-42 ka cal BP shown by dating of kauri wood from New Zealand that is wiggle matched to a modelled ^{14}C record based upon ^{10}Be fluctuations. This is preliminary research and the extent of its significance remains to be determined. The radiocarbon record from Cariaco Basin, which forms the basis for the majority of the points in the calibration curve through the period to 50 ka cal BP is broadly consistent at the age limit which it ought not to be if there is indeed a systematic bias. It is very important to note that whilst successive iterations of the INTCAL curves are subject to

modification and change, the radiocarbon determinations accurately reflect the concentration of ^{14}C measured in the AMS laboratory and will not change.

Bayesian modelling enables the relative stratigraphic information recorded from sites during excavation to be formally incorporated along with the calibrated likelihoods or calibrated probability distributions. Bayes' theorem, which encapsulates the mathematical basis of the Bayesian method, incorporates three principal components, which allow the analysis of the relationship between data (represented by y) and unknown values, or parameters, denoted by θ.

Bayes' theorem is:

$$p(\theta|y) \propto p(y|\theta)\, p(\theta)$$

Here, $p(y|\theta)$ is defined as the 'likelihood', where p is a probability function (the symbol | means 'given'), so the likelihood tells us how likely are the values of the data we observed, given some specific values of the unknown parameters. Calibrated radiocarbon probability distributions represent the likelihood. $p(\theta)$ denotes the 'prior'. This term describes our strength of belief concerning the possible values of unknown parameters before, or prior to, the observation of the data we collect. $p(\theta|y)$, the 'posterior', is a probability function that reflects the level of confidence associated with the values of the unknown parameters after the observation of the data. Bayes' theorem therefore may be written as; 'the posterior belief is proportional to the likelihood times the prior'. In terms of archaeological radiocarbon dating, this can be understood as meaning that 'the modelling results are proportional to the probability derived from the radiocarbon dates multiplied by the probabilities defined by purely archaeological constraints'.

Priors in our chronometric models comprise the relative site information obtained that allow determinations to be placed into `sequences` and `phases` reflecting the sequence of archaeological levels, as well as the presence of hiatuses within them, and the presence of known age layers, such as volcanic tephra, and the like. This so-called 'uninformative' prior information is the basis for the models presented here. It is important to note that there is no one "perfect" model, each model is based on an archaeological interpretation. In addition it is vital that the possibility of sampling and dating intrusive or residual material is minimised by meticulous sample selection. This is challenging, especially in Palaeolithic contexts where sites are often occupied not solely by humans but by other species, such as bears and hyaenas, and where excavations were conducted and recorded in earlier periods when less rigorous excavation and recording methodologies were more

common. In order to determine whether there are problematic determinations that do not agree with the prior framework, an outlier detection method[14] was applied. When there is a lack of agreement with the prior framework, significant outlier results allow us to quantify the degree of difference. Values excessively higher than the prior outlier probabilities applied are automatically downweighted in the models. A posterior outlier probability of 1.00 leads to the result not being included in the modelled calculations, whilst a value of 0.5 means that the radiocarbon likelihood of the sample is only included in half of the runs of the model.

For each model a start and end boundary is included to bracket each archaeological phase. These posterior distributions allow us to determine probability distribution functions (PDF) for the beginning and ending of these phases. A number of functions have been used to interrogate the models further:

- We use the date command in OxCal to determine PDFs spanning periods of interest in the models, for example, from the start boundary of one phase of the Mousterian, to the end boundary of another phase of the same industry. This is the basis for one of the model comparisons in the main paper and allows us to model the complete age ranges for specific Phases associated with the Mousterian at a set degree (usually 68.2 and 95.4%) of probability. These date ranges are given below.
- The order function was used to determine probabilistically the relative order of different boundary PDFs from the various models we ran. This enables us to order PDFs generated within individual site models and determine an order with respect to $t_1>t_2>t_3$ with a calculated probability, where > means younger or older than.
- By comparing different ordered PDFs using the difference command it is possible to determine whether there is a statistically significant difference between two PDFs. If the difference determined between two PDFs overlaps with 0 then we can say that there is no statistical significance between the two. This is the basis for our statistical inferences about the difference between various PDFs that we have compared against each other in the main paper.

Bayesian age model CQL coding is given at the end of this Supplementary Methods section.

All of the models published here were tested for sensitivity and run 4-5 times at 5-50 million iterations or more. We were therefore able to check that the posterior distributions were

reproducible and that the convergence values were high. Specific comments on each model are given where appropriate in either the text or the captions.

OSL and U-Series ages are incorporated in Bayesian models as in the cases of Le Moustier, Saint-Césaire and Abric Romani. It is important to note that these are; a) expressed as calendar years before today (i.e., not AD 1950) and; b) include a combination of both systematic and random errors. OSL and U-series determinations do not have fully independent uncertainties associated with their age estimates. The systematic error is shared among all calculations for a particular batch of samples, and may include, for example, calibration errors for the various pieces of equipment that were used[15]. The error estimate unique to each OSL or U-series age is called the random error and derives predominantly from measurement uncertainties; counting errors, dose rate estimation etc. Where OSL and U-series dates are incorporated in the Bayesian models presented here, these data include systematic and random errors. When ages with common systematic errors and random errors are combined, however, only the latter should be included[16]. While we acknowledge that it is not best practice to include in the Bayesian modeling ages that are based on a combination of systematic and random errors, the differences between corrected and uncorrected data are not significant to the posterior results of these particular models in this time range[17].

The Mousterian

The primary focus of this paper is the chronology and dating of the Mousterian technocomplexes of Eurasia. The Mousterian lithic tradition is primarily a flake-based industry. Recently, the validity of this long-standing, sweeping description –as opposed to the standardized blade character of the Upper Palaeolithic- has been questioned on the grounds that true blades occur well before the Upper Palaeolithic, in several Mousterian contexts[18]. Blades are found in sites both in Europe and the Near East, yet in differing forms and as a result of a different reduction sequence [19, 20, 21, 22]. Technologically, the Mousterian is often identified with Levallois reduction strategies but several other technologies (e.g. Kombewa, discoidal) have been recognized as acting in parallel or independently[23,24]. These assemblages are dominated by sidescrapers, denticulates and notched tools produced on flake substrates.

Mousterian tool typology was formalized by Bordes[19,25] who identified 63 types of flakes and 21 types of biface and categorized the variations in Mousterian industries in six types of industrial facies (Typical Mousterian; Mousterian of Acheulian Tradition (MTA) types A and B; Denticulate Mousterian; Quina and Ferrassie Mousterian, or Charentian Mousterian). These he saw as contemporary variants reflecting the strong cultural affiliations of their makers. However, the idea of contemporaneous cultural phyla with distinct lithic traditions closely co-existing but not interacting with each other was challenged through a series of publications[26,27,28,29,30,31,32].

The unilinear temporal succession of these variants is not established beyond doubt because almost no sites, as yet, are reliably chronometrically dated. In western France, over the general time period of the transition to the Upper Palaeolithic, the final Mousterian is often identified with the MTA B or Typical Mousterian, industries with high frequencies of scrapers, notches and denticulates[33] while in Mediterranean France last Mousterian industries show the use of a large set of technologies, including both Levallois, discoidal flaking, Kombewa and blades/bladelets[34]. In Italy, in the Final Mousterian, predetermined debitage always occurs, mainly represented by the recurrent unipolar Levallois method. Some assemblages present an independent blade/bladelet knapping technique, with a volumetric orthogonal method[35]. In short, Mousterian lithic industries in western Europe at around the time of the transition exhibit considerable variability which requires explanation.

Jaubert et al.[36] have attempted to do this by considering the nature of the lithic technocomplexes that characterise the end of the Middle Palaeolithic in Europe, in particular the important sequences of southwestern France. They identify three different technocomplexes preceding the start of the Upper Palaeolithic. These appear to stratigraphically post-date the industries of the Mousterian of Acheulian Tradition (MTA) dating to MOIS3. The most recent technocomplexes in their view comprise a so-called Discoid-Denticulate Mousterian, followed by a Levallois Mousterian characterised by large scrapers. The former technocomplex is known from the sites of La Quina, Saint-Césaire (Levels 10-12) and Roc-de-Combe. The Levallois Mousterian with large scrapers is also identified by Jaubert et al. as post-dating the MTA at sites including Rochers de Villeneuve, Grotte du Bison at Arcy-sur-Cure, and probably also Level J at Le Moustier. To this might be added level EJOP sup at Saint-Césaire, although some doubts exist regarding potential admixture that might compromise a reliable diagnosis of the industry. As the authors acknowledge, more work is needed to refine the technological assignation and intra- and inter-site distribution of these. Despite this, the authors argue convincingly that the traditionally accepted simple progression of MTA to

Châtelperronian is probably unrealistic. As Shea [37] has suggested, the field of Palaeolithic archaeology is characterised by several named industrial stone tool industries based on a long historical typological tradition of research into the 'Mousterian', and these are often extremely confusing and may act to obscure the evolutionary picture.

The majority of specialists agree that the European Mousterian technocomplex was probably produced by Neanderthals. In other parts of Eurasia this association is also accepted, although the link remains to be proven, since it is known that AMHs and Neanderthals produced similar Mousterian lithic tools in the Near East prior to the initial Upper Palaeolithic. This is unsurprising given the Middle Stone Age record in Africa[38,39]. For the purpose of this paper, however, we have assumed that Neanderthals produced Mousterian industries.

Several so-called 'transitional industries' are also linked with the earliest Upper Palaeolithic, although diagnosing human authorship (AMH or Neanderthal) has been challenging and difficult to resolve. In this paper we analyse two of these industries, the Uluzzian of Italy and Greece, and the Châtelperronian of Franco-Cantabria, both of which have human remains in association that contribute to the diagnosis of authorship. Other European transitional technocomplexes, such as the Bohunician, Szeletian, Bachokiran and Lincombian-Ranisian-Jerzmanowician (LRJ) are not associated with specific human groups, and have few reliable dates associated with them. There are, however, some exceptions. For the LRJ, for instance, Cooper et al.[40] have provided a chronology for the presence of a leaf-point assemblage at the site of Rutland in the UK. The occupation is dated to 44,300-42,500 cal BP. In eastern Europe the Bohunician thus far is poorly dated and there are no published ABOx determinations yet[41]. The Szeletian has one ABOx determination from Vedrovice V[42], again limiting our ability to infer reliable chronologies. The absence of human fossil evidence limits our ability to interpret their significance at this juncture, however, so we have left them to one side in this analysis.

Sampling of archaeological materials

Dating material was carefully selected at each site from the uppermost Mousterian-bearing strata, with the express aim of dating the latest Mousterian occurrence and therefore of the Neanderthals who produced it. A total of 40 archaeological sites across Europe and western Eurasia were sampled. Each contains evidence for late Middle and early Upper Palaeolithic occupation and the

transition between the two, or Neanderthal fossil remains that we have dated. Particular attention was paid to sites with evidence for late Middle and early Upper Palaeolithic occupation and the transition between the two and, in particular, evidence for the last or final Mousterian, as well as 'transitional' industries (the Uluzzian and the Châtelperronian). Each site analysed is discussed below along with the chronometric data obtained and the lithic evidence found. By using a Bayesian modeling approach and incorporating age data from horizons occurring above the Mousterian, containing Upper Palaeolithic artefacts, it is possible to produce PDFs that provide reliable dates for the end of the European Mousterian.

Bone samples were scrupulously examined and the sampling strategy targeted bones with evidence for human cut-marks or modification (e.g. artefacts), permitting dated samples to be linked to human presence as described in the text and tables below. We selected humanly modified bones after sorting carefully through sometimes thousands of bones from these sites. Of course, in some cases we were not able to obtain these ideal samples; they did not exist at the site, or the presence of cutmarked bone was extremely rare (eg Hyaena Den or Pin Hole). In these cases we focused on identifiable animal remains and issue the results with a warning or caveat, but the vast majority of the samples published here are demonstrably humanly modified, as shown in the tables of data accompanying each site.

AMS dating of material from the Palaeolithic is particularly challenging owing to the combined effects of lower ^{14}C concentrations and often poor preservation states, particularly for bone, which was our favoured target. We took 457 archaeological samples from Mousterian and related 'transitional' industry contexts during the course of our project (including Neanderthal remains) and obtained 196 AMS determinations (a failure rate of 58%). Many of the failed samples were those tested prior to extensive sampling by measuring the %nitrogen in the bone. This was achieved by sampling ~3-4 mg of bone powder using a small dental drill and measuring the %N using an Elemental Analyser/Isotope Ratio Mass Spectrometer (EA/IRMS). The method used is outlined in Brock et al[43]. %N values greater than 0.5-0.8% were accepted for full chemical pretreatment. In some cases smaller amounts were also accepted, where additional bone was available in a large enough proportion to be easily sampled. Many bones, particularly from Mediterranean sites such as Gorham's Cave, Cavallo and Castelcivita, were tested using this method, thereby avoiding unnecessary sampling. We recommend that researchers focus on using similar approaches to avoid needless destruction of valuable archaeological material if working in this area. Future work using single amino acid dating might allow us to revisit certain bones that have trace collagen levels in

future[44]. Avoiding the production of unreliable determinations through minimising the dating of very low collagen bones is a sensible approach to reducing the large number of aberrant radiocarbon ages that exist for the Palaeolithic.

Site locations for each site are given in decimal degrees (Lat./Long.).

Archaeological sites

France

Grotte du Renne at Arcy-sur-Cure

The Grotte du Renne site is located at Arcy-sur-Cure in the Paris basin (47.59° Lat., 3.75° Long.). It comprises a sequence of 15 archaeological levels (I to XV, from top to base), covering a depth of about 4 m. Mousterian horizons are located in levels XI and XII. Above them, there are 3 Châtelperronian levels, of which X assumes greatest importance because it contains ornaments and Neanderthal human remains which are central to the debate concerning whether Neanderthals possessed a behaviourally advanced cultural adaptation.

Previous radiocarbon dates from the site covered 28-45,000 ^{14}C BP, with poor general stratigraphic consistency resulting in confusion over the precise age of the Châtelperronian at this site. Two studies have subsequently contributed to attempting to resolve this issue. Higham et al.[45] took samples for radiocarbon dating from 59 pieces of humanly-modified material from levels V to XII and produced 31 new AMS determinations. These disclosed a range in ages that Higham et al.[45] interpreted as evidence for some mixing or instrusion of material within the site's sequence. Hublin et al.[63] subsequently obtained a newer series of 40 dates. Although less rigorously selected in terms of human modification, the determinations appeared to possess fewer outliers and therefore lent support to an alternative model to that of Higham et al.[45], and one in which mixing was argued not to be present to a significant degree. This interpretation has since been questioned[46].

The Hublin et al.[63] dataset contains several newer determinations from the Mousterian (the uppermost level XI), which the Higham et al.[45] dataset did not cover. The Higham et al.[45] data from the Mousterian level XII was subject to some uncertainty due to potential mixing between the uppermost Mousterian and the lowermost Châtelperronian levels (both determinations from Oxford have high posterior outlier probabilities in the model). Given this, we included the Hublin et al.[63] data from the latest Mousterian level at the site (XI) in our Bayesian model for the site. In addition, we included the Hublin et al. cutmarked or humanly modified series of bones from the

Châtelperronian levels. We also included only the Higham et al. Proto-Aurignacian data from Level VII rather than the more varied and poorly selected Hublin et al. data to constrain the uppermost age of the Châtelperronian. We adopted the prior framework of Higham et al.[45]

Initially runs of the model disclosed results that were slow to converge and poor to reproduce. We therefore decided to relax the prior constraints and assume a single phase for Levels X and IX in order to produce a model that constrained the Mousterian phases reliably. The subsequent model (Figure S1) showed acceptable convergence and overall reproducibility after repeat runs, although there are still many outliers. It is this model, consisting only of cutmarked determinations, that we use for our further analysis.

We also determined a PDF for the dated range of the Mousterian of Arcy using the same data which is shown in Figure S1. The age range for the Mousterian (using the `date` command) was 46,690-43,840 cal BP (95%). The end `boundary` for the Mousterian was 45,070-43,720 cal BP (95.4%).

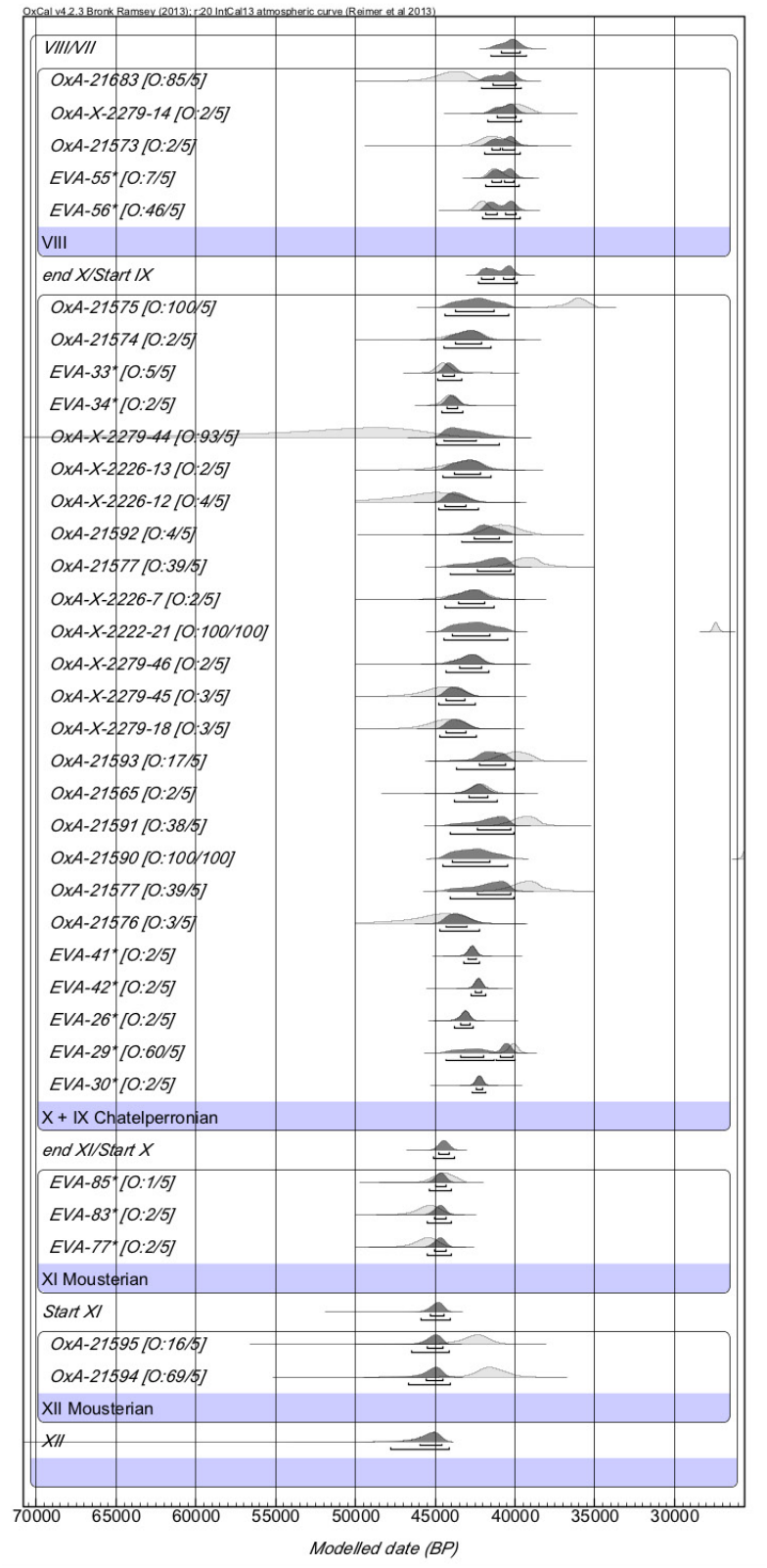

Figure S1: Bayesian age model for the Mousterian and X and XI Châtelperronian levels data after Higham et al.[45] and Hublin et al.[63] Boxes with blue surrounds define individual `phases` in the model. `Boundaries` separate each `phase`. The light grey distributions represent the radiocarbon likelihoods, the dark black distributions are the posterior probabilities, i.e. after Bayesian modelling. `Outliers` are given in the form [O:2/5] where 2 is the prior outlier probability and 5 is the

posterior outlier probability. Data is ordered from lowest at the bottom, to uppermost in the sequence. See text for details.

Le Moustier

Le Moustier is in the Dordogne, near the town of Les Eyzies (44.99° Lat., 1. 05° Long.) and is the type-site for the Mousterian. It consists of an Upper and Lower shelter. The most extensive excavation evidence comes from the lower part of the site, where Peyrony excavated from 1909. The ~4m thick sequence comprises a series of 11 geological levels, consisting of a lower series of waterlain deposits caused by the flooding of the nearby Vezere River, followed in the upper parts of the section by a series of Mousterian levels. It is important to remember that Peyrony excavated in quite large units, which almost certainly amalgamated several lenses or sub-units. The Mousterian phases comprise levels G-J. G and H are characterised by Mousterian of Acheulean Tradition (MTA) layers, I is attributed to a Denticulate Mousterian, J to Typical Mousterian and above these are two more levels; K (Châtelperronian) and L (early Aurignacian). A sequence of TL dates from samples of burnt flint was obtained from a remaining section of the site that was sampled by Geneste in 1982[47]. Mellars and Grün later obtained a series of ESR determinations[48].

Sampling of bone for AMS dating was undertaken in two stages. In the first, a small number of bones (principally bone retouchers/*retouchoirs*) were sampled for direct dating from the Musée Nationale de Préhistoire, Les Eyzies-de-Tayac (see Table S1 for sample details, the first group sampled are represented by Oxford P numbers 22688-22696). The 8 results obtained were used to generate a preliminary Bayesian model that was used as a basis for selecting further samples. We identified another 60 suitable samples for AMS dating from the collections on a second sampling visit to the Les Eyzies, including cut-marked bone and humanly-smashed horse teeth from each of the principal levels. Unfortunately we only received museum permission to attempt dating on 15 of these samples and these had to be sampled at the museum in Les Eyzies rather than in Oxford. Ideally, it would have been preferable to micro-sample the entire suite of 60 bones and teeth and use %Nitrogen methods to screen suitable samples with preserved collagen, as described above, but this was not possible. Only 3 of the 15 samples yielded enough collagen for dating. Sadly, for this reason we have obtained only 11 new radiocarbon results from this important site.

The new AMS determinations are shown in Table S2. The first series of bones analysed were ultrafiltered, as per our usual method, but the blank filter water we measured in the batch of ultrafilters we used yielded a higher than usual humectant background. We therefore re-ultrafiltered

the bone collagen from Le Moustier using new filters. We dated laboratory background bone standards (beyond the radiocarbon limit) in the same batch as these archaeological bones. The results were equivalent to the laboratory background for bone which suggests that the samples were not significantly affected by residual humectant, otherwise we would have expected higher ^{14}C activities, since the humectant has a modern (post-bomb) activity. The re-ultrafiltered bone collagen samples were given OxA-X, rather than OxA- numbers to reflect this non-routine chemistry.

The Bayesian age model we built is shown in Figure S2. The model incorporates the TL dates as well as the radiocarbon results (see above). The model produced a PDF `boundary` for the latest Mousterian of 45,090-40,750 cal BP (95.4%). The `date` range for the Mousterian at the site is 49,480-42,020 cal BP (95.4%).

Sample ID	OxA/OxA-X	Context	Material	%N	Comments	Status
22688	21750	Level H	bone	-	Retoucher on large animal limb bone	d
22689	21751	Level H	bone	-	Retoucher on large animal limb bone	d
22690	21752	Level H	bone	-	Cut large mammal tibia shaft fragment	d
22691		Level I	bone	-	Fractured wild horse lower cheek tooth	f
22692	21753	Level I	bone	-	Indet. cut large mammal limb bone fragment	d
22693	2300-19	Level J	bone	-	Cut large mammal tibia shaft fragment	d
22694	21754	Level J	bone	-	Retoucher on large mammal bone limb fragment	d
22695	2300-21	Level J	bone	-	Retoucher on large mammal bone limb fragment	d
22696	21765	Level J	bone	-	Cut large mammal limb shaft fragment	d
25161		Level L R.H3 B1 REC 06.69	bone	0.28	Partial artiodactyl rib, no visible human modification	f
25162		Level J R.H3 B1 REC 06.63	tooth	0.94	Bovine lower cheek tooth, human impact	f
25163	21789	Level J R.H3 B1 REC 06.64	bone	1.64	Cut small artiodactyl limb bone fragment	d
25164		Level B Box R.H. 3B1 REC 06.50	tooth	0.17	*Equus ferus* lower cheek tooth, complete	f
25165		Level F Box R.H. 3B1 REC 06.55	tooth	1.0	Bovine upper cheek tooth, complete	f
25166		Level B Box R.H. 3B1 REC 06.49	tooth	0.26	Bovine upper cheek tooth, complete	f
25167		Level F Box R.H. 3B1 REC 06.56	bone	0.26	Cut small artiodactyl bone fragment	f
25168		Level G R.H. 3A15 REC 06.14	bone	0.66	Cut limb bone shaft fragment	f
25169	21790	Level G R.H. 3A15 REC 06.14	bone	0.86	Cut large artiodactyl limb bone, no identification	d

25170		Level G R.H. 3A15 REC 06.15	bone	0.56	Smashed *Rangifer tarandus* metacarpal	f
25171		Level G R.H. 3A14 REC 06.06	tooth	0.50	Fractured bovine upper cheek tooth	f
25172		Level G R.H. 3A14 REC 06.01	tooth	0.67	Bovine lower cheek tooth, human impact	f
25173	21791	Level H R.H. 3A16 REC 06.28	bone	0.75	Bovine cut astragalus	d
25174		Level H R.H. 3A16 REC 06.25	tooth	0.44	Bovine upper cheek tooth, human impact	f
25175		Level H R.H. 3A16 REC 06.36	tooth	0.53	*Equus ferus* upper cheek tooth, human impact	f

Table S1: Details of the samples obtained for AMS dating from the site of Le Moustier. Status column: d-denotes dated; f-denotes failed. For failed these were all based on low or no collagen yields or low %N (% nitrogen) values. Pnumbers are the ORAU unique identifier numbers, OxA/OxA-X denote the numbers given to successfully dated samples. %N values are on whole bone powder samples ranging in size from 4-7 mg.

OxA/OxA-X	Date	Error	Used (mg)	Yield (mg)	Yield (%)	%C	$\delta^{13}C$ (‰)	$\delta^{15}N$ (‰)	C:N
2300-19	37600	900	890	5.5	0.6	37.1	-20.5	7.4	3.4
2300-21	40700	1300	690	6.8	1.0	40.9	-20.0	4.8	3.4
21750*	50000	3900	880	20.1	2.3	45.8	-19.4	6.2	3.5
21751*	44100	1900	930	40	4.3	46.4	-20.1	5.8	3.4
21752*	45200	2200	920	23.6	2.6	46.4	-20.0	6.5	3.4
21753*	43300	1700	890	20.3	2.3	45.5	-20.0	6.4	3.4
21754*	45100	2300	570	13.7	2.4	44.9	-20.3	5.4	3.4
21765*	40600	1800	780	8.9	8.9	45.2	-20.3	4.4	3.4
21789	40400	1200	620	17.9	2.9	45.3	-19.3	4.7	3.3

21790	43300	1800	1070	5.94	0.6	41.5	-20.0	6.1	3.3
21791	45000	2100	650	9.45	1.5	44.0	-20.1	5.6	3.3

Table S2: Radiocarbon determinations from Le Moustier. Samples with OxA-X- prefixes are given in preference to OxA- numbers when there is a problem with the pre-treatment chemistry, AMS measurement or when there is a novel or experimental protocol applied in the dating. Asterisked samples are those that were reultrafiltered after a small amount of humectant was detected in background standard measurements of the MilliQ^{TM} water we use in the cleaning process of the ultrafilters before use (see test for details). We therefore re-ultrafiltered the collagen samples for a second time. Date in this table stands for the conventional radiocarbon age, expressed in years BP, after Stuiver and Polach[10]. Errors are the determined standard errors (values are ± one standard error): see Ramsey et al.[49] for details. 'Used' represents the amount of bone powder pretreated in milligrams. Yield represents the weight of collagen or ultrafiltered collagen in milligrams. Yield (%) is the percent yield of extracted collagen as a function of the starting weight of the bone analysed. %C is the carbon present in the combusted collagen and averages 40±2% in the ORAU. Stable isotope ratios are expressed in ‰ relative to vPDB[50] with a mass spectrometric precision of ±0.2‰ for C and ±0.3‰ for N. C:N is the atomic ratio of C to N and is acceptable if it ranges between 2.9-3.5.

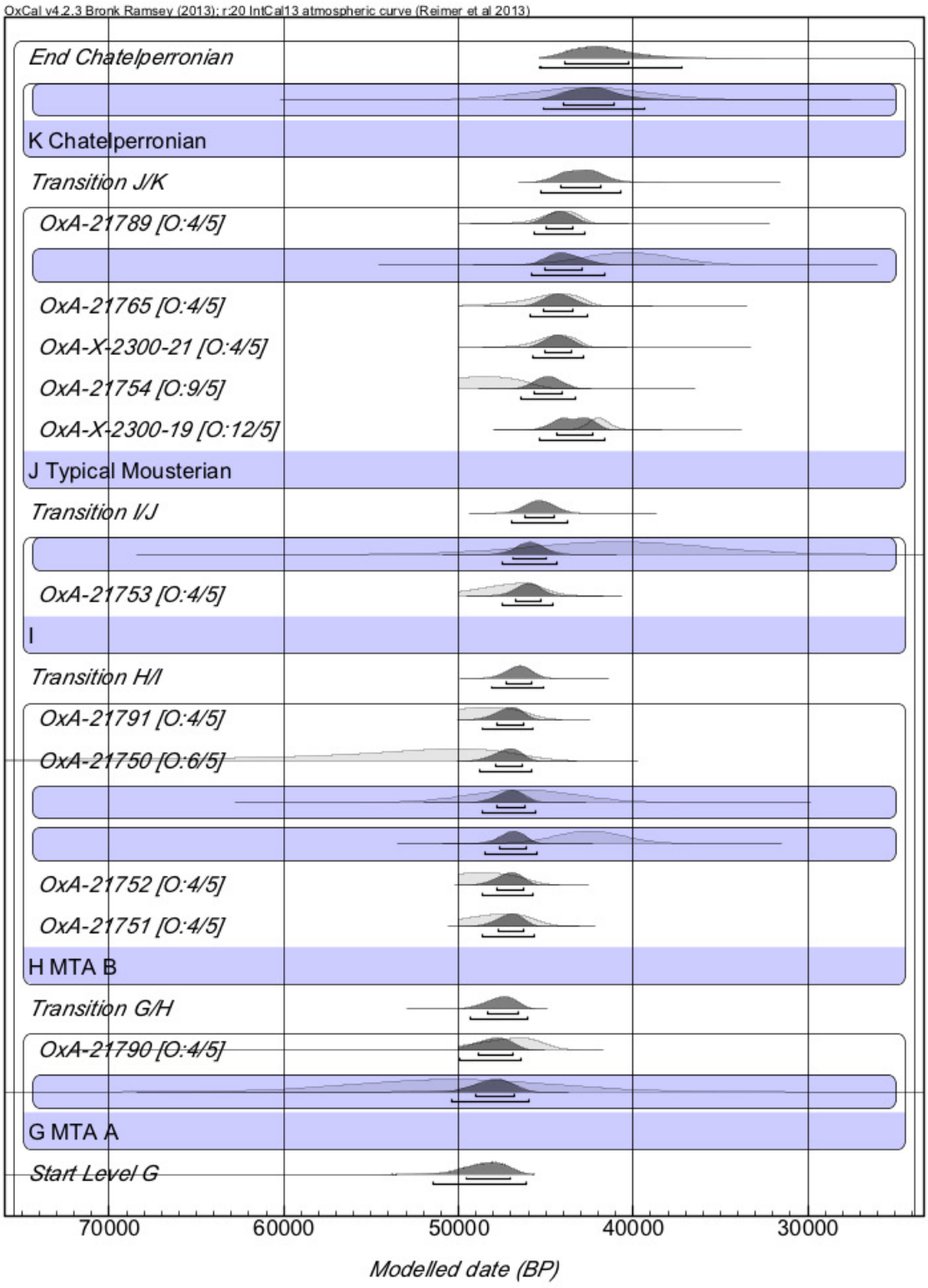

Figure S2: Bayesian age model for the Le Moustier site, Dordogne, France. TL determinations on burnt flint are included within the model after Ref 47, these are denoted by the shaded blue boxes.

La Quina

The site of La Quina is in the Charente region (at 45.30° Lat., 0.17° Long.) and is the type site for the Quina Mousterian. We obtained new radiocarbon dates from the La Quina Amont station part of the site complex[51]. Prior to our work there was little reliable chronometric data for the site. Two dates of burnt bone (GrA-2526 and GrN-4494 at 35250 ± 530 BP and 34100 ± 700 BP respectively) had been obtained from what was defined as the "Final Mousterian". Jelinek[51] suggests these samples are probably from Bed 8. We have severe doubts regarding the reliability of burnt bone as a sample type, as outlined by Higham et al.[52] During excavations by Jelinek and Débenath three samples of bone were dated from Bed 4, 6c and 8, respectively. The results were all very similar and grouped at ~34,000 BP, perhaps lending some credence to them. Later, luminescence dates on burnt flint from beds 8 and 6a were obtained (Mercier and Valladas, 1999)[51,53]. The ORAU later still dated several bone samples for Delagnes and Park[54] using the ultrafiltration method. These were from Bed 3 and Bed 6a-d respectively (see Table S3). These were substantially earlier than all previous dates and mirror the picture that has emerged in the dating of the Middle to Upper Palaeolithic previously in this regard[172] in that more rigorous pretreatment chemistry, improved instrumentation and the use of bone background measurements appears to make a difference to accuracy. Often, the resulting determinations are older that previous measurements on the same material[8].

For this project we sampled further identified (where possible) and humanly-modified bones from the Amont station in collaboration with colleagues in Bordeaux and Saint Germain-en-Laye. The results are shown in Tables S4-6. In addition to sampling material from the Amont beds we also obtained Châtelperronian material from the Aval site, 200 m SW of the Amont sequence, from Bed 4 in Squares B2 and B3 of G. Henri-Martin's 1953-71 excavations (these results are shown in Table S6). Note that there is no Châtelperronian from the Amont station, only from the separate Aval station. The Châtelperronian at the Station Aval derives from Germaine Henri-Martin's work. Later excavations by Veronique Dujardin were confined to the early Aurignacian in Germaine Henri-Martin's Bed 3, separated from the Bed 4 Châtelperronian by a layer of roof fall. Since it is widely accepted that the Châtelperronian postdates the Mousterian, we modeled the determinations from the Châtelperronian as being stratigraphically above the Mousterian determinations that are shown in Table S4. This is an assumption of course, and needs to be field tested in the case of this site.

The results suggest that Bed 6 and those below it appear likely to be at, or beyond, the radiocarbon limit. The alternative explanation is that there is some post-depositional mixing in the sequence. Jelinek[51] suggests that this might be the reason for the late date of OxA-21806, which was found towards the rear of the Bed 6a deposit, and might have originated from Bed 4 or higher.

The Bayesian model for the Mousterian of La Quina is shown in Figure S3. There was one significant outlier identified, this was OxA-21806 in Layer 6a which, at 36,850 ± 800 BP, is clearly too young for its stratigraphic position. The age determined for layers 6a, 6c and below are close to the measureable limit. It is not possible to include the Park results for 6a-d because they are greater than ages. Taken together, it is possible that these levels are at, or beyond, the ORAU age limit of 49.9 ka BP.

The Bayesian modeled results suggest that the `date` range for the Mousterian spans 48,170-42,530 cal BP (95.4% probability). The final `boundary` for the Mousterian layers was 43,830-41,960 cal BP. Modelled as coming after the Mousterian levels (see above), the Châtelperronian `date` range for the site spans 43,320-41,630 cal BP.

(Note that L.B., T.H. R.J., W. Davies, A.J, D. Armand and V. Dujardin are preparing a fuller paper on the La Quina sites "A revised interpretation of the chronology of La Quina Aval, and La Quina Amont, and implications for the Middle to Upper Palaeolithic Transition" planned for submission to the *Journal of Human Evolution*).

OxA	Bed	Date BP	error	Used (mg)	Yield (mg)	Yield (%)	%C	$\delta^{13}C$ (‰)	$\delta^{15}N$ (‰)	C:N
16998	Bed 3 base	41300	1000	860	11.8	1.4	44.6	-20.2	7.4	3.4
16999	Bed 6a	>48300		700	14.4	2.1	45.1	-19.5	8.1	3.4
17000	Bed 6a top	51200	2800	760	14.9	2.0	45.8	-19.8	8.0	3.3
17001	Bed 6d	>49600		880	13.8	1.6	44	-19.5	6.2	3.3

Table S3: AMS dates from the ORAU produced from La Quina for Park[51]. These are all ultrafiltered samples of bone. The caption to Table 2 describes the terms used in this table.

OxA	Bed number	LQ number	Date BP	error	Species and human modifications noted
2326-22	2b	N5-586	37000	800	*Equus ferus*, distal humerus fragment
21805	5	O5-250	41100	1300	Bovid or horse long bone fragment with cutmarks
21806	6a	O4-280	36850	800	Bovid mandibular fragment with cutmarks
21807	8	N4-126	45200	2200	*Rangifer tarandus* radio-ulna with cutmarks
21808	6d	N4-175	44200	1900	Bovid humerus with cutmarks
22153	4b	N6-1059	37500	800	*Cervus elaphus* tibia fragment
22154	Loc 2	F965-327	46900	2700	*Retouchoir* on an *Equus ferus* metatarsal
22155	7	N5-3301	48900	3400	Bovid tibia with faint cutmarks

Table S4: AMS dates from the Mousterian levels at the La Quina Amont site.

OxA	Date BP	error	Used (mg)	Yield (mg)	Yield (%)	%C	$\delta^{13}C$ (‰)	$\delta^{15}N$ (‰)	CN
2326-22	37000	800	485.9	8.1	1.7	40.9	-21.0	7.1	3.4

21805	41100	1300	862	32.0	3.7	41.5	-20.2	6.9	3.4
21806	36850	800	860	48.4	5.6	44.0	-19.6	6.0	3.4
21807	45200	2200	640	25.5	4.0	40.9	-18.7	7.6	3.3
21808	44200	1900	640	33.4	5.2	41.8	-19.9	5.3	3.3
22153	37500	800	830	25.5	3.1	45.4	-18.8	6.6	3.2
22154	46900	2700	532	17.85	3.4	45.2	-20.3	8.2	3.2
22155	48900	3400	855	15.21	1.8	43.8	-20.0	5.0	3.2

Table S5: AMS date analytical data from La Quina Amont. See Table S2 caption for details of the analytical parameters given in this table.

OxA	Date BP	error	Sample	Species	Used (mg)	Yield (mg)	Yield (%)	%C	$\delta^{13}C$ (‰)	$\delta^{15}N$ (‰)	CN
21706	39400	1000	LQa1 C5 couche B3	*R. tarandus* metatarsal, scraped	497	18.7	3.8	45.5	-18.2	4.0	3.4
21707	38100	900	LQa2 C5 couche B2	cf. *R. tarandus* femoral shaft fragment with cutmarks	520.2	25.8	5.0	44.0	-18.5	5.1	3.3

Table S6: AMS dates from the Châtelperronian level at La Quina Amont. Table S2 caption contains details of analytical parameters.

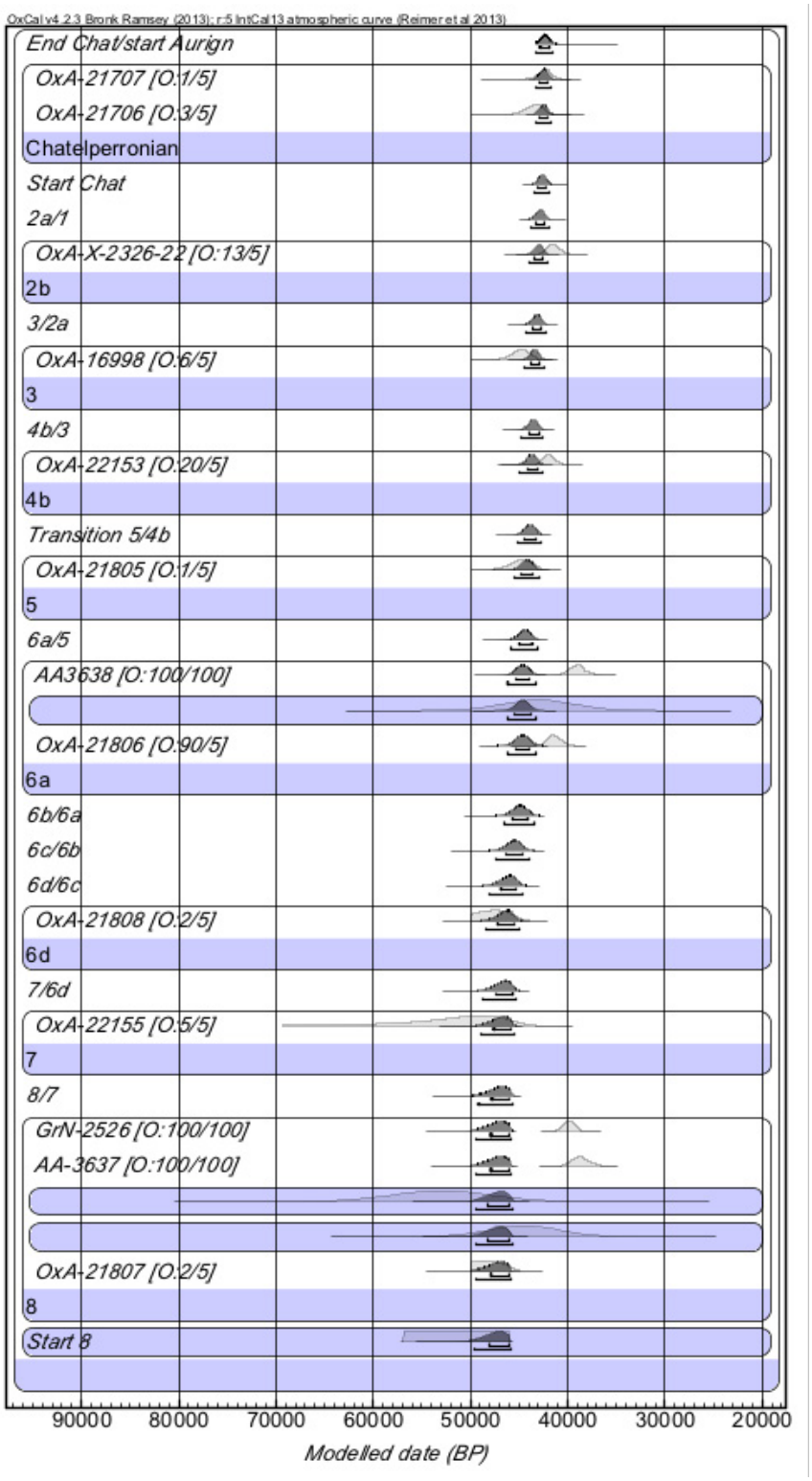

Figure S3: Bayesian age model for the La Quina site. See text for details. The prefix AA denotes the Arizona AMS laboratory, the prefix GrN denotes the Groningen CIO Laboratory (conventional dates). Three determinations were given 100% chances of being outliers in the model due to their significantly young ages and are included for illustrative purposes only, to demonstrate the differences between the previous results and those obtained here. There were no significant ORAU outliers apart from OxA-21806 in Layer 6a. TL determinations are shown in the blue shaded boxes in the model.

Saint-Césaire

Saint-Césaire is located in the Charente-Maritime region (45.76° Lat., -0.64° Long.). It is a key site for understanding the Middle to Upper Palaeolithic transition because in 1979, the partial skeleton of a female adult Neanderthal was excavated within the Châtelperronian level EJOP sup[55,56]. This find assumes major significance because it adds to the evidence that Neanderthals were the authors of the Châtelperronian industry. Prior to this the Châtelperronian had been considered an early Upper Palaeolithic industry linked probably with AMHs. One other site (Arcy-sur-Cure, France) is argued to document this link. Saint-Césaire contains a sequence of Mousterian, Châtelperronian and Aurignacian levels, but its chronology rested, until now, on a small series of TL ages on burnt flint that are imprecise[57].

The stratigraphy of the site consists of a series of Mousterian levels that form the so-called Lower Group (gray) and the bottom of the Upper Palaeolithic-dominated Upper Group of yellow-brown clayey sediments. The Lower Group includes Mousterian levels from the MTA (levels EGB sup and EGC) and Denticulate Mousterian (EGF, EGP, EGPF and EJOP inf). The EJOP sup level, which has been ascribed to the Châtelperronian, contains 26 Châtelperron points as well as other tools common to this technocomplex[58,59]. What is not clear at present is whether the high proportion of sidescrapers and flake-based tools in EJOP sup reflects the continuation of a production mode extending back into the Mousterian, or an amalgamation of Mousterian and Châtelperronian occupations[58,60]. This is crucial because of course it was in this level that the Neanderthal skeleton was excavated[61]. Renewed excavations at the site by François Bachellerie and Eugène Morin should help to resolve this issue. Above are several Aurignacian levels.

Applying the radiocarbon method to the Mousterian levels has proven particularly difficult at Saint-Césaire because of the problems encountered in obtaining enough collagen from bones and teeth, and the lack of charcoal at the site[57]. Levels of collagen in bone are low[62]. We therefore measured the %nitrogen in selected bones from throughout the sequence to screen out low collagen bones. We sampled a large range of bones from the site, then stored in Poitiers, including samples of bone that formed refits[59,60]. This enabled us to improve the rate of acceptability in the samples analysed later and obtain the first reliable dates from this site, as well as eliminate bones that were clearly lacking any collagen (see Table S7). The samples selected for dating were all identifiable

specimens, cut-marked or marrow-cracked bones. Dated samples and radiocarbon results are shown in Table S8.

The Bayesian model built for the site is shown in Figure S4. We included the direct date of OxA-18099 in its proper `phase`, which is the date of the Neanderthal in layer EJOP sup[63]. In addition, we added the TL dates of Mercier et al.[64] These results fit within the dated sequence with acceptable agreement and there were no outliers in the model. The age range (`date`) for the Mousterian levels in the age model was 47,540-42,030 cal BP (95%). The final `boundary` (in this case the transition from EGPF to EJOP inf) for the last Mousterian was determined to be 44,600-41,750 cal BP.

Sample ID and context	C:N atomic ratio	%N
RPB H6 (I) EJOP sup 26 (250–255), *Bos/Bison* tibia shaft fragment	74.9	0.1
RPB H6 (I) EJOP sup 26 (250–255, refit), *Bos/Bison* femur shaft fragment	63.89	0.1
RPB H5 (III-IV) EJOP sup 25 (240–250), *Bos/Bison* tibia shaft fragment	62.82	0.1
RPB D3 (IV) EJOP sup 27 (260–265), *Rangifer tarandus*, humerus shaft fragment	71.44	0.0
RPB 15 (I) EJOP sup 26 (250–260), *Rangifer tarandus*, shaft fragment	74.12	0.0
RPB I6 (I) EJOP sup 24 (230–240), *Bos/Bison*, tibia shaft fragment	68.06	0.1
RPB D3 (1) EJOP sup 248-24-98, *Rangifer tarandus*, metatarsal shaft fragment	60.5	0.1
RPB I5 (I) EJOP sup 26 (250–260), *Rangifer tarandus*, shaft fragment	64.06	0.1
RPB H6 (II) EJOP sup 25 (240–245), *Bos/Bison* tibia shaft fragment	61.58	0.1
RPB E5 (I-IV) EJOP inf 27-28 (265–275), *Rangifer tarandus*, tibia shaft fragment	47.38	0.1
RPB H6 (IV) EJOP inf 26 (255–260)	51.29	0.1
RPB E3 (IV) EJOP inf 27 (265–270), *Equus ferus caballus*, tibia shaft fragment	55.96	0.1
RPB F3 (III+IV) EJOP inf 27 (260–270) *Bos/Bison* shaft fragment	12.48	0.3
RPB D5 (III) EJOP inf 29 (280–290), *Rangifer tarandus*, tibia shaft fragment	58.46	0.1
RPB H6 (III) EJOP inf 24 (230–240), *Bos/Bison* tibia shaft fragment	50.93	0.1
RPB H4 (I) EJOP inf 27 (260–270), *Rangifer tarandus*, tibia shaft fragment	40.06	0.1
RPB E3 EGPF 28, shaft fragment*	29.06	0.1

RPB E3 (II) EGPF 28 (270–280), shaft fragment*	57.75	0.1
RPB E4 (I-II) EGPF 27 (265–270), shaft fragment*	40.34	0.1
RPB E4 (I-II) EGPF 27, shaft fragment*	6.7	0.8
RPB E4 (III) EGPF 28 (270–275), *Rangifer tarandus*, metatarsal shaft fragment	55.6	0.1
RPB E3 (II) EGPF 28 (270–280), shaft fragment*	47.93	0.1
RPB E3 (I) EGPF 30 (290–295), *Rangifer tarandus*, humerus shaft fragment	62.54	0.1
RPB E3 (IV) EGPF 27 (265–270) *Rangifer tarandus*, metacarpal shaft fragment	39.62	0.1
RPB E3 (IV) EGPF 28 (275–280), shaft fragment*	48.72	0.1

Table S7: %N and C:N atomic ratios from bones at the site of Saint-Césaire. In modern bone we would expect 4-4.5% N, and a C:N ratio of about 3.5-4.0. In this case the values are demonstrably different, indicating loss of nitrogen, and no recoverable collagen. The high C:N ratios indicate that these bones are essentially undateable and free of almost all remaining collagen. None of these bones were dated. Precise taxonomic and/or skeletal information for fragments with an asterisk (*) has been lost.

OxA	Sample	Species	Date	error	Used (mg)	Yield (mg)	Yield (%)	%C	$\delta^{13}C$ (‰)	C:N
21699	7. RPB H4 (I) EJOP sup 22 212.50.45(2)	*Rangifer tarandus*, tibia shaft fragment	36000	700	1230	14.01	1.1	44.0	-18.5	3.4
21700	7. RPB H4 (I) EJOP sup 22	*Rangifer tarandus*, tibia shaft fragment	36650	750	1080	9.2	0.9	44.2	-18.7	3.4
21636	7. H3 (III-IV) EJOP sup 24 239.53.05	*Bos*, metatarsal shaft fragment	37200	1000	739	3.2	0.4	41.4	-20.1	3.2
21637	8. F7 (IV) EJOP inf 34 (330–340)	*Equus ferus caballus*, metapodial shaft fragment	40100	1900	696.8	2.2	0.3	39.1	-20.5	3.2
21638	9. F4 IV EGPF 27 (265–270)	*Bos/Bison*, tibia shaft fragment	42400	2100	874.1	5.5	0.6	41.8	-19.7	3.3

Table S8: Radiocarbon determinations from the relevant Mousterian levels at the Saint-Césaire site that were used to build the model in Figure S4. See caption in Table S2 for description of the analytical parameters measured.

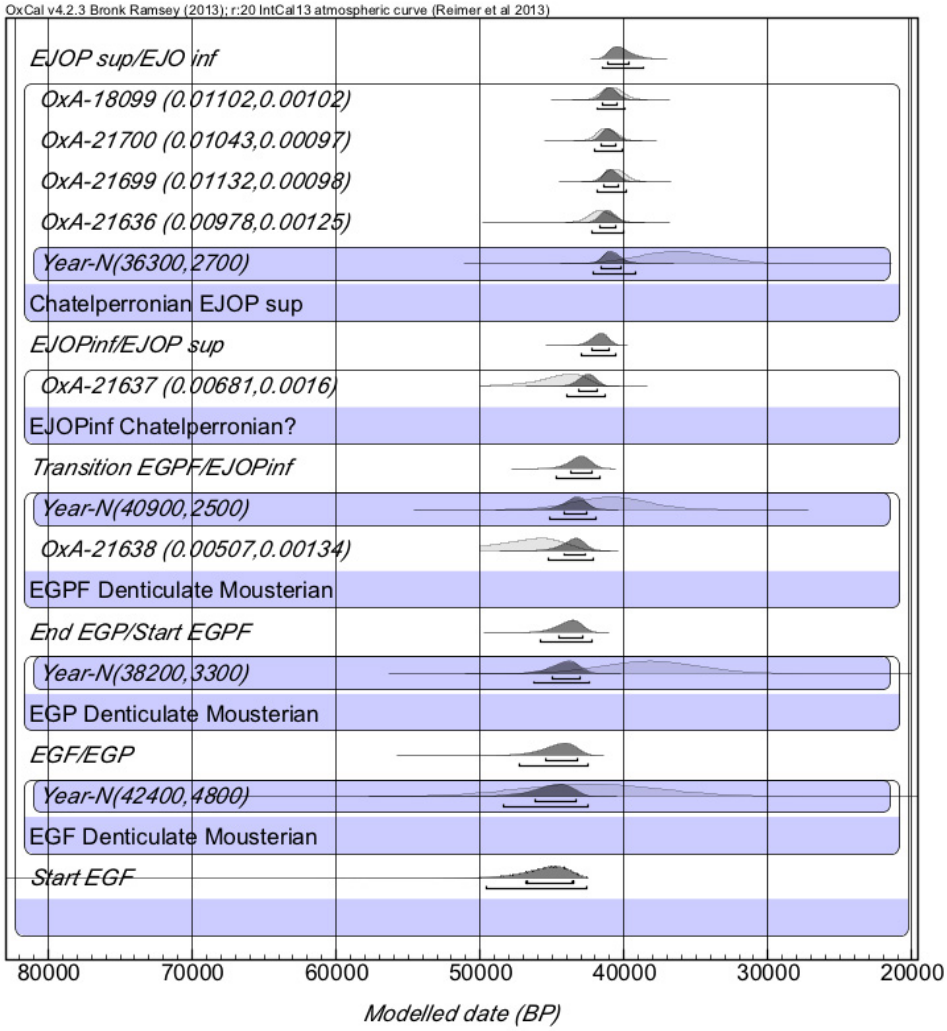

Figure S4: Bayesian age model for the Saint-Césaire Mousterian and Châtelperronian levels. The model includes TL dates as well as the new radiocarbon dates reported in Table S8, and the direct radiocarbon date for the Neanderthal in EJOP Sup dated in Oxford[63]. The latter fits perfectly into the sequence established by the other AMS dates from EJOP sup.

La Ferrassie

Material from the La Ferrassie 1 (44.95° Lat., 0.93° Long.) Neanderthal skeleton (code 23645 1953-25) was sampled at the Musée de l'Homme, Paris. This included a distal right (coded LF 1 in the table below) and a distal left tibia (LF2). The bones underwent a %N test. This yielded a result of ~1.3% nitrogen, therefore encouraging us to proceed with collagen extraction on a large sample.

The first two determinations produced ages in substantial disagreement with each other. We consider both to be unreliable.

We then attempted to isolate single amino acids from the bones (HYP -hydroxyproline and ALA – alanine) using HPLC methods (see Marom et al.[65]). The results are shown in Table S9. The result for the LF1 bone suggests that, even with single amino acid dating, there is a significant contaminant remaining in the sample. This suggests strongly that the contamination is likely to be a proteinaceous contaminant, such as bone or collagen glue. There is a high chance that the same could be influencing the LF2 series of results, albeit in a lower proportion.

We consider these determinations to be inaccurate and so the results were not included in our analysis of the overall results.

OxA-X	Sample	Date BP	Error	PCode/ fraction	Used (mg)	Yield (mg)	Yield (%)	%C	$\delta^{13}C$ (‰)	$\delta^{15}N$ (‰)	C:N
2294-14	LF2 La Fer 1 23645 1953-25	32750	450	HYP				46.1	-22.8	13.4	4.9
2395-26	LF2 La Fer 1 23645 1953-25	35700	1500	Ultrafiltered*	1020	30.7	3.0	46.1	-18.9	11.4	3.4
2403-14	LF2 La Fer 1 23645 1953-25	32100	1800	ALA				25.6	-32.9	7.9	3.1
2294-15	LF1 La Fer 1 23645 1953-25	11540	55	HYP				48.4	-22.9	12.7	4.9
2395-25	LF1 La Fer 1 23645 1953-25	12910	90	Ultrafiltered*	690	19.8	2.9	47.6	-19.3	10.7	3.5
2403-18	LF1 La Fer 1 23645 1953-25	12950	130	ALA				32.5	-24.7	11.1	3.1

Table S9: Radiocarbon data for the La Ferrassie 1 skeleton. LF1 is a distal right tibia and LF2 is a distal left tibia. See Table S2 for caption explanations. * denotes a solvent prewash before collagen pretreatment. HYP is hydroxyproline; ALA is alanine, derived via HPLC separation. For methods see ref 65. Note that C:N atomic ratios for these amino acids differ from bulk collagen and are approximately correct here. The determinations are OxA-X-ed to denote the problems with the accuracy of the results in this instance (see text for details). The bones are contaminated, and almost certainly with proteinaceous-derived material of a modern age.

La Chappelle-aux-Saints

We sampled the important Neanderthal specimen the 'Old Man' of La Chappelle-aux-Saints (Charente) (44.98° Lat., 1.71° Long.) using the methods described above. Sampling was undertaken at the Musée de l'Homme in Paris. The dated sample was a distal left femur (reference 1908-37, 24.483 – 1960-3). A small amount of bone taken from the specimen was tested prior to sampling for dating and provided %N values of 1.07 and 0.95%, suggesting that there was remaining collagen in the bone. A total of 610 mg was therefore later sampled for AMS dating. The resulting determination produced a high C:N atomic ratio (3.6) and was therefore failed for dating (Table S10). We suspect that it was contaminated. Despite the sample being treated prior to AMS dating with a solvent extraction sequence, the sample was not effectively cleaned. We hope to attempt a second determination using a single amino acid protocol in the near future.

Used	Yield	Yield (%)	$\delta^{13}C$	$\delta^{15}N$	C:N	Date BP	Error
590	17.1	2.9	-19.5	13.3	3.6	failed	na

Table S10: Radiocarbon sample analytical details for the attempted date from La Chappelle-aux-Saints.

Néron

We attempted to date the Neronian and Mousterian industries from the site of Néron (44.89° Lat., 4.836° Long.). The Neronian is attested from a number of sites in the Rhône valley and Mediterranean France including Néron I, Grotte Mandrin E, Moula IV, Figuier 1' and Maras 1-1'24[24,68]. The Neronian of Néron I appears to suggest an origin in the Charentian Mousterian[68] but presently it is not known what human species were responsible for this industry. We directly sampled for dating a small piece of cranial fragment from an adult hominin from Néron I, as well as samples of fauna, fractured or cut teeth and bone from Niveau 1 and 2 at the site. We also sampled retouchers for direct dating (Table S11 for details of the samples). Unfortunately, none of the samples proved to be dateable due to lack of collagen. The hominin sample gave a yield of >1% nitrogen but ultimately not enough collagen could be extracted for dating.

Niveau	Veyrier/Combier number	Type of material	Period

1	Veyrier 13	*Equus ferus* fractured left M1/M2 lower	Neronian
1	Veyrier 15	*Equus ferus* fractured left P4 lower	Neronian
1	Veyrier 12	*Equus ferus* fractured left M1/M2 lower also used as a retoucher	Neronian
1	Veyrier 230	*Equus ferus* humeral fragment cut and used as a retoucher	Neronian
2	Veyrier 09	*Equus ferus* metapodial retoucher	Mousterian
2	Veyrier 06	Retoucher and scraped large mammal bone	Mousterian
2	Combier 293	Retoucher	Mousterian
2		Hominin cranial fragment: assumed *Homo neanderthalensis*	Mousterian

Table S11: Samples taken for dating from the Néron site. None of the samples produced sufficient collagen for an AMS date.

Grotte Mandrin

Grotte Mandrin is a vaulted rock shelter located in the Middle Rhône valley around 120km north of the Mediterreanean sea (44.28° Lat., 4.46° Long.). Excavations have been undertaken since 1991. The latest excavations are by Ludovic Slimak and his team. The upper sequence revealed six stratigraphic units (B to G) divided into 6 cultural phases. These include: 1) Ferrassie Mousterian (couche G and F), 2) Quina Mousterian (Couche F), 3) Néronian I (E), 4) Post-Neronian I (D), 5) Post-Neronian II (Cinf, Csup, Binf, Bmed) and 6) Proto-Aurignacian (Bsup)[34,66,67]. These phases cover the final Middle Palaeolithic from ~50-55 ka BP until the early Proto-Aurignacian around ~42 ka cal BP.

Mandrin contains a Middle and Upper Palaeolithic sequence that records all of the cultural phases currently known for the last Neanderthals up to the earliest French Mediterranean Upper Palaeolithic. Each archeological unit contains a rich lithic industry alongside many humanly modified faunal remains. The preservation state of the stratigraphic units is good in the case of units A to D and excellent in the case of units E-F due to windblown local sands and silt being an active agent in the site sedimentation. There is a restricted presence of carnivores and, where they occur, they are represented by coprolites and gnaw marks on some of the bones. Layers B to E have yielded several anthropogenic structures.

All of the radiocarbon samples selected for dating from Grotte Mandrin were bones and only artefacts and humanly-modified bones were sampled. Several retouchers were sampled from the

lower levels of the site. Table S12 contains the radiocarbon measurements and Table S13 the analytical data associated with the results.

The Bayesian model built consists of a sequence of phases ordered sequentially, containing several radiocarbon and luminescence dates (Figure S15). In contrast to previous results (e.g Ly-2755 from level E, which gave a result of 33,300 ± 230 BP)[68] all of the determinations from the Neronian (level E) and below produced infinite determinations, indicating that their age was beyond our measureable limit for bone collagen of 49.9 ka BP (0.002 fM). For this reason these determinations were not included in the modelling. This also includes OxA-21698, which is a finite radiocarbon age from Level D that extends beyond the calibration range. This determination is from a bone from the immediate post- Neronian level and therefore would act to constrain the Neronian below it. The removal of this determination means that the Neronian is constrained instead by the ages from level C. Under the model parameters the estimated probability range for the Neronian is 52,480-48,130 cal BP (68.2% prob.) and 55,260-46,620 cal BP (95.4%). We suggest that given the importance of the TL determination from Level G within the model, and the lack of finite radiocarbon ages within the lower sections of the sequence, that this probability range may well be a minimum age. If the TL determination from G, like that from level Bmed, underestimates the age of the level, then the Neronian age as inferred from our model might likely be older in reality. More work is required from these lower facies.

The model clearly shows that the TL determination from the Bmed Mousterian level is a clear outlier (100% likely)(Figure S5). There are no other significant outliers except for OxA-21691, which has a 37% outlier probability and extends to the older end of the timescale when compared with other determinations from the same context. This determination is flagged as too old for its context, and may be a bone derived in some way from a lower level. In 37% of the model calculations this determination was not included.

The model shows that the Mousterian at Mandrin ended at 44,260-42,590 cal BP (this being the final boundary for the Mousterian level Bmed). The date range for the Mousterian levels we have dated and modelled (Figure S5) was 45,950-42,990 cal BP (at 95.4% prob.).

OxA	Sample	Geol. layer	Material	Date BP	error
21691	15	B	horse tooth fractured by human activity Upper cheek tooth	45300	2200
22121	Man 08 B3 1755	B	Cut bone fragment	40300	1200
21690	11	C	Cut and scraped bone fragment	41700	1400
X-2286-10	10	C	humeral shaft fragment, small bovid size. Cutmarks	38500	1000
21685	5	B	Cut diaphyseal fragment	39000	1000
22120	Man 08 B2 934 No. 47	B	Cut bone fragment	43400	1800
X-2286-13	17	C	Retoucher *cf.* bovid limb metatarsal fragment	43200	2000
X-2286-14	18	C	Retoucher artiodactyl limb fragment	42800	1800
X-2286-15	21	E Niv. 7	*Cervus elaphus* mandibular ascending ramus with cutmarks	>49000	
21692	22	E. Niv.7	Retoucher on horse tibia	>47300	
21693	23	E. Niv.7	Retoucher on horse tibia, cut and smashed	>48600	
21698	36	D Niv.6	Bone with cutmarks	47000	2700
21694	27	D testpit	Retoucher *cf.* reindeer femur	>47100	
21695	28	F testpit	Retoucher with cutmarks and impact (ascending ramus fragment of a bovid or horse sized animal?)	>48200	
21696	30	F testpit	Cut bone small artiodactyl small radius	>49900	
X-2287-24	35	G testpit	Broken horse tooth humanly fractured	>48000	
21697	34	Geol. layer	Cut bone distal femoral articulation horse/bovid sized	>45400	
21701	34	B	Bone with cutmarks	>45200	

Table S12: Material, context and radiocarbon dates from the Mousterian, Neronian and post- Neronian levels at the Grotte Mandrin.

OxA number	Used (mg)	Yield (mg)	Yield (%)	%C	$\delta^{13}C$ (‰)	$\delta^{15}N$ (‰)	C:N
21691	640	9.1	1.4	47.1	-20.3	5.1	3.3
22121	704	26.9	3.8	45.1	-21.3	3.4	3.2
21690	840	33.2	4.0	43.5	-20.5	n.d	3.3
2286-10	830	5.34	0.6	44.5	-19.5	n.d	3.3
21685	540	9.52	1.8	41.8	-19.8	2.3	3.3
22120	510	5.9	1.2	44.8	-20.9	1.5	3.2
2286-13	610	3.71	0.6	44.1	-20.1	3.9	3.2
2287-24	600	3.02	0.5	41.4	-20.0	2.9	3.2
2286-14	620	4.16	0.7	43.4	-18.9	3.7	3.3
2286-15	610	5.5	0.9	45.5	-18.1	3.8	3.4
21692	700	8.58	1.2	47.4	-19.2	4.7	3.3
21693	620	10.35	1.7	47.1	-19.8	3.3	3.3
21698	620	7.68	1.2	46.1	-19.5	3.4	3.3
21694	600	12.57	2.1	46.3	-19.5	6.6	3.4
21695	610	20.91	3.4	46.6	-19.7	4.8	3.3
21696	610	19.71	3.2	47.7	-18.5	4.1	3.4
21697	520	18.94	3.6	45.7	-19.9	2.0	3.4
21701	620	20.66	3.3	45	-19.9	2.3	3.3

Table S13: Analytical data for the radiocarbon dates from the Mousterian, Neronian and post- Neronian levels at the Grotte Mandrin. See Table S2 caption for details of the analytical data.

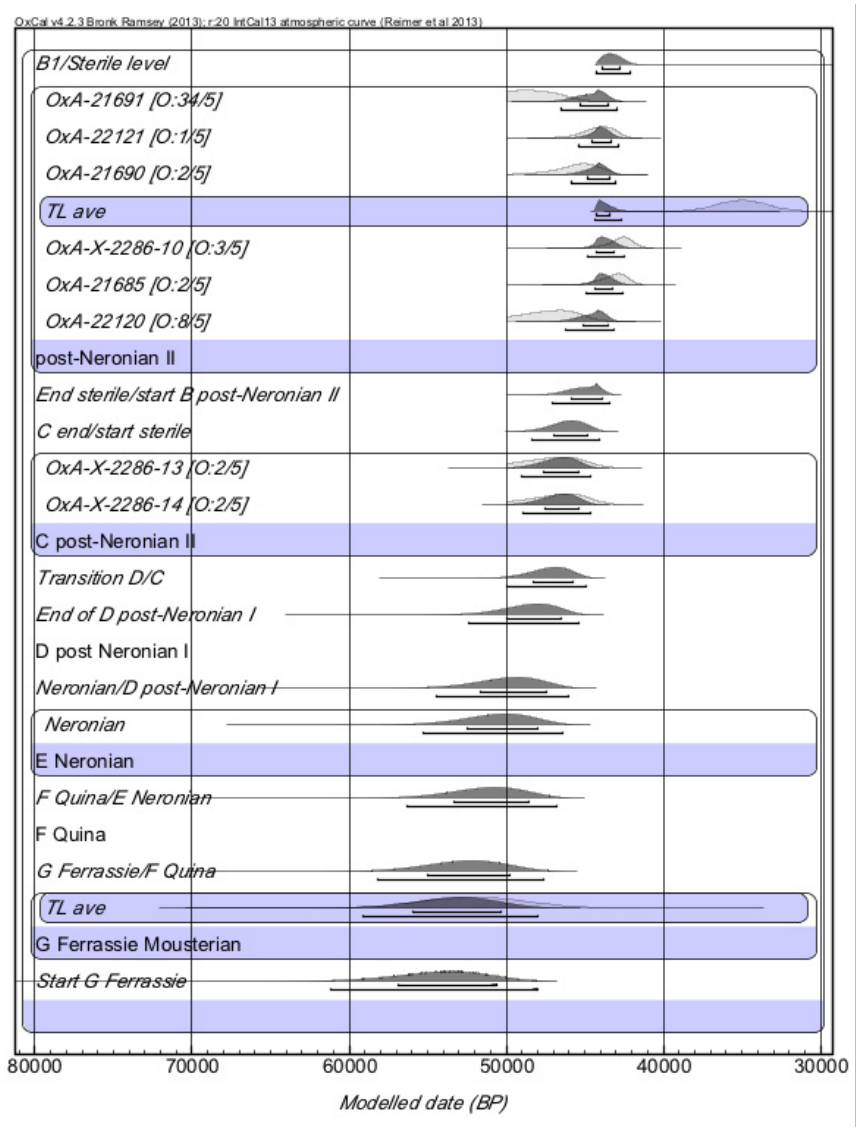

Figure S5: Bayesian age model for the Mousterian and Neronian sequence from the Grotte Mandrin. The `boundary` B1/Sterile level denotes the end of the Mousterian `sequence`. Note also that there is a replacement between the Quina Mousterian and the final Mousterian at the site by the Neronian and post-Neronian `phases`. The Neronian in this model is not directly dated but constrained by determinations from C above it, and the TL average age in Level G. The PDF in E is a distribution generated by a `date` command to provide a preliminary age estimate for the Neronian level.

Les Cottés

This site is located in the southwestern part of the Paris Basin (46.41° Lat., 0.50° Long.), importantly on the periphery of the known distribution of Châtelperronian sites. The site consists of a sequence of Mousterian, Châtelperronian, Aurignacian and Gravettian layers. A series of AMS dates from the site was published by Talamo et al.[69] and the reader is referred to this paper for a wider discussion of the archaeological sequence. Further work is being undertaken to determine the

precise type of Mousterian at the site. Various authors have diagnosed the presence of MTA and La Quina Mousterian variants[69].

We determined a final boundary for the Mousterian at this site of 43,810–42,350 cal BP based on the model in Figure S6. The overall date range for the Mousterian was estimated at 45,540–42,730 cal BP (all at 95.4% prob.). The Châtelperronian range by comparison was 43,100–41,050 cal BP.

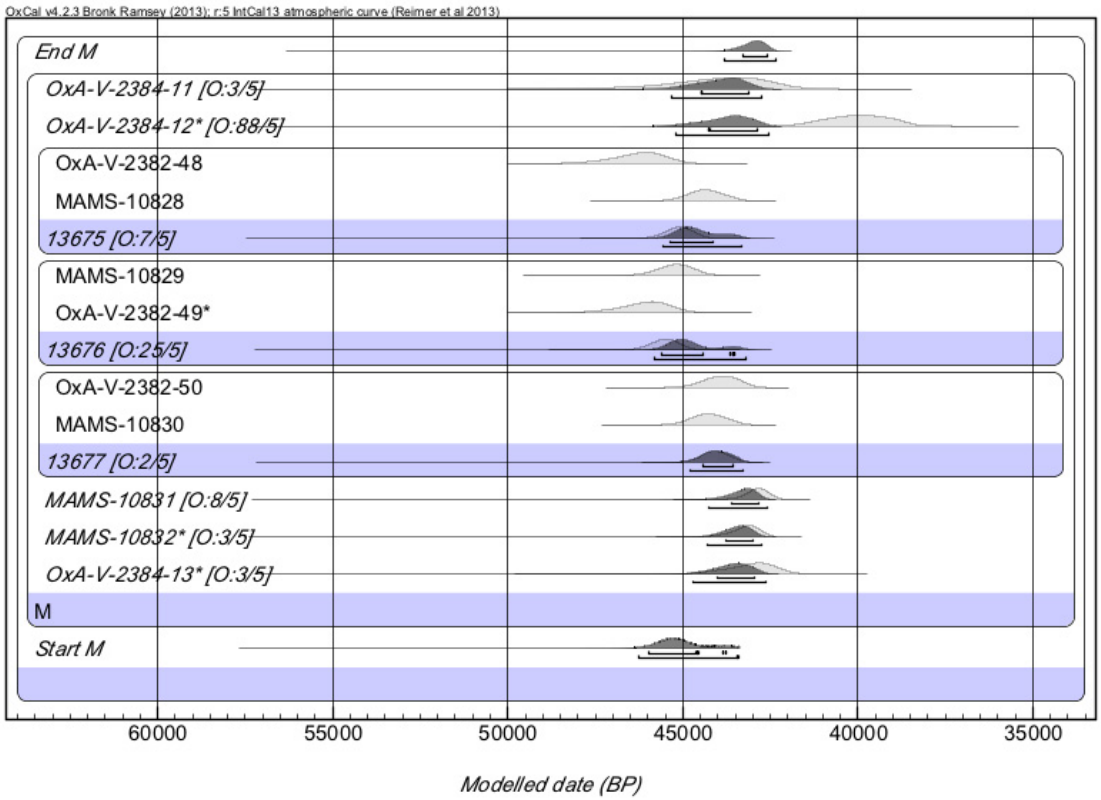

Figure S6: Bayesian age model for the site of Les Cottés, France. See text for details. Data is from Talamo et al.[69].

Pech de l'Azé IV

Radiocarbon dates from the site of Pech de l'Azé IV (44.86° Lat., 1. 25° Long.) have been published by McPherron et al.[70] from renewed excavations. The lithic industry at the site has been diagnosed as MTA with a Levallois technology present and blade and bladelet technologies absent[70]. The lithic industry from layers 3b-3a includes bifaces typical of the MTA as well as backed knives. There is no evidence of any Châtelperronian, Aurignacian or Proto-Aurignacian lithic materials in the site therefore it does not contribute to our understanding of the transition to

the Upper Palaeolithic, but it does document the well-dated presence of this Mousterian variant industry in MOIS3.

The radiocarbon results obtained in McPherron et al.[70] use ultrafiltered collagen methods that are virtually the same as our own. The data have therefore been used to build the Bayesian model below.

The model discloses three outliers of significance (see Figure S7) downweighted in the model. The age range (`Date`) for the Mousterian from this site was 49,100-45,860 cal BP (the posterior probability is skewed heavily to the younger end of this range), with the final `boundary` for 3a equivalent to 47,040-45,740 cal BP (at 95.4% probability).

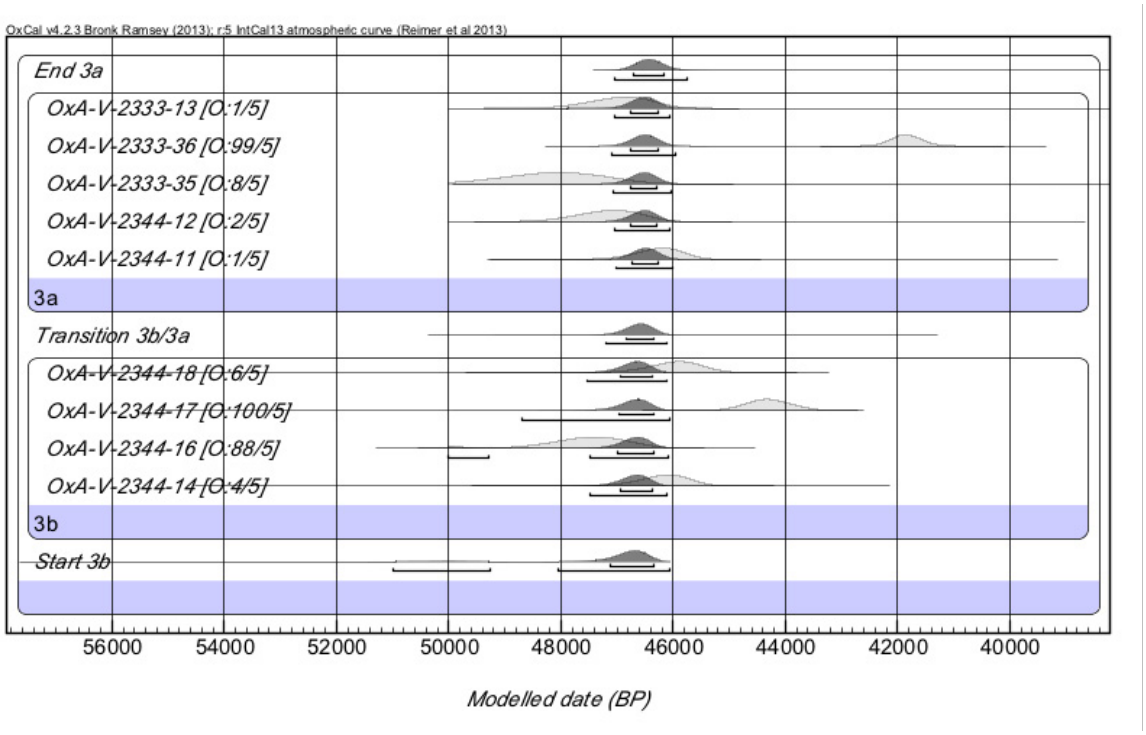

Figure S7: Bayesian age model for the site of Pech de l'Azé IV, data after McPherron et al[70]. Note there are three outliers in the model (two ~100% and one 88% probable as being outliers) that are downweighted. See Figure S1 caption for details of the model parameters.

Spain

Abric Romani

Abric Romaní (41.53° Lat., 1.69° Long.) is in Catalonia, northeastern Iberia[71,72]. It is a travertine rock shelter overlooking the Anoia River, on a high 60m cliff situated below the modern day town of Capellades (~45 km NW of Barcelona). Archaeological excavation began in the early 20th century through the work of Amador Romaní in 1909, and later others, until 1930. Still later excavations were undertaken by Ripoll (1956 – 1962), Ripoll and de Lumley (1975) and Carbonell (1983 – present)[72]. The site is best known for its very long Mousterian sequence. Atop this is a single layer (termed layer A) that has been considered to probably be Proto-Aurignacian. This is separated from the latest Mousterian level (layer B) by a sterile tufa (layer 3). The Mousterian industry at Romaní is considered to be a La Ferrassie-type Mousterian by virtue of the low proportion of denticulates[75]. Vaquero and Carbonell[73] have commented on the attribution made of some of the lithic evidence by Camps and Higham[75] but their comments are not relevant to the chronometric work at the site that we have undertaken.

The latest Mousterian is dated at Romaní by a series of TIMS U-Series dates obtained by Bischoff et al.[74] and these effectively seal the Level B Mousterian below it. Level B itself is dated by two charcoal determinations, one of which is from the ORAU (Table S14).

The Bayesian model for the site is shown in Figure S8. The model shows that the boundary representing the end of the latest Mousterian level B is 43,160-41,130 cal BP. The Mousterian date range covered in the Bayesian model ranges between 49,550-41,190 cal BP, a longer range than we have usually documented, this being due to the large number of U-series determinations from earlier parts of the site sequence.

OxA	Sample ID	Sample	Date BP	error	$\delta^{13}C$ (‰)
OxA-12025	AR102/level B	Charcoal	39,060	350	-24.5

Table S14: Radiocarbon determination from Level B at Abric Romaní, Catalonia[75].

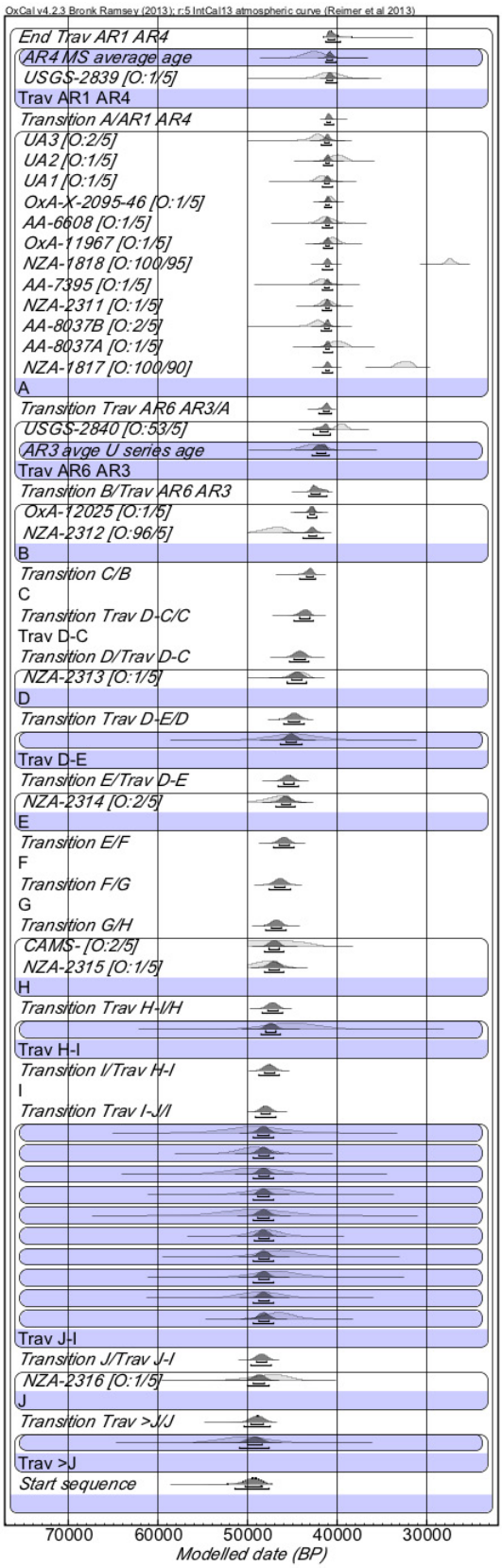

Figure S8: Bayesian age model for the Abric Romaní site[75]. The model includes TIMS uranium series dates obtained by Bischoff et al.[74] These are the distributions with the single blue background (and no lab code) around them.

L'Arbreda

L'Abreda is a collapsed cave in a karstic cascading travertine environment located in Catalonia, northeastern Spain (42.16° Lat., 2.75° Long.). Excavated since the 1970s, the sequence is around 9 m deep and contains archaeological evidence from the Epipalaeolithic to the Middle Pleistocene[76]. The final Mousterian to Gravettian levels are found within a single sedimentological unit, formed of homogenous clay housed between large travertine blocks that fell from the cave roof. The archaeological levels have therefore been defined by the distribution of artefacts[77]. The final Mousterian at the site is in level I. The level above contains an Archaic or Proto-Aurignacian level (H). Both have been radiocarbon dated using bone and/or charcoal, but not treated with the more robust methods used in this paper ([eg in refs 76,78,79]). Level H contained several dates beyond 42 ka cal BP, significantly earlier than most other Aurignacian contexts in western Europe. This has proven controversial[16,80, 81,82]. Some authors[82] suggest that they are not reliable due to mixing of the final Mousterian and Aurignacian level primarily because of difficulties in their stratigraphic separation but Soler et al.[77] have presented piece plotted artefact data that largely rebuts this criticism.

New determinations have been obtained as part of this project by Wood[83] and Wood et al.[84] %N analysis was used to test bone for the presence of collagen and 15 bones obtained from post-1975 excavations were dated from throughout the sequence. Bones from the Aurignacian levels were all anthropogenically modified in some way but because no cutmarked bones were found in level I, only longitudinally fractured bones were dated (Table S15). One charcoal fragment from level I was dated using ABOx-SC[85] (OxA-19994), and this is included in the model below. Only one sample, OxA-21702 (level I), extends beyond the limit of the calibration curve. Dates from the uppermost Mousterian in level I are shown in Table S16.

The model shows that there is some reworking of material from levels above the Mousterian, in some instances. Three obvious outliers, one in level I and two from level H, were given a higher prior outlier probability (50%) to help the model to run. There is no pattern in terms of the location of the intrusive bones. Suspicions that they might be more prevalent in areas closer to roof-fall travertine blocks in the site are not supported by the data. With the exception of these three samples, the radiocarbon dates for the transition between the Mousterian and Proto-Aurignacian appear to be unaffected by the mixing evident from higher in the stratigraphy.

In our model (Figure S9), the `boundary` calculated for the end of the Mousterian is 42,710-40,680 cal BP (95.4% probability). The `date` range for the Mousterian at the site is 44,610-41,050 cal BP (95.4% prob.).

Sample ID	Context	Species identification	Human modification
ABD 13	Level I C4 DC108 871, 64, 6, -536	*Cervus elaphus*, proximal fragment of right metatarsal	Longitudinal fracture
ABD 14	Level I A5 EA112AC 806, 0,75, -557	*Cervus elaphus*, 1st phalanx, posterior side of the distal epiphysis	Longitudinal fracture
ABD 15	Level I C2 BC108 831, 33,5,-540	*Cervus elaphus*, 2nd phalanx, posterior side	Longitudinal fracture
ABD 17	Level I D2 BD118 1204, 62, 48, -581	*Cervus elaphus*, 1st phalanx, posterior side of the distal fragment	Longitudinal fracture

Table S15: Samples selected for dating from the Mousterian Level I at L'Arbreda.

Sample ID	Level	Pretreat. method	Lab. No.	Date BP	error	Yield (mg)	Yield (%)	%C	$\delta^{13}C$ (‰)	$\delta^{15}N$ (‰)	C:N
ABD 15	Level I	AF*	OxA-21663[J]	32,100	450	15.72	4.4	45.6	-19.4	3.1	3.2
		AF*	OxA-21703[J]	32,300	450	27.67	3.6	47.1	-19.6	4.7	3.3
ABD 17	Level I	AF*	OxA-21704	39,200	1000	11.55	2.6	47	-19.4	6.2	3.3
ABD 14	Level I	AF*	OxA-21702	44,400	1900	16.85	2.6	46.1	-19.5	5.8	3.3
ABD 13	Level I	AF*	OxA-21662	37,300	800	35.64	4.3	42.4	-20	4.4	3.2
ABD 5	Level I	XR	OxA-19994	38,350	400	9.15	4.8	39.6	-24.5	na	na

Table S16: Radiocarbon determinations from the Mousterian Level I of L'Arbreda, Catalonia (after Refs 83 and 84). See Table S2 for details of location and context, as well as the type of element and species. ABD 5 is charcoal (*Pinus sylvestris*) and treated with an ABOX-SC treatment (on the ORAU database this is termed an 'XR' treatment), all other results (termed 'AF*') are bone collagen treated using the ultrafiltration method described above but with a solvent extraction first as a precaution, since PVA was applied to some bones during excavation. Note that the duplicate AMS dates for sample ABD 15 were 100% outlying in the model in Figure S9 and are intrusive samples from higher up in the sequence. Radiocarbon dates from the Aurignacian and Gravettian units are detailed in Wood et al.[84] [J] denotes duplicate measurements on the same bone.

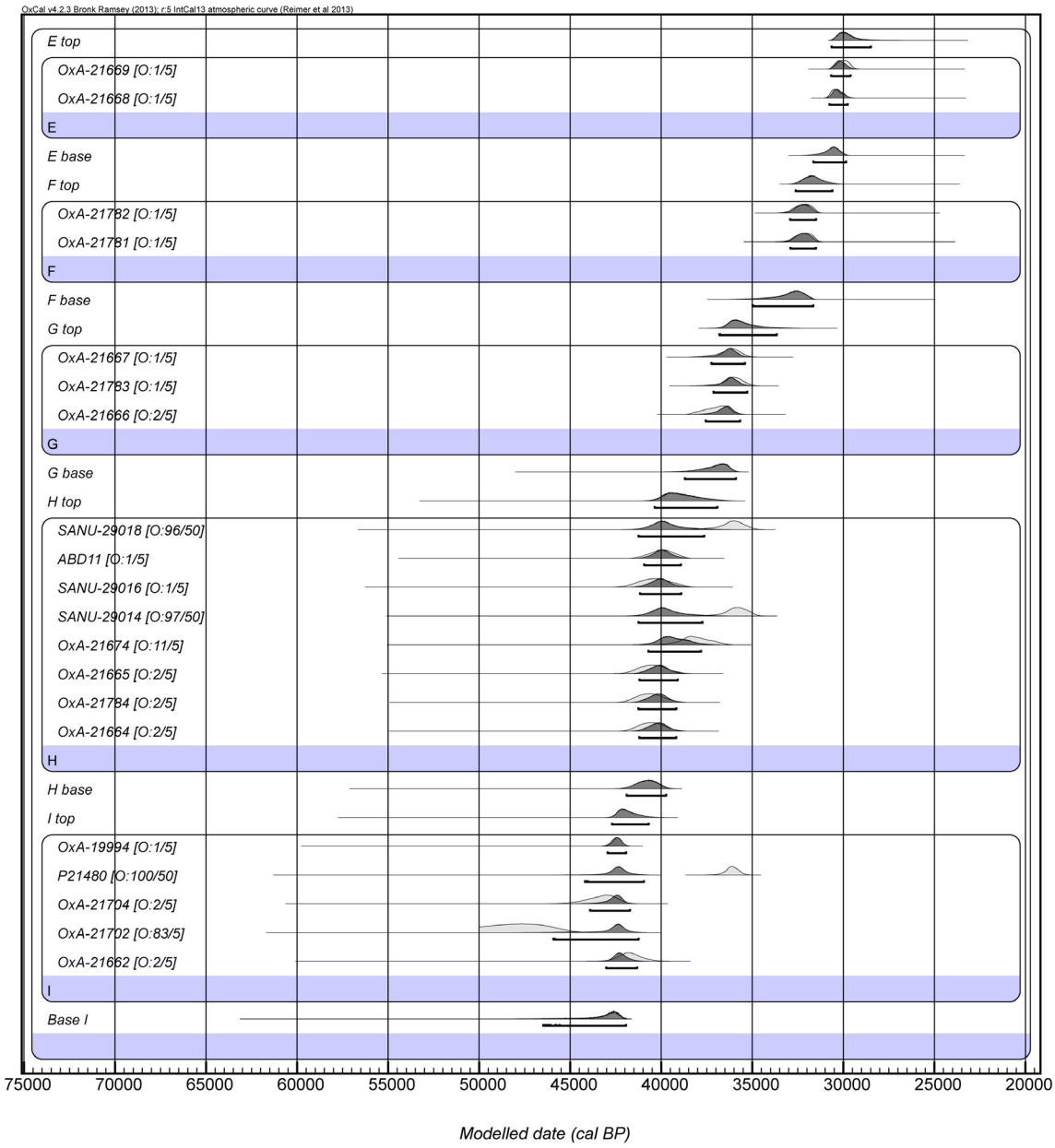

Figure S9: Bayesian age model for the L'Arbreda site, after refs 83 and 84. P21480 denotes the duplicate dates from ABD 15.

Labeko Koba

The site of Labeko Koba (43.06° Lat., -2.49° Long.) is located in the Basque Country. It was discovered and excavated ahead of the construction of a road[86]. The site is key in the early Upper Palaeolithic of the wider region because it contains Châtelperronian (level IX lower) and Proto-Aurignacian (level VII) levels separated by levels (levels IX upper and VIII), which are nearly

archaeologically sterile[86]. There is no Mousterian in the site, but our interest here is in dating the Châtelperronian, linked, as it is currently, with Neanderthals. The assemblage in level IX(lower) is small, consisting of 62 lithics, of which only 11 were retouched. However, these have been identified as Châtelperronian as they include 3 Châtelperron points, an atypical point and an Aurignacian blade, amongst diverse substrate elements[87].

Prior to our work there were eight AMS radiocarbon dates on bone from the site. The bones were treated with acid demineralisation and gelatinisation and are not consistent with the stratigraphic sequence. They also had low pretreatment yields, which raised suspicion over their accuracy.

We dated 9 new samples (Table S17) from levels IX(lower) and IX(upper) after extensive testing of the available bone corpus using %N analysis[83,84]. Most of the bones gave yields >1% weight collagen although one sample failed to produce enough collagen to date.

The Bayesian age model for the sequence is shown in Figure S10. The `date` range for the Châtelperronian was 42,610-41,450 cal BP. The `boundary` for the end of the Châtelperronian was 42,490-41,340 cal BP (at 95.4% probability).

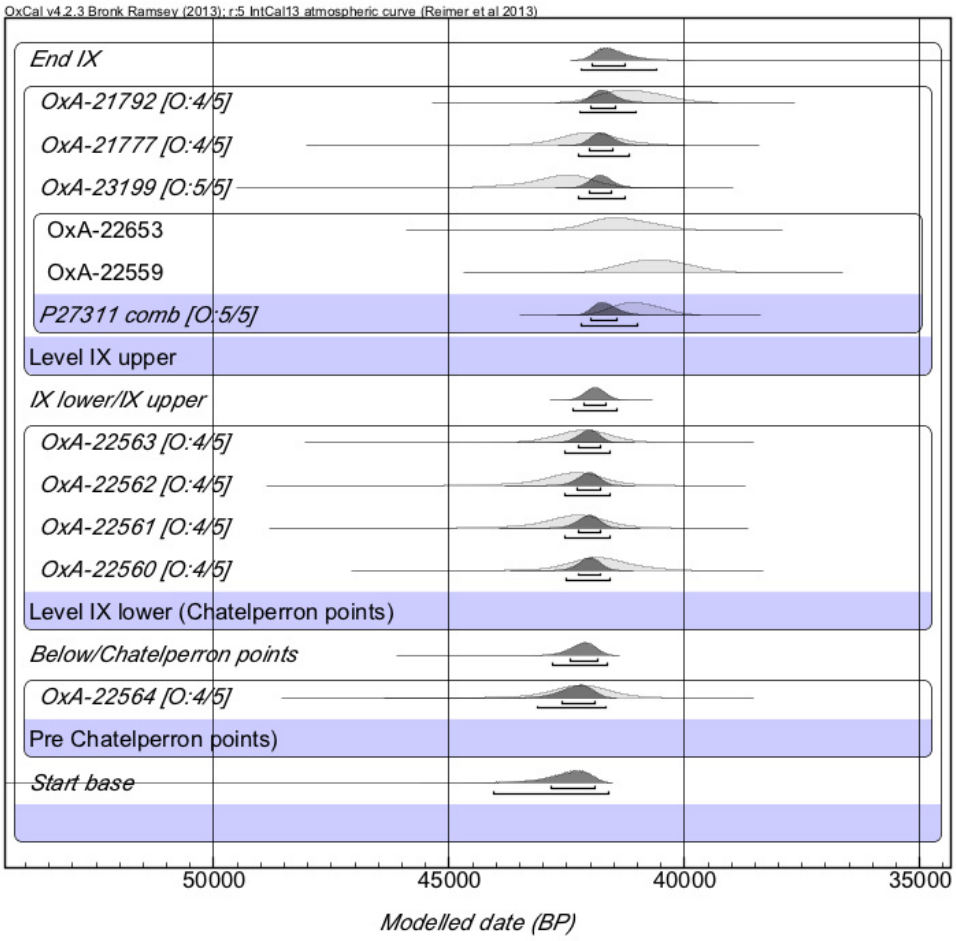

Figure S10: Bayesian age model for the earliest Upper Palaeolithic levels at Labeko Koba[83,84]. See Wood et al.[84] for a model including Aurignacian units.

Code	Lev	Industry	Identification and human modification.	OxA-/OxA-X no.	Date BP	error	Yield (mg)	Yld (%)	%C	$\delta^{13}C$ (‰)	$\delta^{15}N$ (‰)	C:N
LAB-3	IX	Sterile	*Megaloceros giganteus* antler base No modification. Possibly collected by humans to be used as soft hammer and later gnawed	23199	38,400	900	16.6	1.3	41.2	-19.4	7.4	3.4
LAB-22	IX	Sterile	*Bos*, tibia diaphyseal fragment cut marked	22559[J]	36,000	700	11.2	1.5	40.1	-20.6	6.4	3.2
				22653[J]	36,850	800	11.4	1.6	44.7	-20.3	6.9	3.2
LAB-2	IX	Sterile	Artiodactyl. 4 percussion stigma and 2 cut marks	21792	36,550	750	13.6	2.2	43.3	-19.5	5.1	3.4
LAB-1	IX	Sterile	*Equus* sp., right tibia, proximal end retouched by percussion, carnivore gnawing on distal end and proximal epiphysis, but as a secondary agent	21777	37,700	900	17.8	2.6	38.2	-19.1	5.6	3.2
LAB-27	IX	Châtelperronian	*Cervus elaphus*, metatarsal cutmarks and gnaw marks	22563	37,800	900	17.7	2.6	42.3	-20.2	3.7	3.1
LAB-26	IX	Châtelperronian	Cut marked *Cervus elaphus* (juvenile), humerus	22562	38,100	900	11.2	1.3	42.6	-20.1	3	3.1
LAB-24	IX	Châtelperronian	*Cervus elaphus*, distal humerus cut marked	22561	38,000	900	12.5	1.3	41	-20.3	4.1	3.2
LAB-23	IX	Châtelperronian	*Cervus elaphus* radius cut marked	22560	37,400	800	8.5	1	42	-20.6	3.8	3.2
LAB-28	IX	Pre-Châtelperronian	Unmodified *Bos* metatarsal	22564	37,900	900	9.0	0.9	40.9	-19.9	3.4	3.1

Table S17: Radiocarbon AMS dates from Labeko Koba after Wood[83] and Wood et al.[84] See caption for Table S2 and the text for details of analytical data. Glue was observed on two bones. Although the sample was taken away from this glue, the bones were given a precautionary solvent wash prior to extraction of collagen, this is denoted by an asterisk after the pretreatment method code. Details of the samples material selected for dating and the human modifications are included in Refs 88 and 89. [J] denote duplicate measurements.

El Sidrón

El Sidrón is in Asturias, northwestern Spain (43.23° Lat., -5.19° Long.). Speleologists discovered the site, and after preliminary work by the Guardia Civil and excavations since 2000[90], around 2000 fragments of Neanderthal bone from 12 individuals have been uncovered[91]. Alongside this, a small assemblage of lithics (399 pieces) attributed to the Denticulate Mousterian[92] have been identified. Articulation suggests the Neanderthal remains were deposited shortly after death[93], and because they are found within the clays and fine sands of unit III, interpreted as a debris deposit that entered the gallery from a higher level during a collapse and/or storm event, it is thought that they are contemporaneous[92]. Existing direct radiocarbon dates on the Neanderthal remains range from c.10 ka BP to c.50 ka BP, a salutary lesson on the dangers of dating low collagen bones. The oldest dates were produced with the ninhydrin method[94] at the LCSE - Gif-sur-Yvette and are in agreement with OSL, ESR and AAR dates[95].

Twenty-two cortical bone fragments were selected and sampled for %N screening in Madrid, and we also later sampled bone 00/47, which was the one previously dated using the ninhydrin method at the LSCE. This was the only sample of 22 cortical bones that contained sufficient nitrogen/collagen for dating (Wood et al.[96]), and it produced a date of 48,400 ± 3200 BP (OxA-21776). This is identical to the two ninhydrin dates (df=2, T=0.1, χ^2(5%)= 6.0), suggesting that the bone is probably slightly younger than 50 ka BP. The bone was not found within unit III, but was recovered after an initial excavation by the Guardia Civil, however, refits of bone and lithics by Santamaría et al.[92] suggest that the age of this bone is representative of the age of the assemblage from level III. No modelling work was done on the site due to the closeness of the reliable determinations to the limit of the calibration curve.

Arrillor

Arrillor is located in the Basque Country (43.0° Lat., -2.73° Long.). After a test excavation in 1959 that did not produce useful results, Andoni Saenz de Buruaga excavated a series of 21 levels containing Mousterian industries between 1989 and 1997[97,98].

The uppermost Mousterian assemblages are found in a unit derived primarily from cryoclastic action[98]. Level Lam is found above a rich Mousterian assemblage in Lmc, and beneath a

Magdalenian assemblage in La. Lam contains a few intrusive Upper Palaeolithic pieces[98]. Beneath this upper unit, levels Amk and Smk are found in thin, horizontal grey clay deposits within an archaeologically sterile sandy matrix[97,98].

The existing chronology of the site is based upon four stratigraphically consistent radiocarbon dates obtained by the ORAU on charcoal from a hearth in Amk using an acid base acid protocol ('ABA' referred to in the ORAU by the lab code ZR[1]), and small, unmodified bone fragments from Amk, Smk and Lmc[98]. The date from Lmc (OxA-6106, 37100 ± 1000 BP) places the uppermost Mousterian levels within the framework of the Middle to Upper Palaeolithic transition, whilst the three dates within the lower unit fall within the mid-40,000s BP. Although the dates are stratigraphically consistent, they should be viewed cautiously. Both bones from Amk and Smk were treated with an ABA protocol which is now known not to be the most reliable method of pretreating very old samples[2]. Their depleted $\delta^{13}C$ values and odd %C's indicate that the material dated may not have been derived from collagen (Table S18).

Cutmarked bones were selected from Lamc/Ala, Smk and Amk (Table S19). Squares close to the wall were avoided, as were those where the upper levels (Lamc/Ala) were affected by the 1959 excavation. Of 17 bones sampled, 9 contained >0.5 %N. Six of these, two from each level, were sampled for radiocarbon dating. In addition, the bone that yielded the youngest date from Lmc in the original study by Hoyos et al.[98] (OxA-6106) was redated.

With the exception of one bone (ARR12), all samples yielded more than 1% collagen, and all had acceptable isotopic and elemental compositions (Table S20). When ultrafiltered collagen from the bone previously measured in the 1990s was dated, it produced an age of 44,900 ± 2100 BP (OxA-21986), significantly older than the original result. Although the absence of a calibration curve in this period hinders comparisons, the published radiocarbon determinations from Smk and Amk do not appear to be significant underestimations when compared to the dates obtained after ultrafiltration.

Dates of the cutmarked bones confirm that Mousterian industries contained in the upper and middle units at Arrillor fall close to the limit of the radiocarbon dating method (Table S20). No modelling was undertaken for this site owing to the closeness of the measurements to the limit of the calibration curve, although the uppermost sample was included in the model for northwestern Iberia (see below).

Unit	Industry	Dates and analytical data									
		Sample type	OxA No.	Date BP	Error	Method	Treatment	Yield (mg)	Yield (%)	%C	$\delta^{13}C$ (‰)
Lam	Mousterian (possibly with some Upper Palaeolithic intrusions)										
Lmc	Mousterian	Bone	6106	37,100	1,000	AMS	Ion exchanged gelatin[99]	36.1	2.3	40	-19
Smk-I	Mousterian	(Burnt?) bone	6250	43,100	1,700	AMS	ABA	391	3	8.3	-24
Amk	Mousterian	Charcoal	6084	45,700	1,200	AMS	ABA	37	4.4	58.1	-23.8

Table S18: Published dates from Arrillor.[97,98,100] The units are arranged in stratigraphic order. ABA denotes an acid-base-acid treatment.

Sample ref	Species	Element	Modification	Level	Detailed sample location	%N
P6808	Indet.	Indet.	Sample taken from lab store, already crushed.	Lmc		0.9
ARR5	*Cervus elaphus*	Astragalus	Cutmarked	Lamc	AR. A'4(6). 15. Lamc. No. 564	1.4
ARR6	*Cervus elaphus*	Diaphysis fragment	Cutmarked	Lamc	AR. A'4. (6). 15. Lamc 568	1.1

ARR12	*Cervus elaphus*	Humerus diaphysis	Cutmarked	Smk	AR. A'5(4), 37, no. 1412.	0.5
ARR19	*Bovini*	Metapodial diaphysis	Cutmarked	Smkl-h	AR. B'1'(3) 23. 1094.	0.5
ARR17	*Cervus elaphus*	Femur diaphysis	Cutmarked	Amk	AR. A'3. 1176.	1.4
ARR18	*Cervus elaphus*	Tibia diaphysis	Cutmarked	Amk	AR. A'3 (5) 1334.	1.0
ARR1	Not Det.	Epiphysis	Cutmarked	Amk	AR, Amk, A'1, scd 1-9, P33-38. 20/08/97. No. 1030.	0.2
ARR2	Not Det.	Diaphsis	Cutmarked	Lamc	AR. Lamc. B'6. scd 4. P16. 17/9/91. No. 238	0.2
ARR3	Not Det.	Diaphisis	Cutmarked	Lamc/Ala	AR. Lamc/Ala. B'6. Scd. 4. P15. 17/9/91. no. 210	2.6
ARR4	Not Det.	Humerous diaphysis	Cutmarked	Lamc.Ala?	AR. Lamc/Ala? B'6. scd1. 15. 17.9.91. no.158	1.8
ARR9	*Cervus elaphus*	Metapodial	Cutmarked	Lamc	AR. A'3(5). 13+14. Lamc. No. 111	0.2
ARR10	*Bovini*	Femur Diaphysis	Cutmarked	Smk	AR. A'5(8), 38, No. 1842.	0.4
ARR11	*Cervus elaphus*	Metacarpal	Cutmarked	Smk	AR. A'3. 1158-1.	0.2
ARR13	*Bovini*	Humerous Diaphysis	Cutmarked	Smk	AR. B'5, 3594.	0.3
ARR14	*Bovini*	Tibia Diaphysis	Cutmarked	Smk	AR. B'5. 2105.	0.3
ARR15	*Cervus elaphus*	Diaphysis	Cutmarked	Smkq	AR. A'4(4) 38. 1571.	1.1
ARR16	*Cervus elaphus*	Tibia Diaphysis	Cutmarked	Smk	B'4. 1157-7.	0.1

Table S19: details of samples selected for %N and AMS dating from Arrillor.

Sample ref	Context	Treat-ment	OxA	Date BP	Error	Yield (mg)	Yield (%)	%C	$\delta^{13}C$ (‰)	$\delta^{15}N$ (‰)	C:N	Comment
P6808	Lmc	AF	21,986	44,900	2,100	8.42	1.5	37.4	-19.5	6.1	3.2	*cf.* 37,000 ±

												1,000 BP (OxA -6,106)
ARR5	Lamc	AF	22,654	>46,800		42.44	4.2	41.9	-20.7	3.8	3.2	
ARR6	Lamc	AF	22,655	45,600	2,300	35.55	4.0	42.6	-20.9	2.2	3.2	
ARR12	Smk	AF	failed			5.31	0.7					Failed on low % yield
ARR19	Smkl-h	AF	22,658	45,600	2,300	12.59	1.2	41.9	-23.2	2.9	3.2	
ARR17	Amk	AF	22,656	48,500	3,200	15.09	2.7	42.8	-20.7	4.7	3.2	
ARR18	Amk	AF	22,657	>45,200		39	3.9	42.6	-19.8	3.2	3.2	

Table S20: New radiocarbon determinations from the site of Arrillor obtained by Wood[83].

Lezetxiki

Excavations in the karstic tube of Lezetxiki (43.07° Lat., -2.52° Long.), Garagartza, Basque Country) were first carried out by José M. Barandiarán between 1956 and 1968[101]. Modern excavations by Alvaro Arrizabalaga have been undertaken since 1996 in the southern part of the site[102, 103]. The lithic assemblages from levels IVc and IVa, but particularly level IIIa of Barandiarán's excavations, have been extensively studied because they contain a lithic industry with elements resembling those from both the Middle and the Upper Palaeolithic. For example, 90% of the 381 formal tools from IIIa were considered Mousterian by Baldeón[104], with sidecrapers dominating the assemblage. The remaining 10% were considered Aurignacian, being dominated by endscrapers on both flakes and blades, whilst pyramidal and centripetal bladelet cores are also present. Two teeth, likely to be Neanderthal, were found at the base of level IIIa[105] whilst marine and freshwater shells have been uncovered in the most recent excavations of both IIIa and IVc[103]. The assemblage from IIIa has been ascribed to the Mousterian (Freeman and Bernaldo de Quirós, in Ref 102), the Aurignacian[106,107], a mixture of Middle and Upper Palaeolithic industries[104], and the Transitional Aurignacian[108].

Two attempts at radiocarbon dating level IIIa have been unable to clarify this situation[109,110] (Table S21). At less than 20 ka BP, both measurements were considered aberrant when originally published. Altuna (Ref 109, p. 410) thought that the area where the first sample was found may have been disturbed by roots, after excavation in a neighbouring sector. Arrizabalaga et al.[102] suggested that chemical contamination is more likely to have caused the underestimation in both cases.

Twenty-five unmodified ungulate bone fragments from the base of IIIa of Barandiaran's excavation (1966-68) were screened for %N. These were selected by Alvaro Arrizabalaga (Universidad de País Vasco) as part of a project lead by Maroto et al.[85]. The bones selected were most likely to derive from the base of level IIIa.

Only eight bones found in band A closest to the shelter contained more than 0.5%N. Of these, five were selected for radiocarbon dating. Three were found at a depth of -490 cm in square 16A, close to the Neanderthal remains recovered from depths -488 and -505 cm in the same square, and provide an opportunity to examine the consistency in the age of samples recovered from a relatively small area. To examine whether any horizontal variation in age exists, a two further samples from

the base of IIIa in square 10A were selected. Isotopic and elemental data highlight no major problems in the collagen aliquots dated. More than 5mg of collagen was extracted from each bone dated which, in all but one case (OxA-21715), was equivalent to a yield of more than 1%.

Although the dates from level IIIa are consistent with an attribution to the Middle to Upper Palaeolithic transition, they range in age by over 20 ka ^{14}C years (Table S22). Particularly interesting is the cluster of three dates found close to the Neanderthal teeth in square 16A, two of which are infinite in age whilst the other is more consistent with the age of the Early Aurignacian at, for example, Labeko Koba. The two samples from square 10A are in agreement with each other, but even younger at around 34,000 cal BP.

Level IIIa slopes strongly along N – S and W– E axes, and it is possible that the early excavation did not cleanly separate the two units and that bone from the underlying, archaeologically sterile IIIb was dated. Despite this, the dates (Table S22) strongly support the hypothesis that level IIIa may include Aurignacian elements. For this reason the site cannot be used to examine the chronology of the final Neanderthals.

Context	Lab number	Date BP	Error	Method	Reference
IIIa (square E24, depth -462cm)	GrA-11505	8350	70	AMS	(Falguères et al., 2005)[110]
IIIa	I-6144	19340	780	Conventional C14	(Altuna, 1972)[109]

Table S21: Published radiocarbon dates on bone from level IIIa of Lezetxiki. No further information on sample chemistry is available.

OxA no.	Context	Date BP	Error	Yield (mg)	Yield (%)	%C	δ^{13}C (‰)	δ^{15}N (‰)	C:N
21715	Level IIIa, square 16A, z -490cm	>46,500		5.7	0.60	43.0	-18.8	9.6	3.4
21837	Level IIIa, square 16A, z -490cm	34,550	600	32.1	4.58	45.1	-19.2	5.9	3.3
22627	Level IIIa, square 16A, z -490cm	>46,700		15.3	1.00	39.9	-22.6	3.6	3.3
22021	Level III, square 10A, z -420cm	29,250	320	29.5	3.00	40.1	-18.2	4.7	2.9

21838	Level III, square 10A, z -420cm	30,830	380	42.5	5.38	45.3	-18.8	4.3	3.3

Table S22: New radiocarbon dates on unmodified, cf. *Bos* rib and diaphyseal bone fragments from level III of Lezetxiki[85].

La Viña

Located in Manzaneda, Asturias (43.18° Lat., -5.49° Long.), La Viña is a site that was excavated between 1979-1998 by the late Javier Fortea and his team. They uncovered a sequence spanning the Mousterian to the Magdalenian in two different areas of the site. The western sector contains the longest sequence. Here, level XIII basal contains the uppermost Mousterian industry. In levels XIII(inf.) to XI, Aurignacian remains were found, and above this, in X to VII, Gravettian assemblages are evident. It seems clear that there was a powerful erosive event between levels XIII basal and Level III. In some areas Level XIII material was completely removed through this process.

Previous samples have been dated from level XIII basal by the Gif-sur-Yvette lab. These range between 37,700 ± 590 to 48,100 ± 1600 BP, and include one greater than age. Chronometric work at the site focused initially on bone material, but we found that the overall preservation state was poor in the Mousterian and Aurignacian contexts. None of the four samples from the uppermost Mousterian in level XIII basal contained sufficient nitrogen to proceed with collagen extraction. Therefore, we also obtained two charcoal samples from the site, both from XIII basal, although one failed in pretreatment due to low %C. The other sample was dated with both ABOx-SC and ABA methods, producing ages of >62,000 BP (OxA-19144; Table S23) and >59,000 BP respectively (OxA-19196). These results were obtained before the laboratory combustion background was reassessed[9], as such, a more reasonable estimate of their age is >c.55, 000 BP. These results suggest that the material from XIII basal is beyond the radiocarbon limit.

OxA	Treatment	Species	Date (BP)	Used (mg)	Yield (mg)	Yield (%)	%C	$\delta^{13}C$ (‰)
19144	ABOX-SC	*Quercus* sp	>59300	111.56	1.87	1.7	65.2	-22.7
19196	ABA	*Quercus* sp.	>62000	38.59	7.17	18.6	66.2	-23.5

Table S23: Two dates have been obtained on a single fragment of charcoal from the XIII basal level at La Viña, one ABOX result and one using an ABA protocol.

Cueva Morin

Cueva Morín is in Villanueva de Villaescusa, Cantabria (4.32° Lat., -3.51° Long.). Excavations in the early 19th century (described in Maíllo Fernández[111]), between 1966-1969 González Echegaray and Freeman[112,113] and by Maíllo-Fernández in 2005 revealed a sequence of Mousterian to Azilian industries. Level 11 contains the uppermost Mousterian, 10 a Châtelperronian industry, 9 and 8 the Proto-Aurignacian, and 7 and 6 Early Aurignacian industries. The integrity of the Châtelperronian and lowest Proto-Aurignacian levels has, however, been questioned. Laville and Hoyos[114] have suggested that that level 10 corresponds to the soliflucted and cryoturbated contact zone between level 11 (Mousterian) and level 9 (Proto- Aurignacian) and Zilhão[82] has raised the additional possibility that imprecise excavation of both levels may have yielded additional uncertainty. The recent excavation works by J-M. Maíllo-Fernández in 2005, however, have demonstrated that the deposition of levels 11-8 was the result of a low-energy process and not due to solifluction or cryoturbation. Both are ruled out by sedimentological analyses. The morphology of the level profiles, especially that of level 10, is the result of a deformation process due to loading. In terms of the integrity of the lithic collections, these cannot be called into question, except perhaps in the case of level 9 (Proto-Aurignacian), where two sub-levels may have gone unnoticed during the 1966-69 excavations.

Leaving the pre-1980s conventional radiocarbon dates to one side there are two charcoal measurements, sampled from the 1960s excavation section available from levels 8 (Proto-Aurignacian, GifA-96263 36,590 ± 770 BP) and 11 (final Mousterian, GifA-96264 39,770 ± 730 BP)[115]. Levels 9 and 10 also have dates on charcoal samples obtained from the section wall, although these seem somewhat anomalous (GrA-33891 33,430 + 250/-230 BP and GrA-33823 29,380 + 260/-240 BP respectively)[85]. Whilst the date from level 9 was produced using an ABA protocol, the charcoal from level 10 was so poorly preserved it was only given an acid wash and contained only 24.0% carbon. Another level 11 charcoal fragment, also recovered from the remaining wall, was dated at ORAU on behalf of Maroto et al.[85] using both an ABA protocol and an ABOx-SC protocol to assess whether the ABA was able to effectively remove contaminants from charcoal at the site (see Table S24). The ABOx-SC treatment produced a slightly older date (OxA-19459 43,600 ± 600 BP) than the ABA treatment (OxA-19083 41,800 ± 450 BP) (chi-squared test; df=1,T=6.0 χ^2=3.8, 5%)), suggesting that the previous dates may be underestimates of the real age of the deposit.

It was hoped that dating of modified bones from the 1960s excavations would test the accuracy of the dates currently available for the transitional layers and identify whether the Châtelperronian and deepest Proto-Aurignacian levels were disturbed. Fauna was relatively scarce in levels 10 to 8[112,113], and from the outset these aims were regarded as ambitious.

Faunal remains were examined with J.M. Maíllo Fernández at the Museo Regional de Prehistoria y Arqueologia de Cantabria in 2009. Material from four squares at the cave entrance (I-II, A-B) was sampled (Table S25). This area contains all the stratigraphic units mentioned above, and is well away from an area that contains evidence of an intermittent stream. No faunal remains were found from levels 12, 11 or 9 in the collections. Of the fauna examined, surface preservation was extremely poor meaning cut-marks were not preserved. Three of four bones from the Châtelperronian in level 10 contained more than 1% nitrogen. We attempted to extract collagen from two, but neither contained enough to date.

No chronological model has been built for the site, because we are only confident in the accuracy of a single date. Moreover, this date is on a sample of charcoal that is not strongly association with human activity.

OxA	Level	Species	Treat.	^{14}C age (BP)	Error	Yield (mg)	Yield (%)	%C	δ^{13}C (‰)
19083	11	*Quercus* sp.	ABA	41,800	450	5.3	25.3	56.2	–25.2
19459			ABOx-SC	43,600	600	9.04	14.3	84.5	-24.2

Table S24: The effect of ABOx-SC and ABA pretreatments on a single fragment of charcoal from level 11 taken from the 1960s excavation section wall at Cueva Morín[85].

Sample ref.	Species	Context	%N	C:N	Yield (mg)	Yield (%)
MO4	Indet. diaphysis	level 10	0.1	2.0		
MO5	Indet. metapodial diaphisis	level 10	1.1	4.2		
MO6	Indet. diaphysis	level 10	1.8	3.8	2.0	0.3
MO7	Indet. diaphysis	level 10	1.1	4.5	0.6	0.1

Table S25: Percent nitrogen, C:N ratios and collagen yields for bones sampled from level 10 at Cueva Morín.

Esquilleu

Esquilleu, near Castro-Cillórigo (43.22° Lat., -4.60° Long.) in Cantabria, contains a long sequence of units containing Middle Palaeolithic industries[116]. Initial dates suggested that material in the uppermost units were exceptionally late, with a date of 30,250 +500/-430 BP (GrA-35065) on charcoal from level V, a date of 22,840 +280/-250 (GrA-35064) on charcoal from level IV[85] and a date of 12,050 ± 130 BP (AA-29664) on bone from level III[116]. To test this chronology, on behalf of a project undertaken by Maroto et al.[85], we obtained ABOx-SC dates from the deeper units that are particularly rich in charcoal. We also dated small fragments of unmodified bones from the uppermost Mousterian units (levels III and VI).

One charcoal fragment from level XIX was dated with ABA and ABOx-SC. The ABA treatment was not sufficient to remove contamination and resulted in a date more than 10,000 ^{14}C years too young (Table S26). Another four dates on charcoal fragments treated with ABOx-SC from these deeper layers are also beyond or close to the laboratory background. This suggests that all dates on charcoal not treated with ABOx-SC should be treated cautiously. This includes the two dates from V and IV that were fragile and treated only with an acid wash.

Two duplicate dates on a bone from level VI gave statistically indistinguishable results (df=1 T=0.0 (5% χ^2 =3.8)), placing the age of the unit close to the limit of the radiocarbon method. In contrast, two bones from level III suggest that this unit was formed during the Last Glacial Maximum (LGM). Whilst Baena et al.[117] maintain that the industry is Middle Palaeolithic, Maroto et al.[85] have been more cautious. They suggest that the lack of Upper Palaeolithic tool types from level III within an assemblage characterized by expedient flake-based reduction methods on local raw materials

may not be enough to assign the assemblage to the Middle Palaeolithic. Alternatively, it is possible that the bones were intrusive because the samples dated were small and unidentified fragments without human modification. Levels IV to V do not have any dates on rigorously cleaned material, but according to Baena et al.[116] they contain similar industries to level III. Ongoing work at the site should confirm the age and nature of assemblages within levels V - III.

OxA	Sample type	Context	Method	Date BP	Error	Yield (mg)	Yield (%)	$\delta^{13}C$ (‰)	%C	C:N
19967	Bone	III	Ultrafiltration	19300	100	45.7	5.1	-19.2	46.9	3.4
19968			Ultrafiltration	19310	80	40.1	4.8	-19.3	49.1	3.4
19246	Bone	IIIB	Ultrafiltration	20810	110	14.7	2.1	-19.4	44.7	3.3
19965	Bone	ESQ-06, level VI, square F12	Ultrafiltration	43700	1400	12.1	1.3	-19.1	46.2	3.4
19966			Ultrafiltration	44100	1300	13.5	1.4	-19.2	44.4	3.4
19085	Charcoal	XIX	ABA	39280	340	5.2	10.4	-23.5	60.0	na
19086			ABOX-SC	>54600		6.3	5.0	-23.0	62.9	na
20318	Charcoal	ESQ. 05, level XVII	ABOX-SC	53400	1300	9.1		-25.0	71.9	na
20319	*Pinus tipus sylvestris*	ESQ. 05, level XVII	ABOX-SC	>58500		9.5		-22.4	73.8	na
20320	Charcoal	ESQ. 05, level XVII	ABOX-SC	52600	1200	8.7		-23.2	36.8	na
20321	Charcoal	ESQ. 05, level XXI-I	ABOX-SC	>59600		11.0		-22.4	68.3	na

Table S26: Radiocarbon dates from Esquilleu[85] obtained using ultrafiltration and ABOx-SC protocols, compared to the ABA protocol applied to charcoal at ORAU. See the caption for Table S2 for descriptions of the analytical parameters described here.

La Güelga

La Güelga cave is in the same valley as El Sidrón, in Asturias (43.2º Lat., -5.53º Long.), and has been excavated since 1989 by Mario Menéndez-Fernández[118,119,120]. The deposits within excavation area D containing the Late Pleistocene deposits are still under study, and interpretations of the archaeological assemblages are currently only preliminary. Menéndez-Fernández et al.[118,119] suggested that a Châtelperronian industry may have been present based on some very young radiocarbon dates on bone (e.g. Beta-186766, 29,020 ± 260 BP) and the presence of backed knives and degraded bone fragments interpreted as artefacts. This came from within a lithic industry that was otherwise Middle Palaeolithic. In collaboration with projects led by Menéndez-Fernández et al.[120] and Maroto et al.[85] the ORAU dated a series of long bone fragments from a unit containing the Châtelperronian/ Middle Palaeolithic industry (zone D exterior, level 4B) and a unit containing the Mousterian (zone D interior, level 9) (Table S27). The dates fell towards the limit of the radiocarbon dating technique at the ORAU, suggesting that the industry in both levels is more likely to be Middle Palaeolithic. We also report a single determination from the Level 2 inferred Châtelperronian phase obtained using a similar pretreatment protocol by the Cologne radiocarbon dating laboratory. It is interesting to note that in the 4b level, but outside Zone D, there is a Neanderthal premolar tooth.

OxA	Context	Date (BP)	Error	Yield (mg)	Yield (%)	%C	$\delta^{13}C$ (‰)	$\delta^{15}N$ (‰)	C:N
27958	Zona D, Interior sector, Level 2 (Châtelperronian?)	40,300	1200	22.1	3.6	44.3	-20.5	6.5	3.1
19244	Zona D, Interior sector, Level 9	43,700	800	26.4	2.5	44.0	-19.0	5.4	3.3
19245		44,300	1200	15.1	1.7	45.1	-19.0	5.4	3.3
20122	Zona D, Exterior sector, Level 4B	47,400	2700	9.5	1.6	42.1	-20.5	4.6	3.2
20123	Zona D, Exterior sector, Level 4B	>43,200		4.6	0.8	43.8	-19.8	3.9	3.2
20124	Zona D, Exterior sector, Level 4B	48,500	3500	8.2	1.3	46.5	-19.1	2.6	3.2
20125	Zona D, Exterior sector, Level 4B	> 43,600		4.0	0.7	44.5	-19.5	5.1	3.2

Table S27: Radiocarbon dates on ultrafiltered collagen from unmodified diaphysis bone fragments from Middle Palaeolithic contexts at La Güelga. See Table S2 caption for analytical details.

Northwestern Iberia summary

Due to the low number of finite dates associated with the Mousterian in northern Iberia, a chronological model for the region was constructed with data from Arrillor, Cueva Morín, Esquilleu and La Güelga. Finite radiocarbon dates were grouped into a single 'final Mousterian' `phase`. In this model (Figure S11) the `date` range of this final Mousterian was 48,130-46,010 cal BP, and the `boundary` delimiting the end of the Mousterian is 47,880-44,820 cal BP (at 95.4% prob.). It is important to note the strong possibility that the latest Mousterian in the northwest of the Iberian peninsula has not yet been dated.

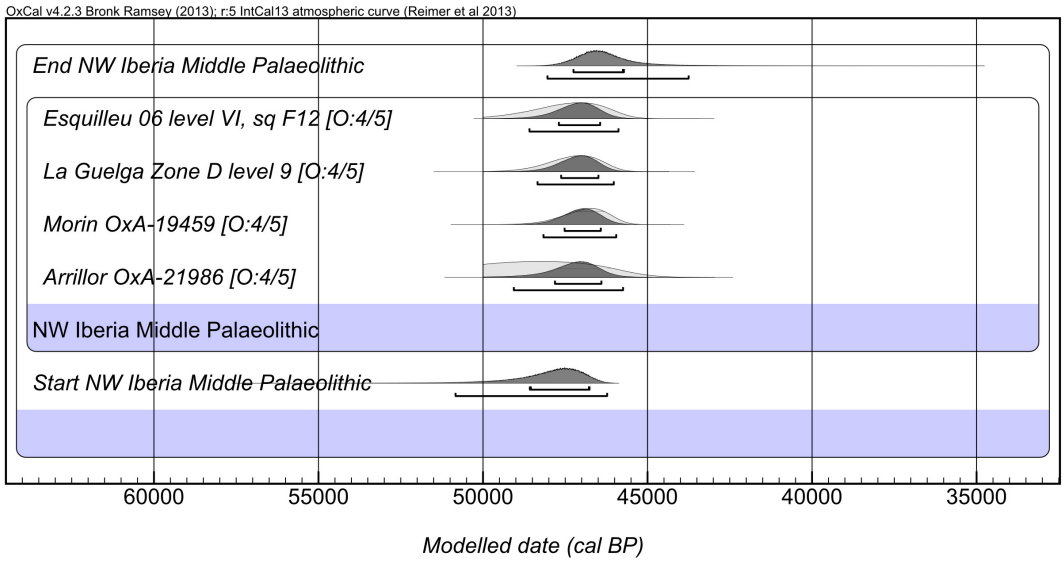

Figure S11: Bayesian age model for final Mousterian sites from NW Spain (after Wood et al.)[121].

Jarama VI

The rock shelter of Jarama VI is located in the Jarama valley, central Spain (40.56° Lat., -3.19° Long.). Excavations between 1989 and 1993[122] uncovered 3 units. The industry in level 1 has recently been identified as Mousterian[123], as have the assemblages in levels 2.1, 2.2 and 3[122], and a metatarsal, tentatively identified as Neanderthal[124] was recovered from level 2.2.

Charcoal has been conventionally dated from level 2.1 (29,500 ± 2700: BP Beta-56638), 2.2 (32,600 ± 1800 BP: Beta-56639), and a burrow, initially thought to relate to level 1 (23,380 ± 500 BP: Beta-56640)[122]. The site is of particular importance for discussions surrounding the late survival of Neanderthals in southern Iberia because of the statistical agreement between the two dates from level 2 and because the sample from level 2.2 was found in a hearth and so is securely associated with human activity[82,125].

We screened 30 cut-marked bones using the %N approach, of which 7 contained >0.5%N. Three samples were dated from levels 1, 2.2 and 3 (Tables S28 and S29)[83,126]. Despite the relatively low collagen yields, two samples produced dates that were beyond the limit of radiocarbon, whilst the third was extremely close to the laboratory background with an standard error of 3700 ^{14}C years, and therefore is also likely to date beyond the limit of radiocarbon. These new radiocarbon dates are now supported by infrared stimulated luminescence (IRSL) of potassium-rich feldspars[123]. The site does not, therefore, contain evidence for a late, post-42 ka cal BP, Neanderthal occupation, instead it is more likely to date to ~50,000 cal BP or older. For this reason we undertook no modeling or calibration of the results from the site.

Sample ref	Species	Element	Modification	Context
JA-6	Indet.	Diaphysis fragment	Cutmarked	Level 1
JA-15	Indet.	Diaphysis fragment	Cutmarked	Level 2.2
JA-18	Indet.	Diaphysis fragment	Cutmarked	Level 3

Table S28: Samples selected for dating from Jarama VI (see Wood et al.[126]).

Sample ref	OxA	Date BP	Error	Treatment	Yield (mg)	Yield (%)	%C	$\delta^{13}C$ (‰)	$\delta^{15}N$ (‰)	C:N	Comment
JA-6	21,714	> 50,200		AF	14.03	1.4	46.9	-19.3	9.5	3.4	
JA-15	X-2,310-22	49,400	3,700	AF	5.42	0.5	43.2	-18.2	7	3.2	Low % yield
JA-18	X-22,90-56	> 47,000		AF	7.38	0.7	45.3	-18.8	10.3	3.3	Low % yield

Table S29: Radiocarbon dates on ultrafiltered bone collagen from Jarama VI (Wood et al. [126]).

Zafarraya

Zafarraya is an important Palaeolithic cave site in Andalucía (36.57° Lat., -4.07° Long.). It was excavated between 1981-1983 and 1990-1994[127], yielding a collection of cut-marked and burned Neanderthal fossils that were initially dated by radiocarbon and U-Series on associated *Capra pyrenaica* (ibex) bone to <42 ka cal BP[128]. Further U-Series, ESR, AAR and radiocarbon dating on *Capra pyrenaica* bone and gamma spectroscopy U-Series dating on a Neanderthal mandible showed the techniques were inaccurate, producing dates ranging over tens of thousands of years on individual *Capra pyrenaica* mandibles[129,130,131]. Many of the techniques used were similar to those published by Hublin et al.[128], casting the late Neanderthal dates into doubt. However, the site continued to be regarded as potentially 'late' by some[125].

Unfortunately it was not possible to directly date the key Zafarraya Neanderthal fossils in our project, despite best attempts. We expected that collagen preservation would be low, but this issue was complicated by the fact that poly-vinyl acetate (PVA) had been applied to many of the bones to conserve them (Higham pers. obs. 2007). We sampled the complete Neanderthal mandible (Z2) and a femur (Z1) in 2006 in the Archaeological Museum of Malaga and tested the amount of collagen likely remaining through a % nitrogen test. These bones come from square Q17 in the Sala del Entrada at Zafarraya. The Z2 mandible sample was obtained by a keyhole drilling through the empty cavity of the M_3. The sample yielded a %N value of 0.01%, whilst the Z1 femur yielded 0.05%. These values are markedly below the minimum values to proceed with fuller pretreatment chemistry. At the time we attempted a simple gelatinisation pretreatment, but recovered no collagen.

We also attempted to date samples of other human bone previously excavated from the site and housed in Lucena. These originate from disturbed areas of the site and were dated to independently determine their age. The bones analysed included samples Z8 (a modern human bone), Z7 (hemi-mandible of a modern human), Z19 (Neanderthal rt. 7th rib), Z21 (a hemi-mandible of a modern human), Z17 (Neanderthal pubic bone) and Z22 (initially assumed to be a Neanderthal humerus fragment). We tested each bone sample for %N analysis and the results were mixed (Z8 – 0.66%, Z7 – 2.14%, Z19 – 0.12%, Z21 – 0.95%, Z17 – 0.32% and Z22 – 0.91%). Again, these bones were not *in situ*, they were found in an upper deposit mixed with ceramic materials of Neolithic, Medieval and modern periods. We dated the three higher %N yielding samples and obtained 3 AMS dates that correspond to the Neolithic period (Z7 – 6596 ± 37 BP (OxA-16414), Z21 – 6480 ±

36 BP (OxA-16415) and Z22 6594 ± 36 BP (OxA-16416). Bone from the site was treated during excavation with PVA or Paraloid B72 and to account for this we included a solvent extraction prior to full bone pretreatment. These consolidants are ^{14}C free and therefore likely not to be a significant factor in explaining these younger dates.

Occupation at Zafarraya was sporadic and brief, and cutmarked bones are correspondingly scarce, so unmodified *Capra pyrenaica* bone was sampled as part of this study. One of the bones dated by Michel et al.[130] to 33,300 ± 1200 BP (OxA-8999) was redated by Wood[83] and Wood et al.[126] to >46,700 BP (OxA-23198). Of 15 unmodified *Capra pyrenaica* bones screened for %N, 5 contained enough to attempt collagen extraction, and 2 contained sufficient collagen (1% yield) to obtain a date (Tables S30 and S31). One produced a result beyond the limit of radiocarbon dating and the other was close to the laboratory background[83,126]. The unmodified *Capra pyrenaica* bones were found in the Sala del Entrada close to, and either within or above the main cluster of Neanderthal fossils around a hearth. The results, therefore, suggest strongly that the Neanderthal fossils fall beyond the limit of the radiocarbon dating method, although direct dating would be the only means to confirm this and as mentioned above, this is not possible with radiocarbon. What these dates do show, however, is that the late radiocarbon dates on ibex bone were inaccurate. This allows us to remove, with confidence, the remaining evidence for a post-42 ka cal BP Neanderthal occupation. Reanalysis of the dataset produced by Michel et al.[129, 130,131] has reached a similar conclusion[132].

Sample ref	Context	Species	Element
ZAF2	Q15, Depth 201 cm	*Capra*	Phalange
ZAF7	Q18, Ensemble D(Sm), Depth 222 cm	*Capra ibex*	Phalange
ZAF32	P20, Depth 170 cm	*Capra pyrenaica*	Metatarsal
ZAF3	Q15, Depth 202.5 cm	Indet.	Diaphysis fragment
ZAF8	Q18, Ensemble D(Sm), Depth 224.4 cm	*Capra ibex*	Astragalus

Table S30: Samples selected for radiocarbon dating from Zafarraya by Wood et al.[126]

Sample ref	Treatment	OxA	Date (BP)	Error	Yield (mg)	Yield (%)	%C	$\delta^{13}C$ (‰)	$\delta^{15}N$ (‰)	C:N	Comment
ZAF2	AF	21810	46,300	2,500	21.26	2	44.6	-19.7	7	3.3	
ZAF7	AF*	21813	> 49,300		13.82	1.4	44.3	-18.9	5	3.4	
ZAF32	AF	23198	> 46,700		62.06	5.4	44.5	-18.9	4.6	3.3	*cf.* 33,300 ± 1200 (OxA-8999)
ZAF3	AF*				2.22	0.3					Fail on low yield
ZAF8	AF				0.74	0.1					Fail on low yield

Table S31: Radiocarbon dates on ultrafiltered bone collagen from Zafarraya (Wood et al.[126]).

Southern Iberia summary

As described above, we attempted to date several sites containing Middle Palaeolithic and Neanderthal assemblages from southern Iberia, defined as south of the 'Ebro Frontier'[82,83,126]. Preservation of bone in this region is particularly poor, and only two sites, Jarama VI and Zafarraya, could be reliably dated. Charcoal from a further site, Cueva Anton, Murcia was dated in collaboration with Zilhão et al.[133]. For discussion of sites that contained bones and or charcoal too poorly preserved to date, the reader is referred to the Supplementary Methods selection of Wood et al.[126] A summary of the sites examined in given here in Table S32. Taken together, there is no robust chronometric evidence, as yet, for late survival of Neanderthals south of the Ebro frontier. Further work may elucidate this.

Site	Location	Contexts sampled	Reason samples were not dated
El Niño	Ayna, Albacete	Middle Palaeolithic; Trench 2, layers 7.4, 7.2, 7.1, 6, 5. 1973 excavation season.	23 bones contained <0.5% N and were considered undatable.
Quebrada	Chelva, Valencia	Middle Palaeolithic; Spits 6, 5 and 2. 2006 – 2007 excavation season.	9 bones contained <0.5% N and were considered undatable.
El Salt	Alcoy, Alicante	Middle Palaeolithic; Units VIII – lower V.	8 of 40 bones selected contained >0.5% N, including one Neanderthal tooth from layer V. Collagen extraction was attempted for three bones and the tooth, but collagen yields were too low for dating.
Sima de las Palomas	Torre Pacheco, Murcia	Neanderthal; Metatarsal SP07200.	%N was <0.5% N and was considered undatable.
Gorham's Cave	Gibraltar	Middle Palaeolithic; 1995-8 Natural History Museum and 2007-ongoing Gibraltar Museum excavations.	49 cut-marked bones were selected but contained <0.5% N and were considered undatable.

Table S32: Middle Palaeolithic sites that did not contain datable bone and/or charcoal examined from southern Iberia. For full descriptions see Wood et al.[126]

Germany

Geissenklösterle

Geißenklösterle is a site in the Ach Valley, in the Swabian Jura of Germany (48.39° Lat., 9.78° Long.). It comprises a sequence of archaeological levels spanning the Middle Palaeolithic to the Magdalenian, divided into a series of 19 geological horizons (GH), and 5 archaeological horizons (AH, numbered I to V). The latter lie within the geological horizons. There are further AH sub-units. The key AH IV is the uppermost Mousterian horizon, and AH III and II comprise the Lower and Upper Aurignacian respectively. Hahn[134] originally attributed the AH III lithic corpus to the Proto-Aurignacian, but both horizons are now considered to be Early Aurignacian[135,136].

Conard and Bolus[135,137] have published more than 80 radiocarbon determinations of bone dated in several laboratories in an attempt to build a coherent chonometric sequence and test the integrity of the stratigraphic sequence at the site. Some of the initial radiocarbon results from the Aurignacian horizons of the site were very early, between ~36-40 ka BP. ESR and TL dates obtained by Richter *et al*.[138] also supported a very early date for some for these levels. These ages have formed the basis of the Danube Corridor and *Kulturpumpe* hypotheses[139,140].

The uppermost Mousterian levels at the site were previously dated by 12 AMS determinations reported by Conard and Bolus[137]. It is clear now that the majority of these determinations underestimated the real age of these levels. This is evident when one considers two determinations from the sterile level III at the site that we dated in Oxford using ultrafiltration and which produced results of 39,400 ± 1100 BP (OxA-21657) and 38,300 ± 900 BP (OxA-21658)[141]. Previously these two bones had been dated at 33 ka BP and 32 ka BP respectively in Oxford. Considerably older ages resulted with new dating, which we attribute at least in part to the additional ultrafiltration preparation applied, to improved instrumentation and background corrections and to problems with previous determinations. These results suggest that material below sterile level III ought to be older than the age of these two bones, unless there are grounds to suggest significant post-depositional movement of material. The radiocarbon dates are shown in Table S33.

OxA	Context/Level	Species and material dated	Date BP	error	Used (mg)	Yield (mg)	Yield (%)	%C	$\delta^{13}C$ (‰)	C:N	Comments
21657	GK 57 IIIc 2430	*Cervus elaphus*, tibia, no human modification	39400	1100	480	20.4	4.2	43.9	-19.4	3.1	*cf.* OxA-6076 (33600±1900)
21658	GK 57 IIIc 2389	*Capra ibex*, left tibia, no human modification	38300	900	420	12.6	3	44.2	-18.3	3.1	*cf.* OxA-6077 (32050±600)
21720	GK 78 IV 1495	*cf. Ursus spelaeus* juvenile shaft fragment. Possible impact.	35500	650	640	14	2.2	46.9	-20.7	3.3	*cf.* KIA19556 (37780+520/-490).
21741	GK 48 VII 456	*Capra ibex*, phalanx I, which articulates with metataurus. No clear cutmarks although two are inferred.	48600	3200	478	38.86	8.1	48.3	-18.7	3.3	

Table S33: Radiocarbon determinations from Mousterian and pre-Aurignacian contexts at the Geiβenklösterle. See caption to Table 2 for details of the analytical parameters. Data previously published in Ref. 141. OxA-21657 and OxA-21658 are from the sterile level that seals the uppermost Mousterian level (AH IV) at the site.

We built a Bayesian model for the lower part of the site's sequence and anchored the older end using the date of a bone from AHVII, which was 48,600 ± 3200 BP (OxA-21741). This date is out of range in calendar terms and a distribution is plotted that essentially forms the equivalent of a calendar range of the radiocarbon age and error term. The new sequence, with the ultrafiltered determinations, is shown in Figure S12. The age range (`date`) we determined for the Mousterian levels was 45,050-41,950 cal BP (95%). The final `boundary` for the last Mousterian was 43,860-41,600 cal BP.

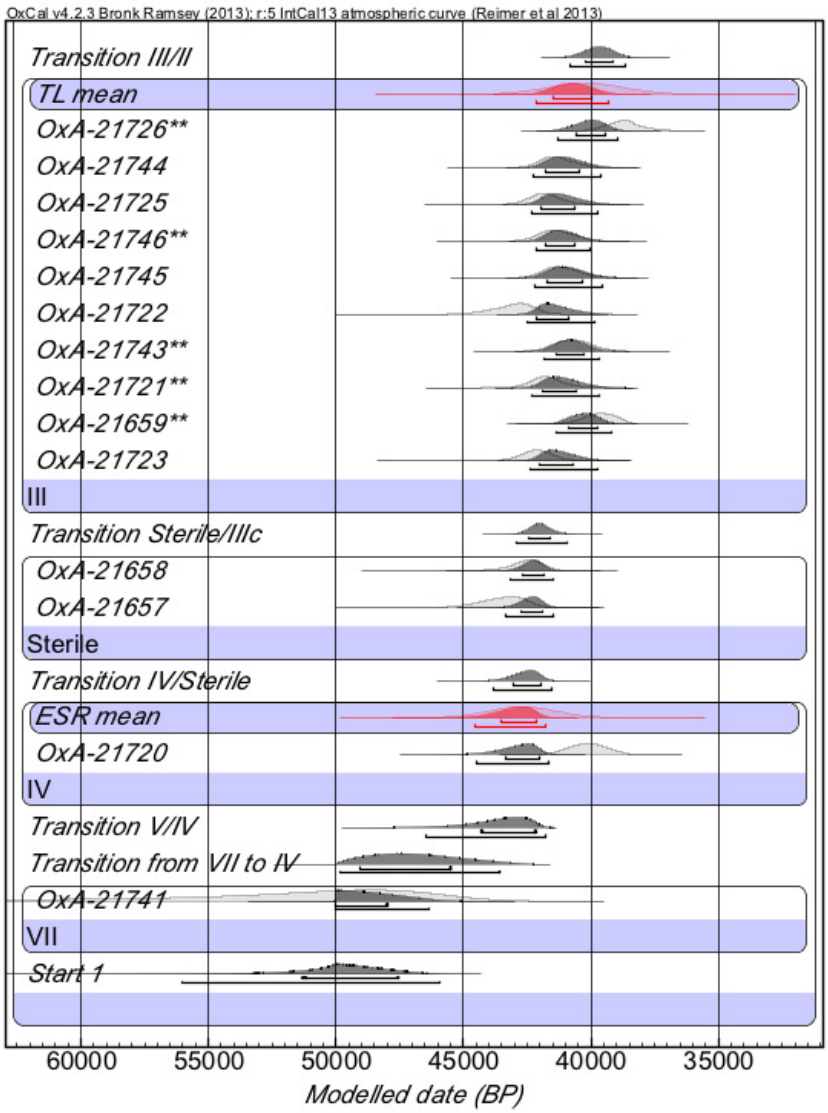

Figure S12: Bayesian age model for the lower horizons of the Geissenklösterle. See text for details and ref 141 for the data in the model. Red outlined probability distributions are non-radiocarbon measurements; a TL burnt flint weighted average and ESR mean dates of teeth respectively[138]. Note the close agreement between the radiocarbon determinations and these measurements. Asterisked samples in AHIII are ones included in the modelling. Those without denote results that are downweighted completely due to the fact that they are not humanly modified bones, rather they were selected for dating to test previously measured results from the chronological data obtained by

Conard and colleagues[137]. There is a marginal shift in the posterior probability distribution of the key boundaries in the model when all of the dates are included (see Higham et al.[141]).

Italy

Grotta del Cavallo

Grotta del Cavallo (40.15° Lat., 17.96° Long.) is situated on the rocky coast of the Bay of Uluzzo, Nardò, in Apulia. The site is located 15m above the present day shore, with a large, 5m wide by 2.5 m high opening facing NW and an approximately circular shaped gallery, about 9 m in diameter. Cavallo was discovered in 1960 and investigated in 1961 by A. Palma di Cesnola. Official excavations took place between 1963–1966[142,143,144], and again between 1986–2008, the latter focusing on the Mousterian parts of the sequence[145,146]. In the interlude between the two series of excavations, looters severely disturbed the central part of the deposits, removing most of the Upper Palaeolithic layers and the freshly exposed Uluzzian layers. Salvage excavations were conducted by the University of Siena (Paolo Gambassini and team) for four seasons in the late 1970s/early 1980s in order for a metal gate to be installed at the entrance of the cave. The surviving sections were cleaned and some free-standing deposits at the entrance of the cave were excavated and correlated to the original stratigraphy. A correlation is given in Benazzi et al.[167]

The site preserves a long stratigraphic succession comprising about 7 m of archaeological deposits directly based on a marine interglacial beach conglomerate (layer O). The archaeological sequence of Cavallo is dominated by Middle Palaeolithic layers (N-F I), capped by a thin layer of green volcanic ash (Fα), which separates Mousterian from the overlying Uluzzian layers (E III- EII - EII/I- DIb)[174]. The Uluzzian deposits, about 80-85 cm thick, were excavated both in the 1960s and in the late 1970s/early 1980s in separate sections of the site. The Uluzzian levels are separated from the uppermost part of the sequence by a stalagmitic crust (D Ia) and two sterile layers of volcanic ash (C II and C Ia-b). The tephra in layer C has been chemically attributed to the Campanian Ignimbrite[174,147].

We attempted to date the sequence initially using bone material. We screened a series of predominantly humanly-modified bone samples from levels D to EIII using %nitrogen methods.

The results are shown in Table S34. All of the bones had almost no remaining nitrogen and for this reason were failed. We turned our attention instead to the dating of shell carbonate samples. Benazzi et al.[167] have previously reported these new determinations, and they have been discussed more recently within a wider chronological framework, by Douka et al.[174] and Moroni et al.[147]

The Bayesian age model for Cavallo is shown in Figure S13. Using the `date` function in OxCal we calculated a PDF for the Uluzzian levels at Cavallo that corresponds to a range between 43,300-39,700 (68.2% prob.) and 46,450-39,200 (95.4% prob.) cal BP. It is important to point out, however, that we could not date the earliest Uluzzian levels, due to the lack of chronometric data from the lowermost Uluzzian level E III. The overall span for the Uluzzian here may change with the addition of new data from this lower phase.

The `boundary` for the start of the Uluzzian (if we model the start from E III) is 45,350–43,000 cal BP (68.2% prob.) or 50,600–42,650 cal BP (95.4% prob.). The long tail towards the older end of this 95.4% range is due to the absence of any determinations below the Uluzzian from the Mousterian levels at the site. The start `boundary` for EII-I, which immediately precedes the EII-I level, however, may be a more cautious estimate for the Uluzzian at the site, because it is a dated level (albeit with only one determination) whereas E III is not. When we model this, the `boundary` start is 46,530-42,890 cal BP (at 95.4%). This is the `boundary` estimate we prefer for the beginning of the Uluzzian at Cavallo. As mentioned, the estimate could change, and probably become earlier, if we are able to date level E III. Precision could also be improved with more determinations. We are working to this end.

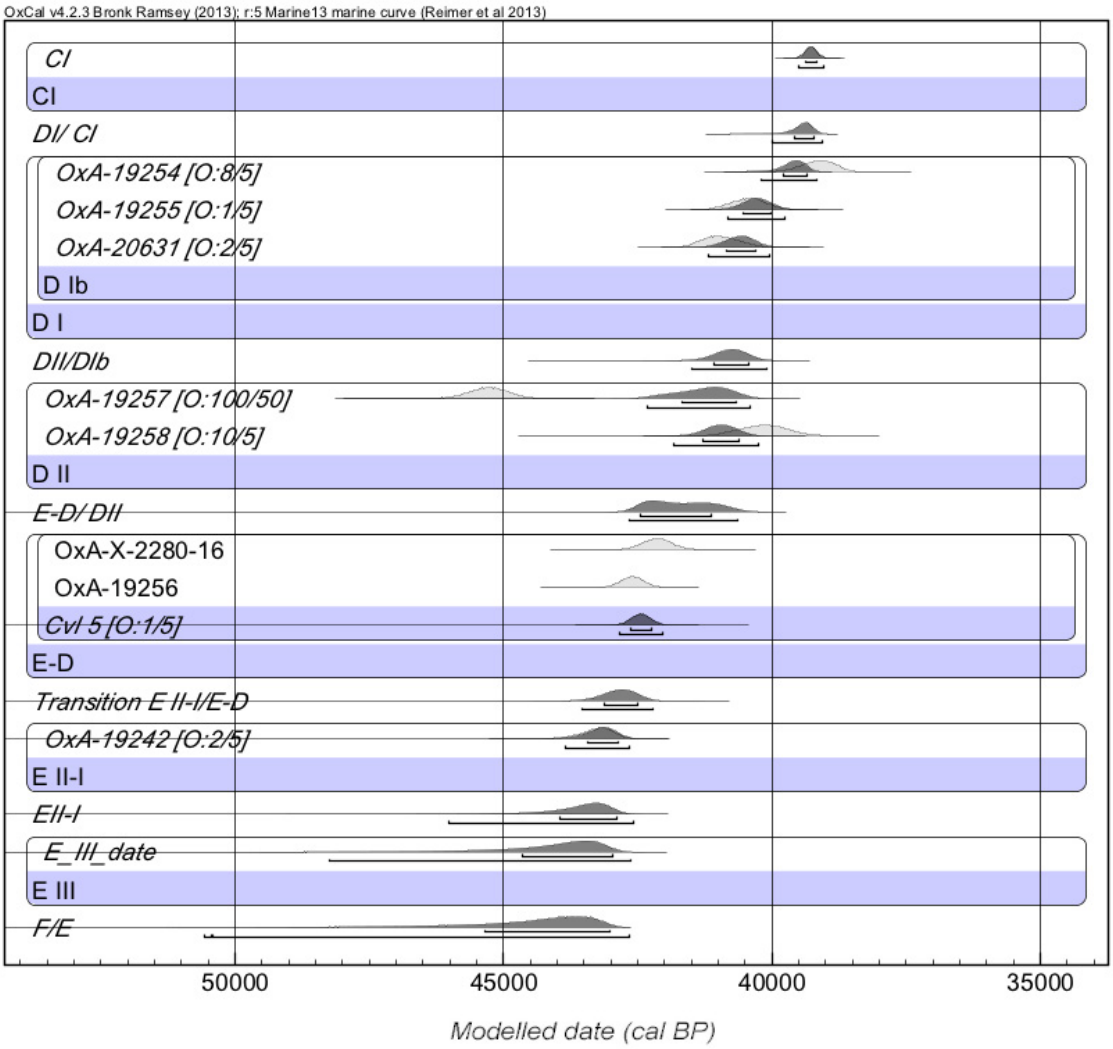

Figure S13. The Uluzzian determinations of Cavallo. For detailed discussion see Benazzi et al.[167], Douka et al.[174] and Moroni et al.[147]

Sample no	Quadrant	Stratum	Square	Cutmarks?	%N	C:N	Species	Bone description
1.	H 11	D	1	-	0.005	44.5	*Bos primigenius*	cut metatarsal
2.	H 11	E	1	-	0.003	90.8	species indet.	Partial vertebra
3.	G11	E III	4	Yes	0.005	43.7	Mammal	Large mammal rib
4.	H7 III	E II	12	Yes	0.003	52.2	species indet.	Cut limb bone fragment
5.	G11	E III	5	Yes	0.018	10.0	species indet.	Cut large mammal bone fragment
6.	F 11	E III	4	-	0.007	21.8	species indet.	Large mammal rib fragment
7.	F 12	E III	5	Yes	0.003	68.4	species indet.	Cut limb bone fragment
8.	F 12	E III	5	Yes	0.033	7.4	species indet.	Cut limb bone fragment
9.	F 12	E III	5	Yes	0.019	9.2	species indet.	Cut limb bone fragment
10.	F 12	E III	5	-	0.009	15.2	species indet.	Large mammal tibia shaft fragment

Table S34: Bones sampled from the Cavallo site. None proved to be dateable on the basis of %N and C:N atomic ratios.

Riparo Bombrini/Riparo Mochi

The rockshelter of Riparo Bombrini (43.78° Lat., 7.53° Long.) is part of the Grimaldi caves complex and lies about 30 m to the east of the site of Riparo Mochi, in NW Italy. Based on the stratigraphic and archaeological sequence it is thought that the two sites were occupied largely contemporaneously, hence we treat them as one entity in this paper. At the time of its discovery in 1938, Bombrini was already badly damaged by the construction of the railway line connecting Genoa with Marseille, completed in 1870. In 1976, G. Vicino performed salvage excavations[148] and renewed excavations were undertaken between 2002–2006 by an Italian-American team (led by F. Negrino)[149,150,151,152]. Both series of excavations[148,151] confirmed the presence of a sequence with late Mousterian and Aurignacian layers. Uppermost layers I and II were mainly identified by Vicino[148] and yielded Upper Palaeolithic tools, although remaining parts of Level II have also been investigated during recent excavations. Below these, three markedly distinct archaeological horizons (III, IV-top, IV-base) were revealed. The deepest, IV-base, is a Mousterian layer probably corresponding to layer I of Mochi. The passage from the Mousterian to the Upper Palaeolithic is characterized by a stratigraphic discontinuity identified by an erosional surface within the quasi-sterile transitional Layer IV-top. The excavators compare layer IV-top of Bombrini to layer H of Mochi, where a semi-sterile level also exists. Level III is a rich Upper Palaeolithic layer, with early Aurignacian affinities. Typically, the deepest spits of Level III are compared to that of the upper spits of Layer G in Mochi. Hence, in Bombrini only the end of early Aurignacian (with Dufour bladelets) is represented without an earlier phase as is the case in Mochi.

We attempted to AMS date samples of bone from Bombrini level IV. We sampled 4 recently excavated bones from collections at the time housed in the Musée de Préhistoire Régionale, Menton, France. These were a bison upper cheek tooth (sample code RB 2005, DD1, IV 4, 367), a cut-marked cervid long bone (RB 2002, IV-1, D1*9), a fragment of a fractured long bone of indeterminate species (RB 2003, AA1, IV-7, A2) and a large unidentified animal bone (RB 2003, AA1, IV-9, 177). The bones were tested for %N and all failed, with virtually no measureable nitrogen. A similar situation, though on a larger scale, was evident when we tested bone samples from throughout the Mochi sequence.

Abundant molluscan remains were identified throughout the Bombrini sequence and these were selected as an alternative target for dating the Mousterian sequence at the site. Twenty-two shells were found during the excavations of Vicino[153] and ~470 in the most recent investigations. In the

lowermost Mousterian layer (IV-base) a few shell remains of edible molluscs were found, but the vast majority of shell comes from Upper Palaeolithic layer III, where personal ornaments appear for the first time. The Bombrini shell assemblage was examined in the premises of the Soprintendenza per i Beni Archeologici della Liguria in Genoa. Eighteen samples, both food refuse and shell beads, were selected for dating.

Nine new radiocarbon dates were eventually obtained from eight samples, a doubling of the total number of radiocarbon dates previously available for Bombrini. Bomb 16 was dated twice using different pretreatment methods (routine and CarDS)(Table S35)[194]. All samples were analysed by XRD and, with the exception of Bomb 16, were shown to be composed almost entirely of aragonite[194]. The dates from the late Mousterian phase span 40–36 ka BP.

In contrast to the chronology from Riparo Mochi[154], the Bombrini radiocarbon series does not clarify the timing of the appearance of the earliest Upper Palaeolithic, since the initial Aurignacian phase is not represented at the site. The most significant contribution, however, is the dating of layer IV. In the Bayesian model built for the site we constrained the age of the Mousterian levels of Bombrini by including a sterile level above which we placed the Proto-Aurignacian modelled dates (published by Douka et al.[154]) from Mochi as a constraint. Given the closeness of the two sites (possibly belonging to the same occupational complex in prehistoric times) and the cross correlation possible between several of the key layers, we felt this composite model was justifiable. Only the Mousterian part of the model, which includes the Bombrini determinations, is shown in Figure S14. We determined that the `date` range for the Mousterian level was 42,190-40,580 cal BP (68.2% prob.) and 43,600-39,100 cal BP (95.4% prob.), whilst the `boundary` for the latest Mousterian was 41,560-40,500 cal BP (at 95.4% prob.). The entire range of the Mousterian here is almost certainly longer, but the `date` range only reflects the ages obtained from the upper part of the composite sequence.

OxA	Sample code	Context (level, square)	Species	Date BP	Error	$\delta^{13}C$ (‰)
19291	Bomb 3	M5 IV, BB1 11	*Mytilus* sp.	38140	250	0.6

19292	Bomb 8	M2 IV, AA1 7	*Trochus* sp.	36540	240	2.3
19862	Bomb 6	M3 IV, AA1 8, 122	*Mytilus*. sp.	40340	390	1.6
20361	Bomb7	M3 IV, AA1 8	*Trochus* sp.	36770	210	4.2
20362	Bomb15	A2 III, DD1 3a	*Ocinebrina* sp. (?)	32950	160	1.8

Table S35: Radiocarbon determinations from the site of Riparo Bombrini, Italy.

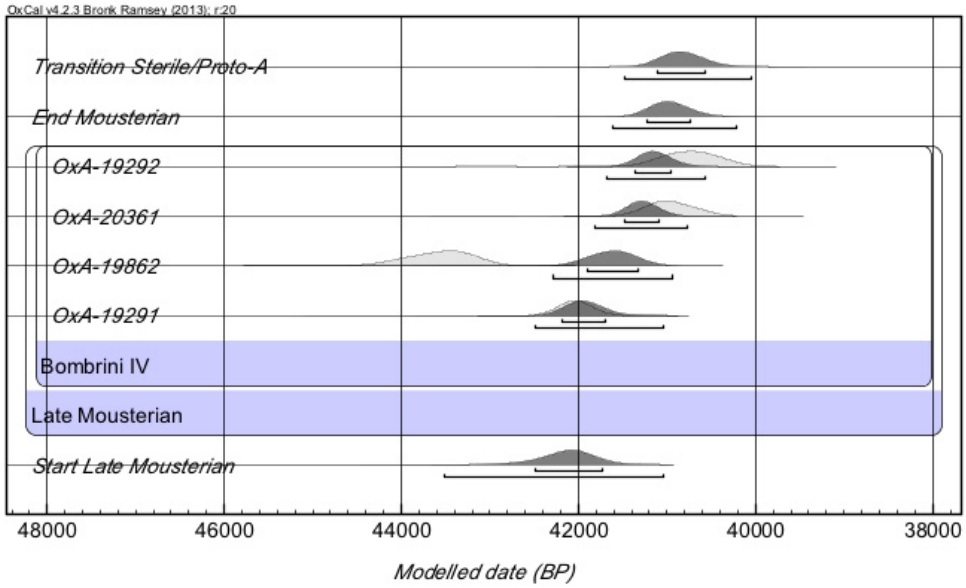

Figure S14: Radiocarbon age model for phase IV at the site of Bombrini. See text for details. All determinations in this model have been calibrated and modelled using the Marine13 calibration curve of INTCAL[12]. The marine reservoir effect is included in the dataset with a ΔR of 0 assumed. The marine reservoir effect in terms of overall uncertainty is less significant at this age range proportionally and we assume stability in the offset due to the nature of the Mediterranean sea and the fact that it is isolated from major changes in ocean circulation patterns in the Atlantic.

Grotta di Fumane

The Grotta di Fumane (45.6° Lat., 10.9° Long.) (hereafter Fumane) is a dolomitic limestone cave at the southern slope of the Venetian Pre-Alps, between the low alluvial plains and the high plateau of Mount Lessini[155]. Systematic excavations started in 1988 and continue to the present day[156]. The excavations have revealed a deep, 12m thick sedimentary succession. On the basis of distinct lithological composition, pedological features and the density and nature of cultural evidence, the stratigraphy has been divided into four main macro-units labelled as S, BR, A and D, covering the Late Pleistocene[157,158].

Macro-units A and D were excavated over a surface of about 80m^2 revealing rich archaeological deposits. Layers A11-A5 have yielded Mousterian lithics, faunal remains and structures[159,160,161,162] and layers A4-A3 have been recently characterized as Uluzzian[163]. Layers A2-A1 and D6-D3 are classified as Aurignacian, the former group usually as Proto-Aurignacian while D3d, D3b and D3a are later Aurignacian units. D1d has yielded a small number of Gravettian artifacts and is attributed to this period[164].

The archaeological sequence of Fumane is central to the discussion of the Middle to Upper Palaeolithic transition in Europe because of a very well preserved and defined Proto-Aurignacian level (Layer A2). This has yielded a significant corpus of evidence for the sudden arrival of anatomically modern humans at the site. These include dwelling structures (hearths, post-holes, midden areas), a rich lithic assemblage with Dufour bladelets, bone and antler tools, painted stones (possibly parietal art), accumulations of ochre and an abundance of perforated molluscan shells[165,153,155,166]. Recently, however, attention has shifted to the Uluzzian within this sequence, as a function of its position now associated with early AMH rather than Neanderthals[167].

The latest Mousterian occurrences are in the stratigraphic complex of levels A5, A5+A6 and A6, which were excavated over the whole entrance area, providing evidence of a well structured use of the living spaces. Areas with combustion structures, close to dumps of combustion debris, are adjacent to areas used for Levallois flake manufacture, tool shaping and curation, use of bone tools, butchering of ungulates and birds[168,159,169,170.]

The Mousterian and Uluzzian levels at the site have been AMS dated using identified charcoal and bone samples obtained from the excavations by Peresani and Broglio. The determinations have previously been published in Higham et al.[171] and Higham[172]. The Bayesian model that has been built is shown in Figure S15. The radiocarbon data is shown in Table S36. The `date` range for the Mousterian levels in the model was 45,300-43,640 cal BP (95.4%). The `boundary` for the end date of the Mousterian (End A5 to Start A4) was 44,800-43,950 cal BP (at 95.4%).

OxA	Sample	Material	Method	Date BP	Error	Used (mg)	Yield (mg)	Yield (%)	%C	$\delta^{13}C$ (‰)	$\delta^{15}N$ (‰)	C:N
2275-45	RF15 A5/88i/3789/struc.III	charcoal	ABOX-SC	41650	650	95	6.5	6.8	24.4	-23.0		
2295-52	RF49 A3/78 79/struc.II/818	bone	Ultrafilter	41300	1300	620	38.64	6.2	45.5	-18.8	7.6	3.3
21736	RF44 A3/69a/53	bone	Ultrafilter	39100	1000	600	17.35	2.9	46.9	-19.6	6.3	3.4
21733	RF28 A4II/86g/367	bone	Ultrafilter	41000	1300	610	17.45	2.9	46.3	-18.8	4.7	3.3
21734	RF29 A4II/100d+g/1120	bone	Ultrafilter	42000	1400	600	20	3.3	48.2	-20.5	3.8	3.4
21735	RF30 A4SII/744	bone	Ultrafilter	42000	1700	600	3.88	0.6	43.7	-19.7	5.8	3.2
21712	RF14 A5/77b/3789	bone	Ultrafilter	40000	1100	720	35.94	5.0	46.7	-20.0	4.6	3.3
17980	Fumane 2 (85 86 95 96 A5)	charcoal	ABOX-SC	40150	350	103	7.43	7.2	74.4	-21.1	-	-
21809	RF13 A5+A6/101f/	bone	Ultrafilter	40200	1200	720	24.95	3.5	39.4	-19.4	4.7	3.2
21757	RF3 A6/105e/688	bone	NRC	41500	1500	22	15.5	69.8	42.9	-19.8	4.5	3.4
21758	RF12 A5+A6/100e/859	bone	NRC	41100	1300	12	9.71	79.6	42.6	-19.4	4.5	3.4
17566	12/A5+A6, q.20	charcoal	ABOX-SC	40460	360	216	7.66	3.5	62.1	-24.4	-	-

Table S36: Radiocarbon determinations from the Mousterian and Uluzzian levels at the Fumane site, Italy. See caption in Table S2 for details. NRC denotes that these samples were reultrafiltered for a second time. All dated bone was clearly cutmarked and humanly-modified. See Refs 171 and 172 for further details of the samples and chemistry.

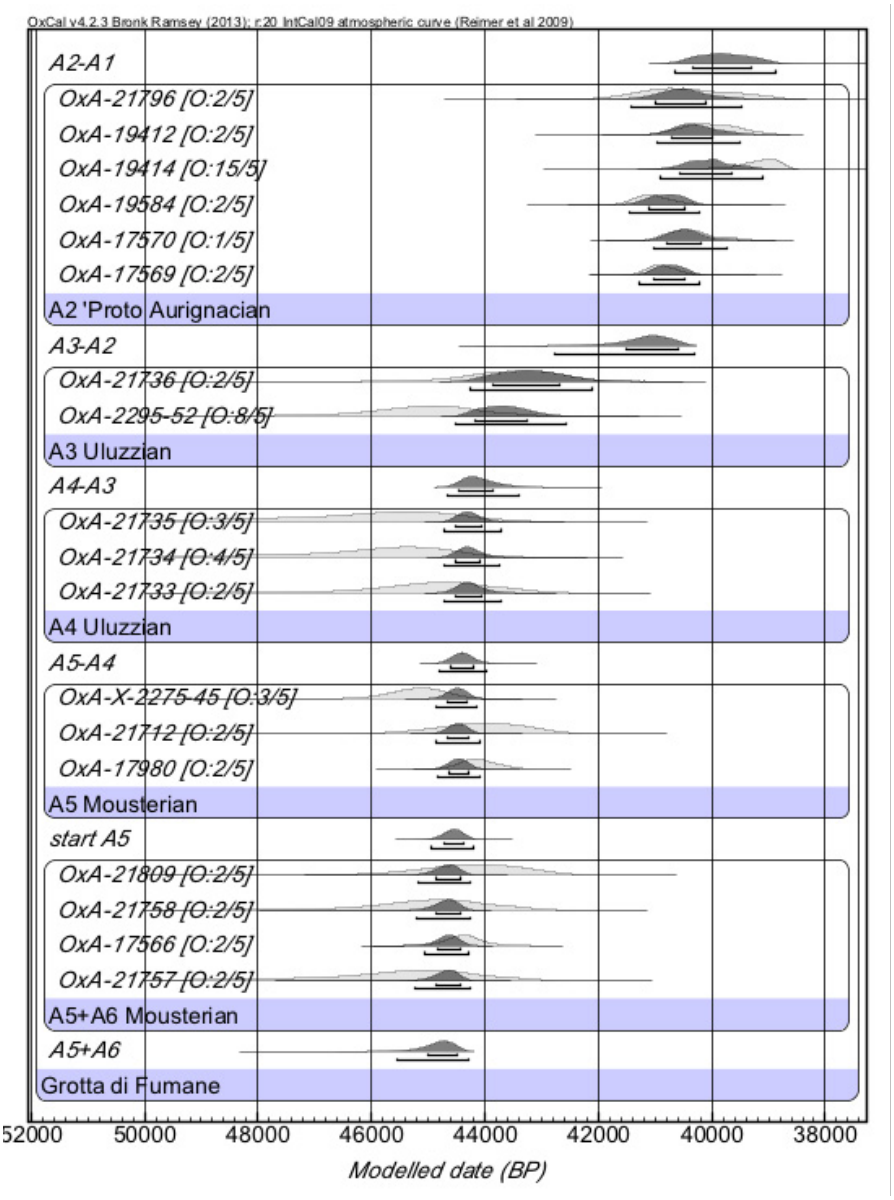

Figure S15: Bayesian age model from the Grotta di Fumane. Dates from the Mousterian are from Levels A5 and A6, and the Uluzzian is represented by levels A4 and A3. See Peresani[163] for additional details concerning the latter industry at the site.

Castelcivita

Castelcivita is located in the Calore river valley, at the foot of the Alburni Mountains (Salerno), 100 m above sea level within a very large karstic network of caves (40.48° Lat., 15.23° Long.). The principal archaeological investigations at the site were undertaken between 1976 and 1988 by Gambassini and his team at the University of Siena[175]. A 3.4 metre sequence of Mousterian,

Uluzzian and Proto-Aurignacian levels was found, topped by the Campanian Ignimbrite with its distinctive two-phase structure[173]. The excavation covered 12 square metres. The three lowermost of the eight human-derived phases were identified as being Mousterian, with a prevalent Levallois unipolar modality. These include levels XIII-VII (cgr-gar-rsi"). There were two conventional radiocarbon dates from Level XI (cgr): 39,100 ± 1300 BP (GrN-13982) and 42,700 ± 900 (GrN-13984) prior to our programme. Levels VI-IIIb (rsi'-pie-rpi-rsa") contained Uluzzian archaeological material. These were characterized by fine red sediment mixed with limestone blocks and were quite distinctive from the Proto-Aurignacian levels above.

ORAU no.	%N	CN	Square	Level	Spit	Excavation date	Cutmarks
1	0.43	7.97	F14	PIE	LA 20	6.8.76	Y
2	**0.74**	**5.95**	F12 I	PIE	LB 20	6.8.76	Y?
3	0.42	8.68	H14 II	PIE	LBA 19	16.7.84	N
4	0.34	10.49	G13 - 15	PIE	-	10.7.75	N
5	0.37	8.74	F14 II	RPI	LA 20	9.8.78	Y
6	**0.60**	**6.46**	F14 II	RPI	LA 20	9.8.78	Y
7	**0.63**	**6.11**	F14 II	RPI	LA 20	9.8.78	Y
8	0.13	16.89	G12 III	RPI	LB 13	3.8.76	N
9	**0.71**	**6.19**	G13 II	RPI	LB 12	4.8.76	N
10	0.44	7.79	G14 II	RPI	LB 13	5.8.76	N
11	0.09	26.81	F14 II	RPI	LB 17	7.9.76	Y
12	0.26	11.19	F14 II	RPI	LB 20	9.8.76	Y
13	0.62	6.73	F14 II	RPI	LB 20	9.8.76	Y
14	0.27	11.34	F14 II	RPI	LB 20	9.8.76	Y
15	0.06	38.54	G13 II	RPI	LB 13	5.8.76	Y
16	0.10	41.92	G13 II	RPI	LA 12	4.8.76	N
17	0.33	9.95	H14 III	RSI	LA 20	11.7.84	N
18	0.57	7.08	H14 III	RSI	LB 20	11.7.84	Y
19	**1.09**	**5.17**	H14 III	RSI	LB 19	11.7.84	Y
20	0.29	10.52	H14 III	RSI	LB 19	11.7.84	Y
21	0.46	6.56	H14 III	RSI	LB 18	11.7.84	Y
22	0.33	16.54	H12 I	RSA	LA 11	2.8.76	Y
23	0.15	50.85	H12 I	RSA	LA 11	2.8.76	N
24	0.06	40.7	H13 I	RSA	LB 9	31.7.76	N

25	0.16	18.28	H13 II	RSA	LA 11	4.8.76	N
26	0.53	7.28	H13 IV	RSA	LA 10	3.8.76	N
27	0.28	12.33	H13 IV	RSA	LB 10	4.8.79	N
28	0.38	8.64	G14 II, G13 I-II	GAR	26	24.7.84	Y
29	0.27	10.75	G14 II	GAR	26	24.7.84	Y
30	0.30	8.86	G14 II	GAR	25	24.7.84	Y
31	0.16	14.99	G13 I - II	GAR	LBA 24	24.7.84	Y
32	0.34	8.61	F12 I	GAR	LBA 23 - 24	1.7.84	N
33	0.28	10.76	G13 I - II	GAR	25	24.7.84	Y

Table S37: Samples of bone selected for AMS dating from the site of Castelcivita. Samples from cgr-gar-rsi" are from Mousterian levels, whilst those from rsi'-pie-rpi-rsa" date the Uluzzian. Samples with %N that were acceptably high were analysed further, but no collagen yield of sufficient amount was extractable, the samples were failed.

We attempted to AMS date bone from the Mousterian and Uluzzian sequence. We obtained 33 samples from the site for analysis. Nitrogen screening revealed that only 5 of the 33 samples had enough N to encourage us to proceed with collagen extraction (Table S37). The 5 samples that we did attempt to analyse failed to produce enough collagen to allow a successful AMS date, so were all failed. In the absence of any bone results we turned to anthracological samples stored for analysis. Sadly, several of the charcoal samples from the Proto-Aurignacian, Uluzzian and Mousterian levels failed when treated with ABOx. We did, however, manage to obtain a single new AMS determination from this corpus, from the Uluzzian level rsa", spit 11. The data we obtained has been published in Wood et al.[4] and Douka et al.[174]

We obtained two AMS dates from the same piece of charcoal. OxA-22622 was treated with an ABOx-SC pretreatment and produced a significantly older result than its pair (OxA-22660), which was treated with the routine ABA result. As previously described, we favour the ABOx-SC determination, and use it in our comparative models. We compare this new result against previous dates from the Uluzzian of the site (Table S38). It can be seen that the previous analyses are on burnt bone, a largely unreliable sample type. The new result (Table S39) was significantly different from the previous level rsa" corpus, with the exception of the greater than age. In a simple Bayesian model we also included two previous determinations from the Mousterian levels of the site obtained by the Groningen laboratory[175]. These are included in the model (Figure S16). These should be seen as minimum determinations only, again obtained on highly variable material (burnt bone). The results suggest an end boundary for the Mousterian of 45,770-41,300 cal BP (95.4% prob.) with a

date range of 47,620-41,140 cal BP. We ought to be cautious here, however, the modelled determinations are very few. More data is required.

Laboratory number	Date BP	error	Material	Context
F-71	32,470	650	Burnt bones	rsa
F-106	>34,000		Burnt bones	?
F-107	33,220	780	Burnt bones	pie
GrN-13985	33,300	430	Burnt bones	rpi
GrN-13983	33,800	13000	Burnt bones	cgr, level 11, spit 27-28
GrN-13982	39,100	1300	Burnt bones	cgr, level 11, spit 29-30
GrN-13984	42700	900	Burnt bones	cgr, level 11, spit 29-30

Table S38: Previous dates from Castelcivita Cave after Gambassini (1997)[175].

Laboratory number	Date BP	error	Treatment	Material	Context	Comments
OxA-22660	33,350	310	ABA	Charcoal c.f. *Ilex aquifolium*	rsa", spit 11	$\delta^{13}C$=-24.8 %C=63.7
OxA-22622	36,120	360	ABOx-SC			$\delta^{13v}C$=-24.0 %C=76.7

Table S39: New dates from Castelcivita Cave after Wood et al.[Error! Bookmark not defined.] and Douka et al.[174]. The two determinations are on the same piece of charcoal, but the pretreatment protocols applied are different. The ABOx-SC determination (OxA-22622) ought to be favoured.

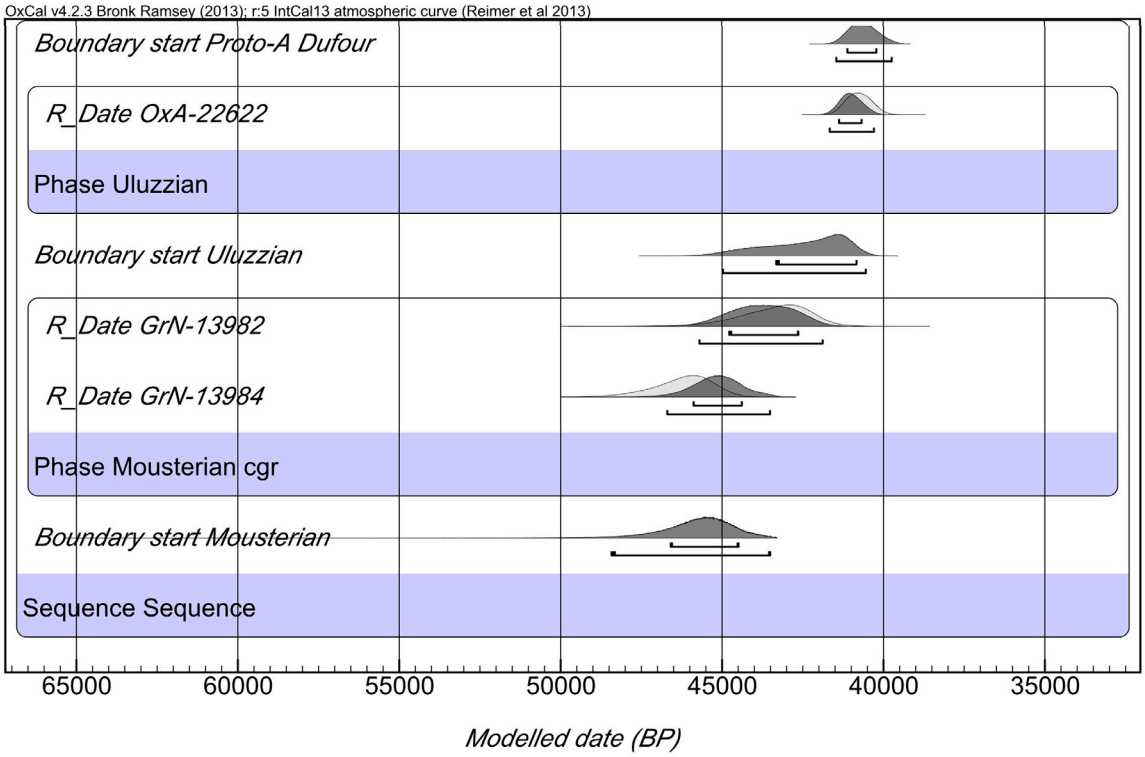

Figure S16: Bayesian age model from the site of Castelcivita. The two modelled dates included for the Mousterian are the Groningen results[175].

Oscurusciuto

The rock shelter of Oscurusciuto is located in southern Italy (Ginosa, Apulia)(40.35° Lat., 16.45° Long.). The site, discovered in 1998, comprises a Middle Palaeolithic sequence more than 6 metres thick. The estimated occupied area is ~60 square metres. In the first part of the stratigraphic sequence excavated to date (Units 1-15) the lithic industry is characterized by a prevalent recurrent unipolar modality and a secondary production of bladelets, with a volumetric orthogonal method.

Several well-preserved hearths were recovered in four different stratigraphic units. Most of the hearths are placed in small circular pits 3-5 cm deep, whose diameter is 20 to 50 cm. A burnt bone from the lower part of Unit 1 has been conventionally dated by radiocarbon to 38,500±900 BP (Beta-181165) [176, 177]. Furthermore, a thick tephra layer (Unit 14), that seals a palaeosurface currently under study (US 15), has been attributed to the Green Tuff of Mount Epomeo of Ischia wich dates around 55ky BP (R. Sulpizio pers.com.).

We attempted to date samples of bone from the site, but they contained no significant nitrogen and, therefore, no collagen. The samples we obtained and their %N values are shown in Table S40.

Sample No.	%N	C:N	Level	Bone Type	Cut Marks
1	0.027	7.99	4	Bovid bone retoucher	No
2	0.006	27.71	4	Bovid bone retoucher	No
3	0.013	8.76	4	Bovid bone	Yes
4	0.006	47.11	4	Bovid bone	Yes
5	0.019	10.34	2 Quad. G9	Bovid bone	No

Table S40: %nitrogen and C:N atomic ratios for whole bone tested from the site of Oscurusciuto, Italy. None of the bone had a high enough level of nitrogen to warrant full collagen pretreatment chemistry.

Greece

Lakonis Cave I

The site complex of Lakonis (36.78° Lat., 22.58° Long.) is located on the eastern coast of the Mani Peninsula, 3 kms east of the town of Gytheio, southeast Peloponnese, Greece. It consists of a cave and several collapsed karstic formations, referred to as sites I to V. Of all sites in the complex, Lakonis Cave I preserves the longest and richest archaeological sequence, while sites 2c and 4a also appear to be archaeologically rich. Lakonis I has been investigated in a series of systematic excavations since 1999[178,179]. It contains a ~7 m deep stratigraphic sequence covering 250 m^2. There are five broad lithostratigraphic units (I to V). Unit V at the base is sterile. Units IV to Ib contain a rich lithic assemblages dating to the Middle Palaeolithic and the terminal phase of this period. Unit Ia is an Initial Upper Palaeolithic (*sensu* Kuhn, 2003[180]). Both MP and IUP deposits are sealed under the collapsed overhang.

We attempted to date charcoal from the Middle Palaeolithic layer of the site but the samples did not survive ABOX pretreatment. Following this, two marine shells (non-ornamental bivalves) from the Middle Palaeolithic levels were dated (Table S41). All specimens are non-ornamental bivalves (non ornamental) shell species. The third specimen gave a much younger age of ~13 ka BP, probably corresponding to the time of the collapse of the rockshelter.

In addition to the Oxford determinations, there are three AMS results from well-defined combustion zones in the uppermost burnt sub-layers of Unit Ib (Late Middle Palaeolithic). These determinations were obtained by the Rehovot laboratory in Israel using the ABA method. We tested and included these in our model alongside the new dates, despite the fact that they were not ABOX- treated and should therefore be considered as minimum ages.

OxA-19843 and OxA-19761, as well as the Rehovot charcoal dates, were incorporated into a model which includes only stratigraphic units Ia,Ib and Ic (Figure S17). OxA-19843 was identified as an outlier.

The `date` range for the Middle Palaeolithic was 48,800-44,830 cal BP. The `boundary` for the end of the Middle Palaeolithic was 46,240-44,330 cal BP (at 95.4% probability). Note that at Lakonis there is no clearly identifiable stratigraphic break between the IUP and the latest Mousterian, hence, in our model, we include a single `boundary` between the two (Ib/Ia `boundary` in Fig. S17). It seems likely that a brief span of time may have elapsed between the replacement of the Mousterian here by the bearers of the IUP industry.

Sample	OxA	Date BP	error	Context/ Unit/ m asl	Species	Arag/Cal %
Lak 2	19843	38380	260	Hearth lenses/ Ic/ 4.63	*Pinna nobilis*	100- 0
Lak 3	19761	43010	350	"kitchen midden"/ Ib/ 5.44	*Pecten jacobaeus*	0- 100

Table S41: New AMS determinations from the Mousterian levels of Lakonis, after Douka[194]. The aragonite calcite percentages were determined using optimized XRD methods outlined in Douka et al.[6]. Note that *Pecten* is entirely composed of calcite in nature, while *Pinna* is entirely aragonitic.

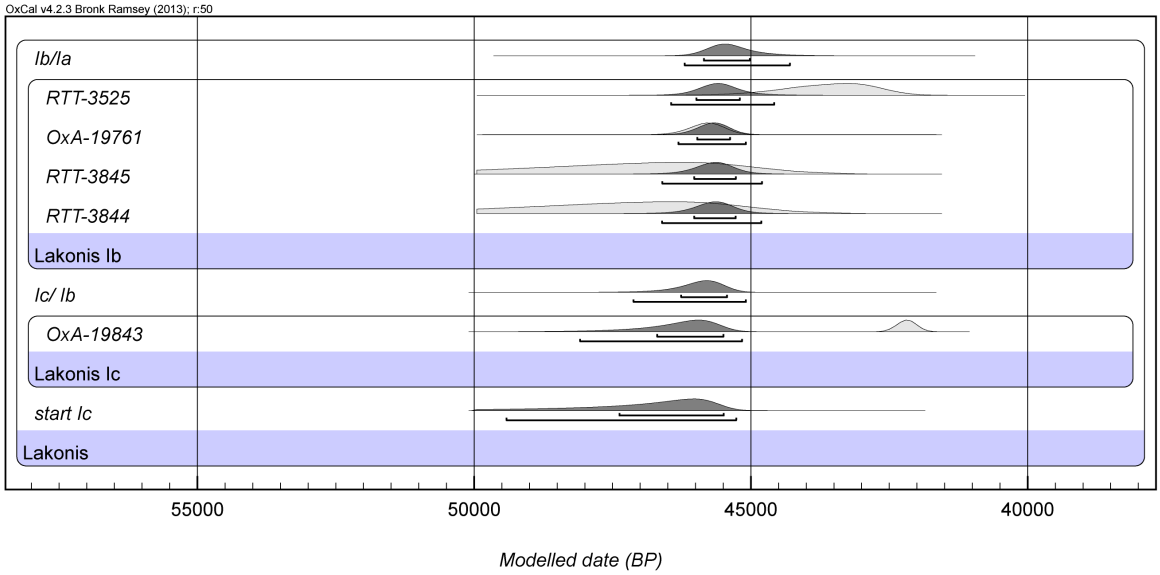

Figure S17: Bayesian age model from the site of Lakonis. Terminal Middle Palaeolithic is found in levels Ic and Ib. See text for details.

Belgium

Spy

The Belgian site of Spy (50.47° Lat., 4.67° Long.) contains directly dated Neanderthal remains that are of key importance in any discussion of the disappearance of the population. We included the site in our analysis for this reason. Sadly, it is not possible to date the Mousterian industries at the site because of the fact that the original excavations were conducted over a century ago and were not of modern standard. Recent work has focussed on reassessing the collection of human and faunal material excavated from the site over the last century. Several human remains, including both Neandertals and AMH, were recovered. This work has been described by Rougier et al.[181], Semal et al.[182] and Crèvecoeur et al.[183]. According to Pirson et al.[184] at least 24 new Neanderthal remains have been identified and some of the material refits with two adult Neanderthals Spy I and Spy II from the original 1886 collection. New radiocarbon dates were obtained directly from some of these specimens[182,183] and fortunately those that came from unsorted faunal collections were not conserved with preservatives and glues. Two of the dated samples (GrA-32626 - a left I1 [Spy 92b]: dated at 36,350 +310/−280 BP and GrA-32623 – [Spy 94a]: a right M3 with maxillary bone dated at 35,810 +260/−240 BP) refit to each of the adult Neanderthals Spy I and II respectively. The two

determinations compare well with OxA-10560 (36,250±500 BP[185], a fragmentary human vertebra that was found below Spy Cave.

There are other dates on Neanderthal remains but contamination is suspected due to prior treatment in some cases (as shown in some examples by high C:N atomic ratios)[182].

Of course single AMS determinations are not ideal because they yield wide uncertainties when calibrated. Our modelling is therefore simple, as it must be for samples without context. Including these determinations in a single Bayesian `phase` results in the model in Figure S18. The `date` range is equivalent to 42,580-38,950 cal BP whilst the end `boundary` is 41,210-37,830 cal BP.

More recently, Crèvecoeur et al.[183] have ascribed six samples to an immature individual termed Spy VI. An upper right di1 was dated in Oxford at 33,950±550 BP (OxA-21610: initially the determination was 34700±550 BP but this was recalculated in accordance with improved background corrections) and a right hemi-mandible was dated in Groningen at 32,970 +200/-190 BP (GrA-32627).

Were we to add the Oxford (ultrafiltered) determination for Spy VI to the model this would yield a wider range to the `phase` and extend it to 43,270-36,480 cal BP, with an end `boundary` of 37,690-34,620 cal BP (95.4% prob.) (Figure S19). We favour a more conservative approach, however, and lend our support to model 1, since radiocarbon ages of this antiquity are far more likely to be minimum ages and these are single ages with no corroborating determinations constraining them. In this we follow Semal et al.[186] in favouring the three oldest direct dates. The radiocarbon dates suggest a late survival of Neanderthals at Spy, a picture complicated by clear evidence for some contamination that is probably unremoved in several cases, but supported by determinations on material that was certainly not conserved.

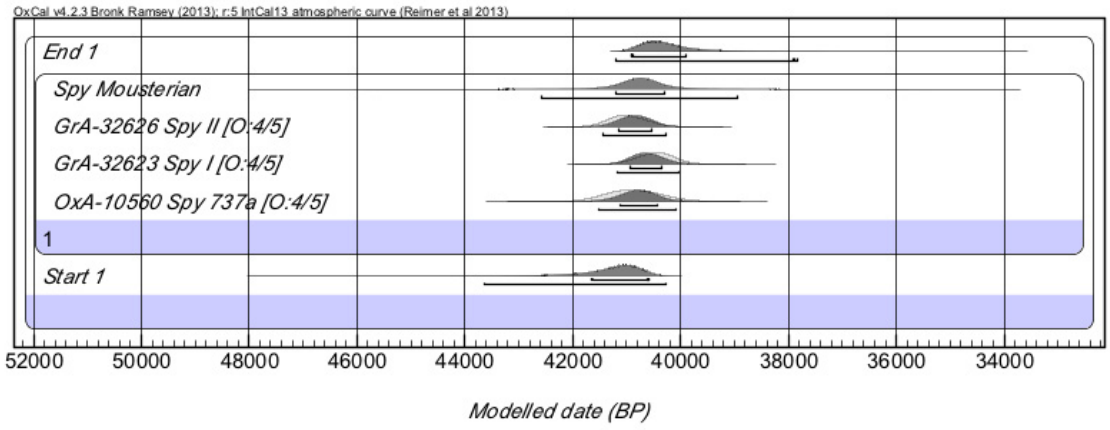

Figure S18: Bayesian model of the Spy Neanderthal dates. The model assumes that the dated specimens belong to a single `phase` of activity at the site (this is termed model 1 in the text). The PDF Spy Mousterian is the `date` range for the phase.

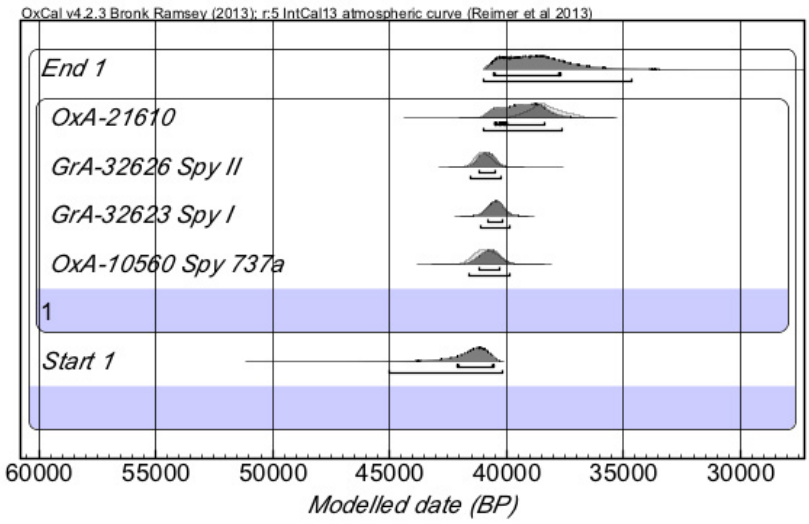

Figure S19: Bayesian model of the Spy Neanderthal dates including the determination from Spy VI (OxA-21610)(termed model 2 in the text).

Grotte Walou

Grotte Walou is a site in Belgium near the town of Trooz (50.58° Lat., 5.67° Long.). Excavations have most recently been undertaken between 1985-1990 and then 1996 to 2004[184]. A 3-volume report on the latter excavations has been published recently by Draily and colleagues[187,188,189].

The sections of the site that concern us focus around Layer CI-8 which contains a rich Mousterian and a human tooth which has been identified as belonging to a Neanderthal (first lower left premolar)[190]. A typical Mousterian industry is present including items showing unifacial debitage, various types of scrapers, some backed knives and a few denticulate pieces[189]. The lithostratigraphic

sequence outlined by Pirson et al.[187,191] is summarized in Figure S19. According to Pirson et al.[184] stratigraphic unit CII-1, directly underlying the CI-8 unit, could be the Les Vaux soil, which is dated to around 42-40 ka cal BP. This date has been used to estimate a *TPQ* for the Neanderthal tooth of younger than 40,000 cal BP. As Pirson et al.[184] note, the tooth has a very reliable context and dating it is important given the rarity of well-provenanced human material from the Middle Palaeolithic in northern Europe. We attempted to date samples above and below it in order to better constrain its age. Above it in the sequence, CI-6 contained some Mousterian artefacts but there is a possibility that these are derived from CI-8, so caution is required in this regard.

We obtained new AMS dates of unmodified *Ursus spelaeus* teeth and bone. More than half of the 12 samples we attempted to date failed to produce any significant amount of collagen. Obviously it is not ideal to date a sequence such as this with non-humanly modified fauna but there was no modified material available. For this reason we are conservative in our interpretation of the site chronology.

The radiocarbon determinations obtained are shown in Table S42 and in Figure S20 with respect to the lithostratigraphic sequence.

The CI-8 level has previously been dated by Lv-1838 (>42,000 BP). Our new date for this level is 47,900 ± 3500 BP (OxA-21608). CI-6 was previously dated by Lv-1642 at 35,380 ± 1870 BP, the new Oxford date is >42,500 BP (OxA-21603). Below the CI level in CII we also obtained two new dates of close to background age, these were OxA-21609 (>48,600 BP) and OxA-21619 (44,200 ± 1900 BP), both from CII-2.

Taken together the new results suggest the possibility that the sediments are older than previously thought. They also, by virtue of the date for OxA-21618, suggest a possible *TAQ* for the Neanderthal tooth of 35,400 ± 650 BP (the date for a bear bone from CI-2-5) which overlies the CI 6-8 levels. The date of OxA-21608 at 47,900 ± 3500 BP from the same level as the tooth may suggest that the real age of the context is considerably older, however the presence of solifluction in and around the CI-8 level might mean that material has been reworked[187], and this should also be borne in mind when considering the range of radiocarbon determinations obtained thus far. More work is required to place the sequence in a tighter chronological framework.

Lithostratigraphy		*Industry*	Lab number	^{14}C age	±
C1	1	Aurignacian			
	2	Indeterminate	OxA-21618	35400	650
	3		Lv-1641	33830	1790
	4				
	5				
	6	Mousterian	OxA-21603	>42500	
		or	Lv-1642	35380	1870
	7	Middle			
	8	Palaeolithic	OxA-21608	47900	3500
CII	1				
	2		OxA-21619 OxA-21609	44200 >48600	1900
	3				
	4				
	5				
	6				
	7				
C III	1				
	2				
	3				

Figure S20: Lithostratigraphic sequence and radiocarbon determinations from Grotte Walou (after ref. 187, 188). Lv denotes radiocarbon results from the Louvain-la-Neuve laboratory. This laboratory is no longer operational. These determinations consist of an amalgamation of several different bones from the same context.

OxA	Sample	Context	Material	Date BP	error	Used (mg)	Yield (mg)	Yield (%)	%C	$\delta^{13}C$ (‰)	$\delta^{15}N$ (‰)	CN
21618	W5. 03 (WA00 J18.41)	CI-2 to CI-5	bone	35400	650	640	12.1	1.9	40.8	-21.5	4.7	3.2
21603	W2. 08 (WA00 J1852)	CI-6	tooth	>42500		520	2.9	0.6	38.7	-22.1	3.5	3.2
21608	W6. 42 (WA98 H20.136)	CI-8	tooth	47900	3500	500	3.8	0.8	42.1	-21.9	8.9	3.2
21619	W4. 27 (WA98 J20.109)	CII-2	bone	44200	1900	640	31.9	5.0	41.8	-21.4	2.9	3.2
21609	W1. 55 (WA02 H19.107)	CII-2	bone	>48600		500	11.0	2.2	43.5	-21.4	5.0	3.3

Table S42: New AMS determinations from Mousterian and near Mousterian contexts in the Grotte Walou (Belgium). All determinations are of unmodified *Ursus spelaeus* bones or teeth. See caption to Table S2 for details of the analytical data in the table.

United Kingdom

Two sites have been dated in the United Kingdom, but caution is required in their interpretation because both are hyaena dens and the material dated is not humanly modified. We include them because we believe that the radiocarbon results cover the broad age of Neanderthals at the sites and this is useful since the data document the presence in the very furthest parts of northwestern Europe during this part of MOIS3.

Pin Hole

Pin Hole is located at the western end of Creswell Crags, a gorge in Derbyshire (53.26° Lat., -1.20° Long.). It has an extensive history of excavation, starting from 1875. Determinations used in this paper come from the excavations of Armstrong (1924-1936). Armstrong's descriptions and measurements of the excavated lithic and bone assemblage were used by Jacobi et al.[192] to reconstruct the cave's use. Armstrong recorded distances into the cave and their depth below the cave floor. Jacobi et al.[192] reconstructed the 3D location of many samples of bone and teeth and selected from them a subset for dating (see Jacobi et al.[192]: Fig 6). The samples used in the simple model built here derive from bone, teeth and antler samples that overlap in their vertical distribution with Late Middle Palaeolithic artefacts. These determinations, without any relative stratigraphy, were placed into a single `phase`. We do know that they post-date the age of a *Coelodonta antiquitatus* right radius at 58,800 ± 3700 BP, which was found at a depth below any recorded archaeology (this determination would now be a greater than age but at the time of measurement we did not have a limit imposed by a bone-specific background correction after Wood et al.[9]). In addition, the uranium series dating of a broken speleothem below the humanly occupied sediments yielded a determination of c. 64 ka BP providing a *TPQ* for the archaeological material in the cave. A small group of samples from the site come from contexts that are apparently above the level of Middle Palaeolithic artefacts. They form a *TAQ* for the archaeological sequence of this period. One determination, OxA-11980 (37,760 ± 340 BP), from a reindeer antler, dates this and is included in the model as post-dating the Middle Palaeolithic samples.

It is important to note that there are no cutmarked or modified bones from the site, therefore it is difficult to precisely date the presence of Neanderthals based on Late Middle Palaeolithic

implements through the sequence. Rather, we provide a range through our modelling over which it is considered highly likely that Neanderthals were present at some time or another. It is not possible to extend our conclusions further than this with the available data. The reader is recommended to consult Jacobi et al.[192] for a more in-depth assessment of the site and context.

Many of the radiocarbon determinations from the Middle Palaeolithic of Pin Hole are close to, or beyond the radiocarbon calibration limit (8 of the 13 available determinations). All appear robust, however, based on the usual analytical parameters we measured. The occupation of the site fits broadly into the period 50-55 ka cal BP until ~43 ka cal BP.

The Bayesian model utilises only the most recent group of determinations from the site (Figure S21). It suggests that the Middle Palaeolithic industries end at the `boundary` immediately prior to the Upper Palaeolithic, which is equivalent to a 44,570-42,030 cal BP, and cover a `date` range from 49,200-42,730 cal BP.

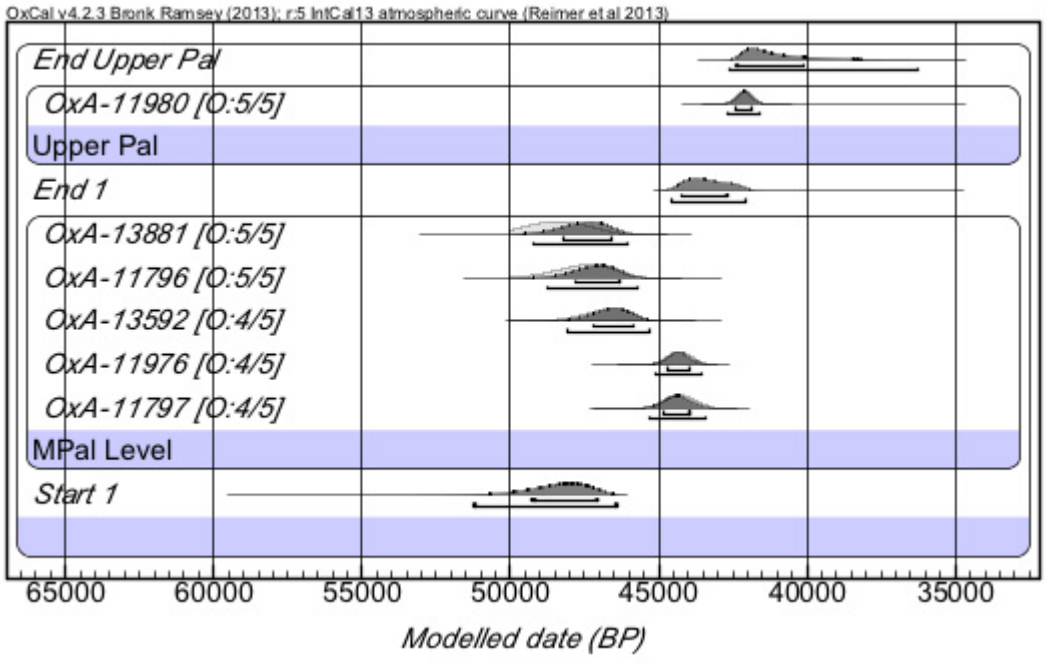

Figure S21: Bayesian model for the Pin Hole site, England. There are 8 further determinations from the Middle Palaeolithic level that approach the radiocarbon calibration limit and have therefore been left out of the model. These data are included in Jacobi et al.[192] and Higham et al.[7].

Hyaena Den

The Hyaena Den is a site on the east side of Wookey Hole ravine in Somerset (51.22° Lat., -2.67° Long.). The site has been explored since 1859. The cave was almost completely full of sediment when discovered but has been almost completely excavated. The lithic evidence in the cave consists of Middle and Early Upper Palaeolithic material. The former includes sub-triangular and cordiform handaxes and some denticulate tools. The Early Upper Palaeolithic blade-points found are made of flint.

Dating of the Hyaena Den had been based on a directly dated red deer (*Cervus elaphus*) incisor with evidence for cut marks. The result (40,400 ± 1600 BP (OxA-4782) was obtained using the ion-exchanged gelatin method. Four samples from the 1992 excavations were dated using ultrafiltration and provided older results. These are shown in Table S33. One (OxA-13914) is of a digested bone fragment in silts below the cave earth that contains the archaeology in the site. This date is a *TPQ* for the Middle Palaeolithic and provided a date that is equivalent to the laboratory background. Three determinations in the Middle Palaeolithic cave earth provided three results (Table S43) indistinguishable between 45-48 ka BP and therefore close to background. Other results dated from Late Middle Palaeolithic contexts were all of burnt and carbonized bone and unreliable or minimum ages[192].

OxA	Date BP	error	Species	Used	Yield	Yield (%)	%C	$\delta^{13}C$ (‰)	$\delta^{15}N$ (‰)	C:N
13914	52700	2000	Unidentified bone	580	31.8	5.5	43.5	-19.8	6.0	3.3
13915	45100	1000	*Cervus elaphus*	400	21.6	5.4	41.7	-20.1	4.2	3.3
13916	47000	1700	Unidentified bone	500	14.45	2.9	42.7	-19.4	3.3	3.3
13917	48600	1000	*Crocuta crocuta*	640	54.8	8.6	43.8	-18.4	8.9	3.3

Table S43: AMS determinations from the Middle Palaeolithic of the Hyaena Den at Wookey Hole, England. See caption to Table S2 for details of the analytical data in the table. These results were previously published by Jacobi et al.[192]

Lebanon

Ksar Akil

The Ksar Akil rockshelter is located in Lebanon (35.62° Lat., 33.92° Long.) around 10 km northeast of Beirut. It sits below a high limestone cliff near the Antelias River valley in the foothills of the Lebanon Mountain range. After initial discovery in 1922, excavations at the site began in 1937-1938 by a team of Jesuit priests (Joseph G. Doherty, S.J. Doherty and by J. Franklin Ewing) from Boston College, Massachusetts. After an interruption during the war, Ewing returned for a further season (1947-1948).

The base of the excavation reached 23 metres below datum. A total of 36 levels were recorded, I-XXXVI from top to bottom[194]. Today scholars recognise 3 major archaeological phases. The Middle Palaeolithic (a Levantine Mousterian) embraces levels XXXVII–XXVI. Above this is an IUP phase (XXV–XXI/XX), known as "Ksar Akil Phase A" or "Phase 1"[193,194].

The first Middle Palaeolithic occupation, XXXVI to level XXVI (19.4–15 m below datum, respectively) occurred during a period of occasional flooding in the cave[195]. Between *c.*-17-16 m the stream seems to have changed course and the rockshelter became less prone to flooding. The lithic evidence from these lower levels has been assigned to the Tabun Mousterian Phase 3/Layer B (and possibly Phase 2/ Layer C). Others have assigned the lower levels (XXVIIIB and XXVIIIA) to Phase 1/ Tabun D Mousterian based on the presence of ovoid blanks, Levallois and discoidal cores, and Mousterian tool types, and the uppermost levels (XXVIIB to XXVIA) to Phase 2/ Layer C Tabun type Mousterian due to the presence of blade and point forms[196]. Above the Middle Palaeolithic occupation a series of sterile or semi-sterile layers were excavated. These are termed the "Stone Complex" and consist of a red clay layer separated by layers of limestone flakes. The lowermost Stone Complex is important because it separates the Middle and Initial Upper Palaeolithic layers of the site and it is where an undiagnostic human fossil ("*Ethelruda*") was discovered. There is debate about the formation processes surrounding this feature[197,198].

Prior to our work there were two radiocarbon determinations from the Middle Palaeolithic part of the sequence: GrN-2579: 43750 ± 1500 BP (XXVI/XXVII, 16m) and Gro-2574/75: 44400 ± 1200 BP (XXVII, 16m) coming from the clay layer of the Stone complex. van der Plicht et al.[199] also

reported four U-series determinations from two Mousterian bones from the bottom of the sequence (XXVI and XXXII), but the results were inconclusive.

Douka et al.[194] obtained 26 new determinations as part of our extensive dating programme at the site. Four dates were obtained from 2 marine shell specimens from the Mousterian level XXVIII (16.6 m below datum), just below Stone Complex 3. An *Ostrea* sp. valve was dated three times because of problems identified with the composition of the carbonate. The results were variable (OxA-X-2344-23: 35,900 ± 400 BP; OxA-X-2361-17: 33,810 ± 180 BP; OxA-20491: 39,310 ± 330 BP)(Table S44). The $\delta^{13}C$ values for the first two ranged from -2.6 to -3.8‰, which suggests the possibility of meteoric diagenesis and the uptake of some of terrestrially sourced carbon. Because *Ostrea* sp. is dominated by calcite in nature it is difficult to screen and discriminate secondary, post-depositional mineral formation, such as low-Mg calcite. A further determination (OxA-20491) was obtained. This sample came from a different part of the valve closer to the thicker umbo area, away from the previously sample area. This is most reliable determination, not only because it is the oldest but its $\delta^{13}C$ value falls within the expected range for marine carbonates (1.6‰).

A second *Ostrea* sp. valve from the same level (XXVIII) was analysed to date layer XXVIII more reliably. Based on morphometric comparisons this second valve could belong to the same animal as the previous specimen. The new date, OxA-25656: 39,530 ± 330 BP, is identical to OxA-20491, and its $\delta^{13}C$ value (1.0‰) is also comparable. Taken together, this suggests that the age of level XXVIII is ~39.5 ka BP.

When comparing the results with the previous dates obtained in the 1960s it is clear that the new estimated age is a lot younger. Sediment clay, however, the previously dated medium, is a problematic material because determining the origin of the measured carbon is very complicated. We consider the determinations of OxA-20491 and OxA-25656 to be a more reliable estimate for the age of the latest Mousterian at the site. The earlier Mousterian levels are undated. If the U-series determinations from levels XXXII are accepted, then the Mousterian must have certainly started before 50 ka and ended at the boundary around 43.5-42.5 ka cal BP. The Mousterian was replaced by the IUP soon after; the latter lasted for a couple of millennia until 41-40 thousand years ago.

The Bayesian model for the Mousterian section of the site is shown in Figure S22. The results show that the basal and terminal Mousterian has a `date` range of 53,160-42,070 cal BP. The final `boundary` for the phase ranges between 43,010-41,680 cal BP.

Sample ID	OxA-/X code	Date BP	error	Level, square, depth	Material	$\delta^{13}C$ (‰)
KA 54	X-2361-17	33810	180	XXVIII, F 5, -16.55–75	*Ostrea* sp.	-3.4
KA 54	X-2344-23	35900	400	XXVIII, F 5, 16.55–75	*Ostrea* sp.	-2.6
KA 54 *	20491	39310	330	XXVIII, F 5, 16.55–75	*Ostrea* sp.	1.6
KA 55 *	25656	39530	330	XXVIIIA, F 5, 16.55–75	*Ostrea sp.*	1.0

Table S44: New determinations from the Mousterian of Ksar Akil. For more details see Douka et al.[194] and Douka[193]. Note that the results from KA54 are variable due to reprecipitation of carbonate in all probability. The age of the Mousterian in XXVIII is best estimated by the two determinations OxA-20491 and OxA-25656 shown with an asterisk.

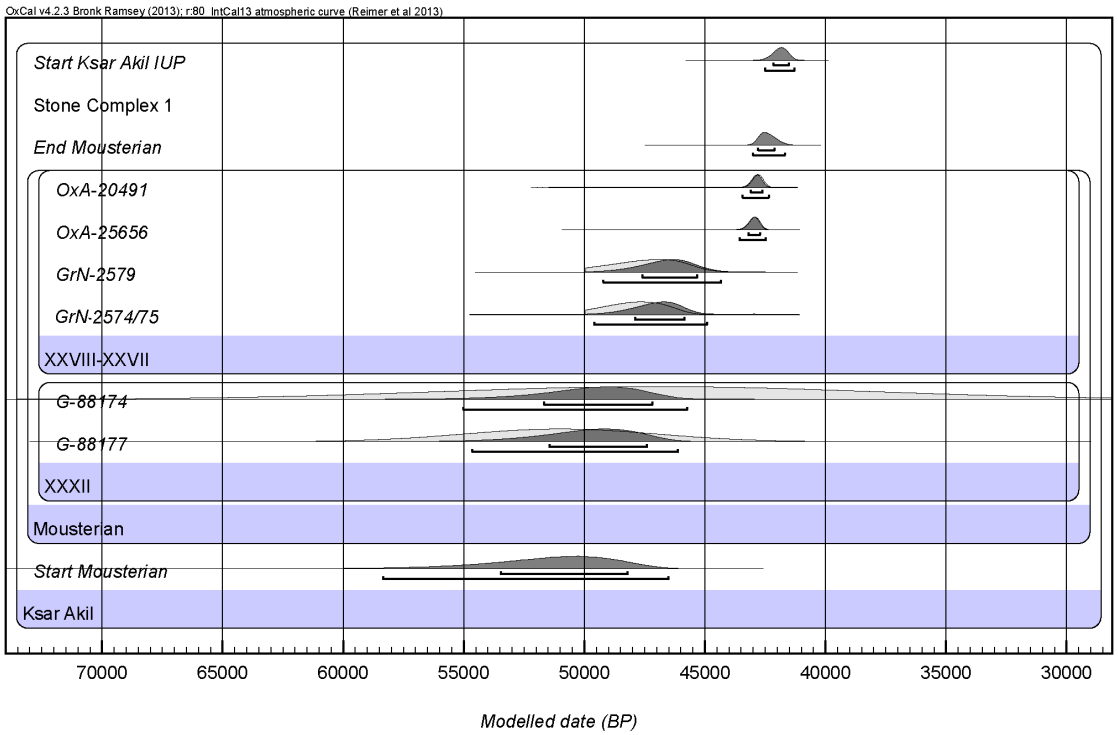

Figure S22: Bayesian age model for the Ksar Akil site, Lebanon. The model shows the lower sections only. For a full site model the reader is referred to Douka et al.[193]

Russia

Mezmaiskaya

Mezmaiskaya Cave is a site in the Russian north Caucasus located at 1,310 m above sea level on the Azish-Tau karst ridge (44.20° Lat., 39.99° Long.). It has been excavated since 1987 by Golovanova and Doronichev[200,201,202]. There are three Holocene layers (1-1, 1-2, and 1-2A) which overlie eight Upper Paleolithic layers (from top to bottom): 1-3,1-4, 1A-1, 1A-2, 1A-3, 1B-1, 1B-2, and 1C. Stratum 1D represents the MP-UP transition and is sterile. The Middle Paleolithic layers in the site consist of seven (from the top): 2, 2A, 2B-1, 2B-2, 2B-3, 2B-4, and 3. Pleistocene layers (4–7) contain no archaeological material. Approximately 80 square metres of the site have been excavated down to around 5 m depth.

Pinhasi et al.[203] published a radiocarbon chronology of the site that included a series of AMS dates from the ORAU, and the data used in this paper comes from this work. The new determinations from the Mousterian level 2 are shown in Table S45. The age model built is shown in Figure S23.

The age range (`date`) calculated for the uppermost Mousterian levels 2 and 2A in the age model was 50,400-40,410 cal BP (95% probability). The final `boundary` for the last Mousterian was 42,300-39,220 cal BP.

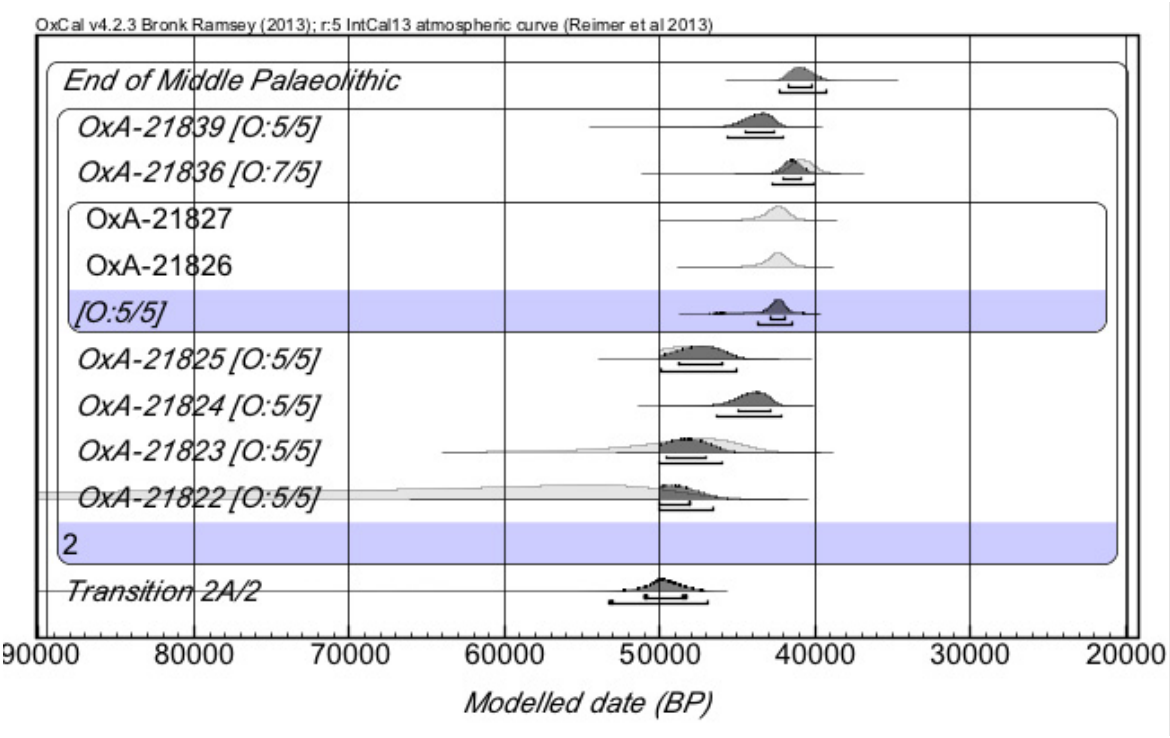

Figure S23: Bayesian age model for the Mezmaiskaya Middle Palaeolithic. (See Golovanova et al.[200], Golovanova et al.[201], Golovanova et al.[202] and Pinhasi et al.[203] for more information on the site and sequence). OxA-21822 and -21823 extend out of range of the calibration curve whilst OxA-21825 may extend outside the range.

OxA	Year of excavation /Layer/Context	Date BP	Error	Used (mg)	Yield (mg)	Yield (%)	%C	$\delta^{13}C$ (‰)	$\delta^{15}N$ (‰)	C:N
21822	MZM 1994 2 Quad. P19	>46200		596	6.2	1	40.4	-19.6	9.6	3.2
21823	MZM 1994 2 Quad. N19	47200	2800	650	33.94	5.2	41.3	-19.6	5.2	3.2
21824	MZM 2002 2 Quad. N17 49	40200	1200	700	17.48	2.5	42.9	-19.0	5.9	3.4
21825	MZM 2002 2 Quad. O17 64	44500	2000	640	25.91	4	41.2	-19.4	7.3	3.2
21826	MZM 2002 2 Quad. N17 38	38200	900	710	37.85	5.3	44.6	-19.2	6.9	3.2
21827	MZM 2002 2 Quad. M17 92	38200	1000	810	51.62	6.4	41.1	-19.1	7.4	3.2
21836	MZM 2002 2 M17 91	36200	750	920	29.04	3.2	41.8	-19.0	5.9	3.3
21839	MZM 1994 2 Quad. N 19 human cranial fragment 13	39700	1100	740	108.3	14.6	44.1	-17.4	0.0	3.2

Table S45: AMS determinations from the Middle Palaeolithic level 2 at Mezmaiskaya, OxA-21839 is a cranial fragment of a Neanderthal infant (Mezmaiskaya 2). All other bones are unidentified but they are cut marked or humanly modified bones. See Table 2 caption for details of the relevant analytical parameters listed.

Bayesian Analysis Summary

The final Mousterian boundary data from the sites described in this Supplementary Methods are summarised in Table S46. We used OxCal4.2[11] to analyse these end boundaries further. We placed the boundaries (inserted as priors) within a single Phase model to determine the end boundary for the joint data. The results are shown in the main paper (see Fig. 1b). The boundary 'End of Mousterian' in the figure provides a PDF for the end of this technocomplex amongst the sites we studied. In Figure S24 we show the model output when we add the Châtelperronian sites we analysed to this. We assume here that the Châtelperronian is associated with Neanderthals. This produces an "End Neanderthals" boundary in Figure S24.

A glance at the boundaries for the start of the Uluzzian in Fig. 2b of the main paper shows that the technocomplex begins around 46-44,000 cal BP, resulting in a difference between the final Neanderthal PDF of ~5000 years. If we assume that the Uluzzian is an industry associated with AMHs, as argued by Benazzi et al.[167] and confirmed by Bailey et al.[204] on the basis of the reanalysis of human teeth found in the lower levels of the Cavallo site, then this difference would effectively be a measure of the overlap between AMHs and Neanderthals Europe wide. In Figure S25 we show the PDF we calculated for the difference between the boundary of the first Uluzzian at both Fumane and Cavallo caves and this "End Neanderthals" boundary as determined in OxCal. The ranges for the differences were 3310-5250 years (at 95.4% prob.) for the former and 2600-5400 years in the case of Cavallo.

We used the OxCal order command to undertake the relative ordering of different events from sites in our model. We focused on the boundaries for the end of the Mousterian, and compared them with the boundaries for the start of the two transitional industries. This enables us to determine the relative probability that one PDF precedes another (the results of this analysis are in tabular format in the Extended Supplementary Online Data 1). We calculated the difference between different parameters measure the significance of the order results. This shows that some 'transitional' industry start boundaries significantly precede Mousterian end boundaries in some parts of Europe. Some of the more interesting of these examples include the result from Arcy-sur-Cure, where the boundary for the start of the Châtelperronian significantly precedes the end

boundary for the Mousterian at Abric Romaní (difference = 950-3460 years at 95.4% probability). It is 99% likely that the Arcy Châtelperronian pre-dates the end of the Mousterian at Romaní. The same start boundary for the Arcy Châtelperronian also precedes significantly (99% likely) the end of the Mousterian level AHIV at Geissenklösterle (difference = 390-3060 years at 95.4% prob.). This suggests that there is a spatio-temporal pattern to sites yielding evidence for the latest Mousterian even though, in the case of Arcy and Geissenklösterle, they are within reasonably close proximity to one another. The end of the Mousterian at sites such as Romaní and L'Arbreda also significantly post-dates the start boundary of the Uluzzian level at Fumane, suggesting a punctuated process in the movement of AMHs along the Mediterranean rim. The final Mousterian at Bombrini/Mochi is also significantly later than Fumane's Uluzzian, as mentioned in the main text. Taken together the results reveal regional differences in the end dates of the Mousterian as reflected in the ranges for different boundaries at the sites we have studied.

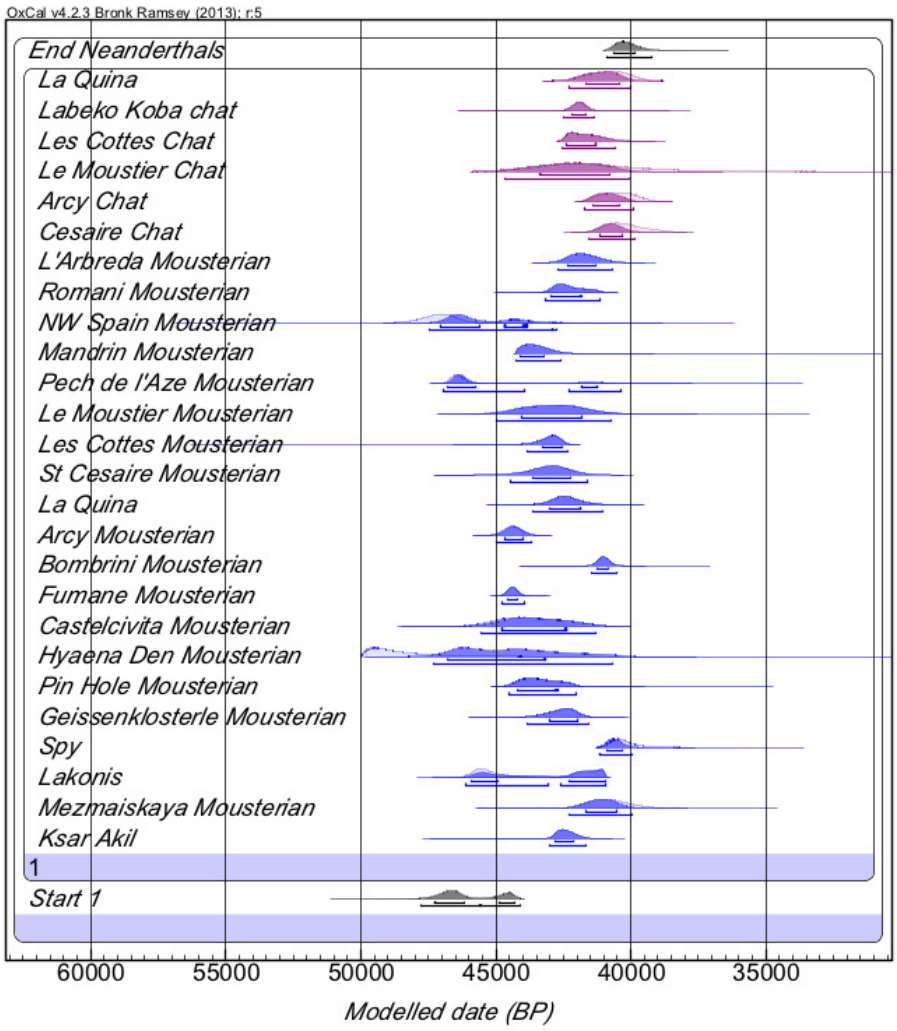

Figure S24: Bayesian age model of end boundaries for Mousterian (in blue) and Châtelperronian (purple) sites. The results are placed into a single Phase in OxCal to determine the start and end boundaries. The end boundary represents a PDF for the terminal age of both technocomplexes amongst the corpus of sites studied here (see boundary 'End Neanderthals').

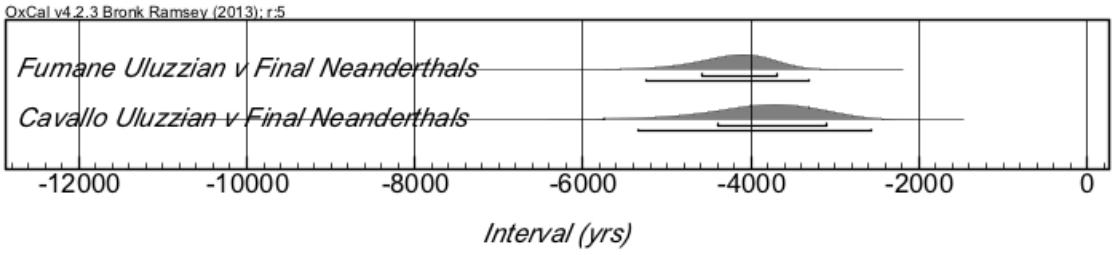

Figure S25: PDF for the difference between the first Uluzzian at Cavallo and at Fumane, compared with the last Neanderthals PDF (determined using the data in Fig. S24 above and comparing it with end boundary for the dated Uluzzian sites we examined). This suggests that there is a significant difference between the start of the Uluzzian and final Neanderthals (the start boundary for the Uluzzian and the final boundary PDF for the Neanderthals) because the distribution does not overlap zero at 95.4% probability.

We tested the sensitivity of our modelling to changes in the type of model applied. We used a trapezium model to examine the effects of changing uniform boundaries on the single Phase model to one using a trapezium model. The difference in the trapezium model[205] is that it includes two transition parameters that provide flexibility and reflect archaeological situations in which start and end boundaries could be more realistically expressed by a slow transition period from the beginning to a peak, and a similar transitional decline towards the end. One can compare it with archaeological phases that go through a slow increase and blooming phase, followed by a gradual decline.

The end of the final Mousterian boundary in the trapezium model (Figure S26) was 40,580-39,240 cal BP (at 68.2% probability) and 40,900-37,890 cal BP (at 95.4%). This compares with the final boundary for the Uniform phase model in the main text (40,790-39,990 cal BP (68.2%) and 41,030-39,260 cal BP (95.4%). One can see considerable overlap in the ranges, with the trapezium model differing only in the wider range to younger ages.

In addition, we checked the robustness of the final Mousterian boundary (based on the latest boundaries for Mousterian sites described in the main paper) to test how sensitive it was to varying the priors in the model. We do not have reason to doubt the reliability of the individual PDFs (see below), but the test is useful to assess robustness. Spy appears to be the latest PDF in the

group of PDFs analysed. When we removed the Spy PDF from the model the final Mousterian PDF became 41,450-39,610 cal BP at 95.4% probability, compared with 41,030-39,260 cal BP when it is included. This means it is older at the earlier end of the range but shows no difference at the younger end. In statistical terms it is not significantly different. We also further tested the model by removing the Bombrini/Mochi boundary PDF from the model. The end boundary for the Mousterian then became 42,240-40,050 cal BP. Again, the various boundaries overlap markedly and are not statistically different from one another. The overall conclusion; that the Mousterian ended by ~40,000 cal BP, is not significantly different. In general, due to the challenges of decontaminating all samples for AMS dating, the PDF for the final Mousterian and last Neanderthals is more likely to become older rather than younger. It is worth remembering too that the direct date of the Saint-Césaire Neanderthal skeleton (OxA-18099) agrees closely with the Spy Neanderthal model results, suggesting that the modelled end boundary for Spy (in Model 1 above in the Spy section) is probably not aberrantly young. The comparison results are shown in Figure S27.

Finally, we also checked the reproducibility of different models by running them several times and comparing the posterior results. These disclosed acceptable levels of reproducibility when compared. We observed that key boundary parameters were usually within 50-100 years of one another with repeat model runs, even in models such as Arcy with high numbers of outlying likelihoods. We conclude that the data is reproducible.

Site	Cal range 68.2% probability		Cal range 95.4% probability	
Arcy-sur-Cure	44730	44060	45070	43720
Le Moustier	44180	41890	45090	40750
La Quina	43260	42350	43830	41960
St Césaire	43650	42200	44580	41580
Mandrin	44120	43210	44260	42590
Les Cottés	43290	42570	43810	42350
Pech de l'Azé IV	46700	46160	47040	45740
Abric Romaní	42980	41850	43160	41130
L'Arbreda	42350	41270	42710	40680
NW Iberia	47750	46390	47880	44820
Geissenklösterle	43060	41980	43860	41600
Bombrini - Mochi	41240	40800	41560	40500
Fumane	44600	44200	44800	43950

Castelcivita	45040	42530	45770	41300
Lakonis	45860	45020	46240	44330
Spy	40910	39880	41210	37830
Pin Hole	44230	42690	44570	42030
Hyaena Den	49930	48060	...	44270
Ksar Akil	42800	42100	43010	41680
Mezmaiskaya	41690	40180	42300	39220

Table S46: Summary of `boundary` data for each dated latest Mousterian context in this paper. These are the final end `boundaries` determined from each Bayesian model listed above. The Hyaena Den model falls at the limit of the calibration curve so does not produce any data for the entire range at 95.4% probability. Data is rounded to the nearest 10 years.

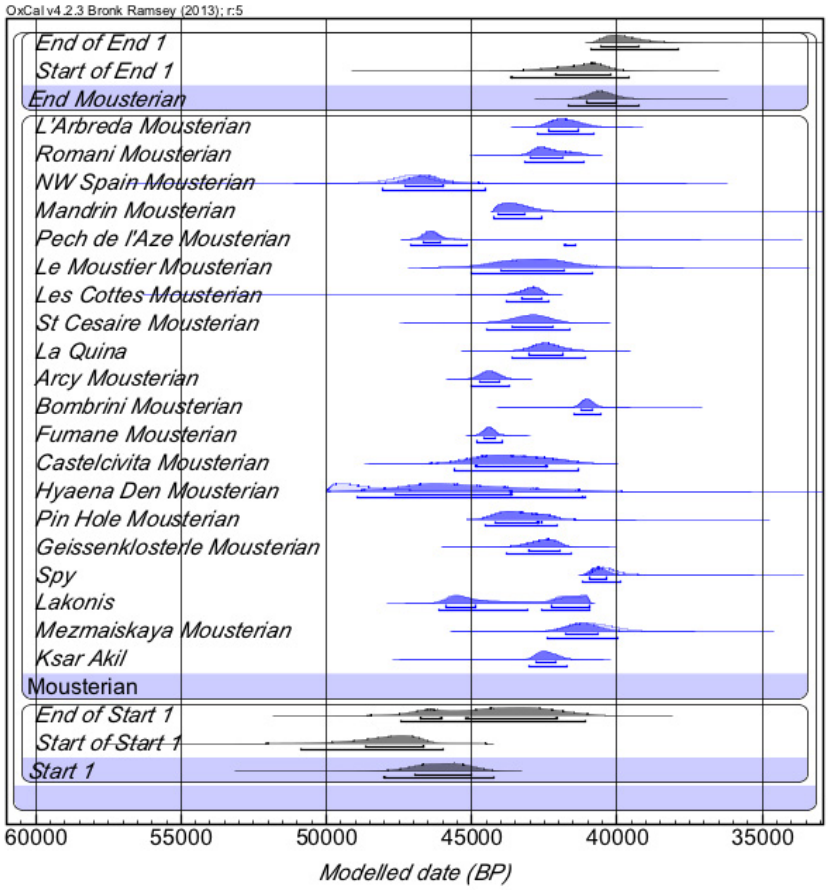

Figure S26: `Phase` model for Mousterian end boundaries using a `Trapezium` model.

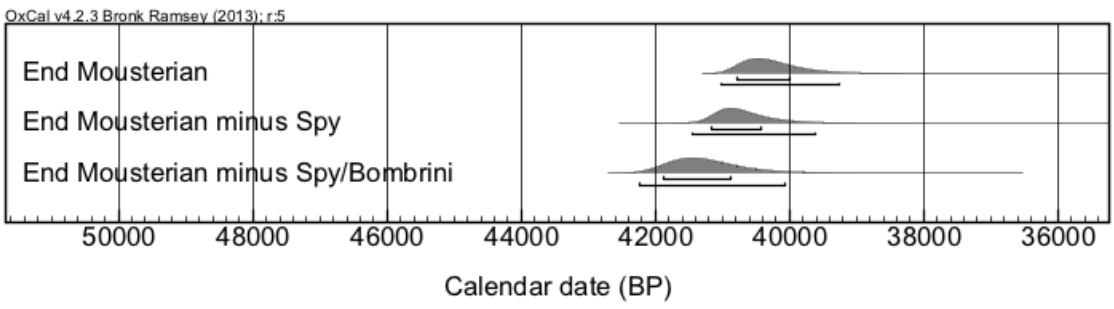

Figure S27: Comparison of the End Mousterian boundary and how it changes when the PDF data from Spy and then from Spy and Bombrini/Mochi is removed.

Bayesian CQL code

Arcy-sur-Cure

```
Options()
 {
  Resolution=20;
 };
 Plot()
 {
  Outlier_Model("General",T(5),U(0,4),"t");
  Sequence()
  {
   Boundary("XII");
   Phase("XII Mousterian")
   {
    R_F14C("OxA-21594",0.00996,0.00126)
    {
     Outlier("General", 0.05);
    };
    R_F14C("OxA-21595",0.00862,0.00127)
    {
     Outlier("General", 0.05);
    };
   };
   Boundary("Start XI");
   Phase("XI Mousterian")
   {
    R_Date("EVA-77*", 42120, 805)
    {
     Outlier("General", 0.05);
    };
    R_Date("EVA-83*", 41980, 821)
    {
     Outlier("General", 0.05);
    };
    R_Date("EVA-85*", 40900, 719)
    {
     Outlier("General", 0.05);
    };
   };
   Boundary("end XI/Start X");
   Phase("X + IX Chatelperronian")
   {
    R_Date("EVA-30*", 37980, 284)
```

```
{
 Outlier("General", 0.05);
};
R_Date("EVA-29*", 35500, 216)
{
 Outlier("General", 0.05);
};
R_Date("EVA-26*", 39390, 334)
{
 Outlier("General", 0.05);
};
R_Date("EVA-42*", 38070, 311)
{
 Outlier("General", 0.05);
};
R_Date("EVA-41*", 38730, 333)
{
 Outlier("General", 0.05);
};
R_F14C("OxA-21576",0.00621,0.00131)
{
 Outlier("General", 0.05);
};
R_F14C("OxA-21577",0.01338,0.00132)
{
 Outlier("General", 0.05);
};
R_Date("OxA-21590",21150,160)
{
 Outlier("General", 1.00);
};
R_F14C("OxA-21591",0.0132,0.00126)
{
 Outlier("General", 0.05);
};
R_F14C("OxA-21565",0.00895,0.00099)
{
 Outlier("General", 0.05);
};
R_F14C("OxA-21593",0.01231,0.00132)
{
 Outlier("General", 0.05);
};
R_F14C("OxA-X-2279-18",0.00639,0.001)
{
 Outlier("General", 0.05);
};
R_F14C("OxA-X-2279-45",0.00618,0.00102)
{
 Outlier("General", 0.05);
```

```
};
R_F14C("OxA-X-2279-46",0.00807,0.001)
{
 Outlier("General", 0.05);
};
R_Date("OxA-X-2222-21", 23120, 190)
{
 Outlier("General", 1.00);
};
R_F14C("OxA-X-2226-7",0.0083,0.00134)
{
 Outlier("General", 0.05);
};
R_F14C("OxA-21577",0.01338,0.00132)
{
 Outlier("General", 0.05);
};
R_F14C("OxA-21592",0.01102,0.00149)
{
 Outlier("General", 0.05);
};
R_F14C("OxA-X-2226-12",0.0057,0.00137)
{
 Outlier("General", 0.05);
};
R_F14C("OxA-X-2226-13",0.00782,0.00136)
{
 Outlier("General", 0.05);
};
R_F14C("OxA-X-2279-44",0.00233,0.00104)
{
 Outlier("General", 0.05);
};
R_Date("EVA-34*", 40520, 389)
{
 Outlier("General", 0.05);
};
R_Date("EVA-33*", 40970, 424)
{
 Outlier("General", 0.05);
};
R_F14C("OxA-21574",0.00794,0.00127)
{
 Outlier("General", 0.05);
};
R_F14C("OxA-21575",0.01837,0.00129)
{
 Outlier("General", 0.05);
};
};
```

```
Boundary("end X/Start IX");
Phase("VIII")
{
 R_Date("EVA-56*", 37710, 533)
 {
  Outlier("General", 0.05);
 };
 R_Date("EVA-55*", 36630, 452)
 {
  Outlier("General", 0.05);
 };
 R_F14C("OxA-21573",0.01018,0.0013)
 {
  Outlier("General", 0.05);
 };
 R_F14C("OxA-X-2279-14",0.01215,0.00112)
 {
  Outlier("General", 0.05);
 };
 R_F14C("OxA-21683",0.00684,0.00099)
 {
  Outlier("General", 0.05);
 };
};
Boundary("VIII/VII");
Phase("VII Aurignacian")
{
 R_F14C("OxA-21569",0.01062,0.00166)
 {
  Outlier("General", 0.05);
 };
 R_F14C("OxA-21570",0.01347,0.00137)
 {
  Outlier("General", 0.05);
 };
 R_F14C("OxA-21571",0.01444,0.00132)
 {
  Outlier("General", 0.05);
 };
 R_F14C("OxA-21572",0.01343,0.00127)
 {
  Outlier("General", 0.05);
 };
 R_F14C("OxA-21682",0.0128,0.001)
 {
  Outlier("General", 0.05);
 };
};
Boundary("VII/VI");
};
```

```
 Sequence()
 {
  Boundary("=end XI/Start X");
  Date("Arcy Chatelperronian");
  Boundary("=VIII/VII");
 };
 Sequence()
 {
  Boundary("=VIII/VII");
  Date("Arcy Protoaurignacian");
  Boundary("=VII/VI");
 };
 Sequence()
 {
  Boundary("=XII");
  Date("Arcy Mousterian");
  Boundary("=end XI/Start X");
 };
};
```

Le Moustier

```
Options()
 {
  Resolution=20;
 };
 Plot()
 {
  Outlier_Model("General",T(5),U(0,4),"t");
  Sequence()
  {
   Boundary("Start Level G");
   Phase("G MTA A")
   {
    Age("", N( 50300, 5500))
    {
     Outlier(0.05);
    };
    R_F14C("OxA-21790",0.00454,0.001)
    {
     Outlier(0.05);
    };
   };
   Boundary("Transition G/H");
   Phase("H MTA B")
   {
    R_F14C("OxA-21751",0.00412,0.00095)
    {
     Outlier(0.05);
```

```
 };
 R_F14C("OxA-21752",0.00359,0.00097)
 {
  Outlier(0.05);
 };
 Age("", N( 42500, 2000))
 {
  Outlier(0.05);
 };
 Age("", N( 46300, 3000))
 {
  Outlier(0.05);
 };
 R_F14C("OxA-21750",0.00198,0.00097)
 {
  Outlier(0.05);
 };
 R_F14C("OxA-21791",0.0037,0.00098)
 {
  Outlier(0.05);
 };
};
Boundary("Transition H/I");
Phase("I")
{
 R_F14C("OxA-21753",0.00457,0.00097)
 {
  Outlier(0.05);
 };
 Age("", N( 40900, 5000))
 {
  Outlier(0.05);
 };
};
Boundary("Transition I/J");
Phase("J Typical Mousterian")
{
 R_F14C("OxA-X-2300-19",0.00927,0.00102)
 {
  Outlier(0.05);
 };
 R_F14C("OxA-21754",0.00366,0.00104)
 {
  Outlier(0.05);
 };
 R_F14C("OxA-X-2300-21",0.00632,0.001)
 {
  Outlier(0.05);
 };
 R_F14C("OxA-21765",0.00635,0.00142)
```

```
   {
    Outlier(0.05);
   };
   Age("", N( 40300, 2600))
   {
    Outlier(0.05);
   };
   R_F14C("OxA-21789",0.00654,0.00097)
   {
    Outlier(0.05);
   };
  };
  Boundary("Transition J/K");
  Phase("K Chatelperronian")
  {
   Age("", N( 42600, 3200))
   {
    Outlier(0.05);
   };
  };
  Boundary("End Chatelperronian");
 };
 Sequence()
 {
  Boundary("=Start Level G");
  Date("Mousterian");
  Boundary("=Transition J/K");
 };
 Sequence()
 {
  Boundary("=Transition J/K");
  Date("Chatelperronian");
  Boundary("=End Chatelperronian");
 };
};
```

La Quina

```
Options()
 {
  Plot()
  {
   Outlier_Model("General",T(5),U(0,4),"t");
   Sequence()
   {
    Boundary("Start 8",U(-55000,-44000));
    Phase("8")
    {
     R_F14C("OxA-21807",0.00361,0.00099)
```

```
 {
  Outlier(0.05);
 };
 Age("", N( 44500, 3600))
 {
  Outlier(0.05);
 };
 Age("", N( 53000, 5000))
 {
  Outlier(0.05);
 };
 R_Date("AA-3637", 34200, 700)
 {
  Outlier(1.00);
 };
 R_Date("GrN-2526", 35250, 530)
 {
  Outlier(1.00);
 };
};
Boundary("8/7");
Phase("7")
{
 R_Date("OxA-22155", 48900, 3400)
 {
  Outlier(0.05);
 };
};
Boundary("7/6d");
Phase("6d")
{
 R_F14C("OxA-21808",0.00407,0.00098)
 {
  Outlier(0.05);
 };
};
Boundary("6d/6c");
Phase("6c")
{
};
Boundary("6c/6b");
Phase("6b")
{
};
Boundary("6b/6a");
Phase("6a")
{
 R_F14C("OxA-21806",0.01017,0.00098)
 {
  Outlier(0.05);
```

```
 };
 Age("", N( 43000, 3600))
 {
  Outlier(0.05);
 };
 R_Date("AA3638", 34450, 725)
 {
  Outlier(1.00);
 };
};
Boundary("6a/5");
Phase("5")
{
 R_F14C("OxA-21805",0.006,0.00099)
 {
  Outlier(0.05);
 };
};
Boundary("Transition 5/4b");
Phase("4b")
{
 R_F14C("OxA-22153",0.00939,0.00099)
 {
  Outlier(0.05);
 };
};
Boundary("4b/3");
Phase("3")
{
 R_F14C("OxA-16998",0.00588,0.00076)
 {
  Outlier(0.05);
 };
};
Boundary("3/2a");
Phase("2b")
{
 R_F14C("OxA-X-2326-22",0.00998,0.00103)
 {
  Outlier(0.05);
 };
};
Boundary("2a/1");
Boundary("Start Chat");
Phase("Chatelperronian")
{
 R_F14C("OxA-21706",0.00741,0.00096)
 {
  Outlier(0.05);
 };
```

```
    R_F14C("OxA-21707",0.00873,0.00099)
    {
     Outlier(0.05);
    };
   };
   Boundary("End Chat/start Aurign");
  };
  Sequence()
  {
   Boundary("=Start Chat");
   Date("Chatelperronian");
   Boundary("=End Chat/start Aurign");
  };
  Sequence()
  {
   Boundary("=Start 8");
   Date("Mousterian");
   Boundary("=2a/1");
  };
 };
};
```

Saint-Césaire

```
Options()
 {
  Resolution=20;
 };
 Plot()
 {
  Outlier_Model("General",T(5),U(0,4),"t");
  Sequence()
  {
   Boundary("Start EGF");
   Phase("EGF Denticulate Mousterian")
   {
    Age("", N( 42400, 4800))
    {
     Outlier(0.05);
    };
   };
   Boundary("EGF/EGP");
   Phase("EGP Denticulate Mousterian")
   {
    Age("", N( 38200, 3300))
    {
     Outlier(0.05);
    };
   };
```

```
Boundary("End EGP/Start EGPF");
Phase("EGPF Denticulate Mousterian")
{
 R_F14C("OxA-21638",0.00507,0.00134)
 {
  Outlier(0.05);
 };
 Age("", N( 40900, 2500))
 {
  Outlier(0.05);
 };
};
Boundary("Transition EGPF/EJOPinf");
Phase("EJOPinf Chatelperronian?")
{
 R_F14C("OxA-21637",0.00681,0.0016)
 {
  Outlier(0.05);
 };
};
Boundary("EJOPinf/EJOP sup");
Phase("Chatelperronian EJOP sup")
{
 Age("", N( 36300, 2700))
 {
  Outlier(0.05);
 };
 R_F14C("OxA-21636",0.00978,0.00125)
 {
  Outlier(0.05);
 };
 R_F14C("OxA-21699",0.01132,0.00098)
 {
  Outlier(0.05);
 };
 R_F14C("OxA-21700",0.01043,0.00097)
 {
  Outlier(0.05);
 };
 R_F14C("OxA-18099",0.01102,0.00102)
 {
  Outlier(0.05);
 };
};
Boundary("EJOP sup/EJO inf");
Phase("Aurignacian? EJO inf")
{
};
Boundary("EJO inf/EJO sup");
Phase("Proto Aurignacian EJO sup")
```

```
  {
   R_F14C("OxA-21633",0.01805,0.00133);
   {
    Outlier(0.05);
   };
   R_F14C("OxA-21628", 0.01572, 0.00101)
   {
    Outlier(0.05);
   };
   R_F14C("OxA-21634", 0.01381, 0.00131)
   {
    Outlier(0.05);
   };
   R_F14C("OxA-21635", 0.01584, 0.00134)
   {
    Outlier(0.05);
   };
   R_F14C("OxA-21629", 0.01448, 0.00101)
   {
    Outlier(0.05);
   };
   Age("", N( 32100, 3000))
   {
    Outlier(0.05);
   };
  };
  Boundary("EJO sup/EJF");
 };
 Sequence()
 {
  Boundary("=Start EGF");
  Date("Mousterian");
  Boundary("=Transition EGPF/EJOPinf");
 };
 Sequence()
 {
  Boundary("=EJO inf/EJO sup");
  Date("Protoaurignacian");
  Boundary("=EJO sup/EJF");
 };
};
```

Grotte Mandrin

```
Options()
 {
  Resolution=20;
 };
```

```
{
 Plot()
 {
  Outlier_Model("General",T(5),U(0,4),"t");
  Sequence()
  {
   Boundary("Start G Ferrassie");
   Phase("G Ferrassie Mousterian")
   {
    Age("TL ave", N(52000,3350))
    {
     Outlier(0.05);
    };
   };
   Boundary("G Ferrassie/F Quina");
   Phase("F Quina")
   {
   };
   Boundary("F Quina/E Neronian");
   Phase("E Neronian")
   {
    Date("Neronian");
   };
   Boundary("Neronian/D post-Neronian I");
   Phase("D post Neronian I")
   {
   };
   Boundary("End of D post-Neronian I");
   Boundary("Transition D/C");
   Phase("C post-Neronian II")
   {
    R_F14C("OxA-X-2286-14", 0.00485, 0.00108)
    {
     Outlier(0.05);
    };
    R_F14C("OxA-X-2286-13", 0.00463, 0.00113)
    {
     Outlier(0.05);
    };
   };
   Boundary("C end/start sterile");
   Boundary("End sterile/start B post-Neronian II");
   Phase("post-Neronian II")
   {
    R_F14C("OxA-22120", 0.00448, 0.00102)
    {
     Outlier(0.05);
    };
    R_F14C("OxA-21685", 0.00781, 0.001)
    {
```

```
     Outlier(0.05);
    };
    R_F14C("OxA-X-2286-10", 0.00832, 0.00101)
    {
     Outlier(0.05);
    };
    Age("TL ave", N(35000,1600))
    {
     Outlier(0.05);
    };
    R_F14C("OxA-21690", 0.0056, 0.00098)
    {
     Outlier(0.05);
    };
    R_F14C("OxA-22121", 0.00666, 0.00098)
    {
     Outlier(0.05);
    };
    R_F14C("OxA-21691", 0.00354, 0.00096)
    {
     Outlier(0.05);
    };
   };
   Boundary("B1/Sterile level");
  };
 };
};
```

Abric Romani

```
Options()
 {
  Resolution=20;
 };
 Plot()
 {
  Outlier_Model("General",T(5),U(0,4),"t");
  Sequence()
  {
   Boundary("Start sequence");
   Phase("Trav >J")
   {
    Age ("", N( 50400, 2600))
    {
     Outlier(0.05);
    };
   };
   Boundary("Transition Trav >J/J");
   Phase("J")
   {
```

```
 R_Date("NZA-2316", 47100, 2100)
 {
  Outlier(0.05);
 };
};
Boundary("Transition J/Trav J-I");
Phase("Trav J-I")
{
 Age("", N( 46500, 1500))
 {
  Outlier(0.05);
 };
 Age("", N( 48600, 2300))
 {
  Outlier(0.05);
 };
 Age("", N( 46900, 2600))
 {
  Outlier(0.05);
 };
 Age("", N( 46300, 2400))
 {
  Outlier(0.05);
 };
 Age("", N( 48000, 1600))
 {
  Outlier(0.05);
 };
 Age("", N( 49200, 3300))
 {
  Outlier(0.05);
 };
 Age("", N( 47400, 2500))
 {
  Outlier(0.05);
 };
 Age("", N( 49300, 2700))
 {
  Outlier(0.05);
 };
 Age("", N( 49300, 1600))
 {
  Outlier(0.05);
 };
 Age("", N( 49200, 2900))
 {
  Outlier(0.05);
 };
};
Boundary("Transition Trav I-J/I");
```

```
Phase("I")
{
};
Boundary("Transition I/Trav H-I");
Phase("Trav H-I")
{
 Age("", N( 45100, 3100))
 {
  Outlier(0.05);
 };
};
Boundary("Transition Trav H-I/H");
Phase("H")
{
 R_Date("NZA-2315", 44500, 1200)
 {
  Outlier(0.05);
 };
 R_Date("CAMS-", 44100, 5900)
 {
  Outlier(0.05);
 };
};
Boundary("Transition G/H");
Phase("G")
{
};
Boundary("Transition F/G");
Phase("F")
{
};
Boundary("Transition E/F");
Phase("E")
{
 R_Date("NZA-2314", 43200, 1100)
 {
  Outlier(0.05);
 };
};
Boundary("Transition E/Trav D-E");
Phase("Trav D-E")
{
 Age("", N( 44900, 2500))
 {
  Outlier(0.05);
 };
};
Boundary("Transition Trav D-E/D");
Phase("D")
{
```

```
 R_Date("NZA-2313", 40680, 940)
 {
  Outlier(0.05);
 };
};
Boundary("Transition D/Trav D-C");
Phase("Trav D-C")
{
};
Boundary("Transition Trav D-C/C");
Phase("C")
{
};
Boundary("Transition C/B");
Phase("B")
{
 R_Date("NZA-2312", 43500, 1200)
 {
  Outlier(0.05);
 };
 R_F14C("OxA-12025", 0.00770, 0.00030)
 {
  Outlier(0.05);
 };
};
Boundary("Transition B/Trav AR6 AR3");
Phase("Trav AR6 AR3")
{
 Age("AR3 avge U series age", N( 42700, 1300))
 {
  Outlier(0.05);
 };
 R_Date("USGS-2840", 35000, 500)
 {
  Outlier(0.05);
 };
};
Boundary("Transition Trav AR6 AR3/A");
Phase("A")
{
 R_Date("NZA-1817", 28440, 650)
 {
  Outlier(0.90);
 };
 R_Date("AA-8037A", 35400, 810)
 {
  Outlier(0.05);
 };
 R_Date("AA-8037B", 37900, 1000)
 {
```

```
 Outlier(0.05);
};
R_Date("NZA-2311", 36590, 640)
{
 Outlier(0.05);
};
R_Date("AA-7395", 37290, 990)
{
 Outlier(0.05);
};
R_Date("NZA-1818", 23160, 490)
{
 Outlier(0.95);
};
R_Date("OxA-11967", 35900, 600)
{
 Outlier(0.05);
};
R_Date("AA-6608", 36740, 920)
{
 Outlier(0.05);
};
R_F14C("OxA-X-2095-46", 0.01060, 0.00030)
{
 Outlier(0.05);
};
R_Date("UA1", 37200, 900)
{
 Outlier(0.05);
};
R_Date("UA2", 35400, 800)
{
 Outlier(0.05);
};
R_Date("UA3", 37900, 1000)
{
 Outlier(0.05);
};
};
Boundary("Transition A/AR1 AR4");
Phase("Trav AR1 AR4")
{
R_Date("USGS-2839", 36300, 1300)
{
 Outlier(0.05);
};
Age("AR4 MS average age", N( 42600, 1100))
{
 Outlier(0.05);
};
```

```
  };
  Boundary("End Trav AR1 AR4");
 };
 Sequence()
 {
  Boundary("=Start sequence");
  Date("Mousterian");
  Boundary("=Transition B/Trav AR6 AR3");
 };
};
```

L'Arbreda

```
Options()
 {
 Resolution=20;
};
 Plot()
 {
 Outlier_Model("General",T(5),U(0,4),"t");
 Outlier_Model("SSimple",N(0,2),0,"s");
 Sequence()
 {
  Boundary("Base I");
  Phase("I")
  {
   R_F14C("OxA-19994", 0.00846, 0.00044)
   {
    Outlier("General", 0.05);
   };
   R_F14C("OxA-21704", 0.00761, 0.00096)
   {
    Outlier("General", 0.05);
   };
   R_F14C("OxA-21702", 0.00399, 0.00096)
   {
    Outlier("General", 0.05);
   };
   R_F14C("OxA-21662", 0.00959, 0.00098)
   {
    Outlier("General", 0.05);
   };
   R_Combine("P21480")
   {
    Outlier("General", 0.05);
    R_F14C("OxA-21663", 0.01838, 0.00101)
    {
     Outlier("SSimple", 0.05);
    };
```

```
 R_F14C("OxA-21703", 0.01789, 0.00099)
 {
  Outlier("SSimple", 0.05);
 };
};
};
Boundary("I top");
Boundary("H base");
Phase("H")
{
 R_F14C("OxA-21674", 0.0149, 0.00099)
 {
  Outlier("General", 0.05);
 };
 R_F14C("OxA-21664", 0.01149, 0.00096)
 {
  Outlier("General", 0.05);
 };
 R_F14C("OxA-21665", 0.01152, 0.00099)
 {
  Outlier("General", 0.05);
 };
 R_F14C("OxA-21784", 0.01129, 0.001)
 {
  Outlier("General", 0.05);
 };
 R_Date("SANU-29018", 32100, 540)
 {
  Outlier("General", 0.05);
 };
 R_Date("SANU-29016", 35700, 830)
 {
  Outlier("General", 0.05);
 };
 R_Date("SANU-29014", 31900, 530)
 {
  Outlier("General", 0.05);
 };
 R_Combine("ABD11")
 {
  Outlier("General", 0.05);
  R_Date("SANU-29017", 34800, 760)
  {
   Outlier("SSimple", 0.05);
  };
  R_Date("SANU-29019", 35900, 860)
  {
   Outlier("SSimple", 0.05);
  };
 };
```

```
 };
 Boundary("H top");
 Boundary("G base");
 Phase("G")
 {
  R_F14C("OxA-21666", 0.01694, 0.00098)
  {
   Outlier("General", 0.05);
  };
  R_F14C("OxA-21667", 0.018, 0.00097)
  {
   Outlier("General", 0.05);
  };
  R_F14C("OxA-21783", 0.01841, 0.00102)
  {
   Outlier("General", 0.05);
  };
 };
 Boundary("G top");
 Boundary("F base");
 Phase("F")
 {
  R_F14C("OxA-21781", 0.02967, 0.00103)
  {
   Outlier("General", 0.05);
  };
  R_F14C("OxA-21782", 0.02958, 0.00106)
  {
   Outlier("General", 0.05);
  };
 };
 Boundary("F top");
 Boundary("E base");
 Phase("E")
 {
  R_F14C("OxA-21668", 0.03883, 0.00103)
  {
   Outlier("General", 0.05);
  };
  R_F14C("OxA-21669", 0.04037, 0.00107)
  {
   Outlier("General", 0.05);
  };
 };
 Boundary("E top");
};
};
```

Labeko Koba

```
Options()
 {
 Resolution=20;
};
 {
 Plot()
 {
 Outlier_Model("SSimple",N(0,2),0,"s");
 Outlier_Model("General",T(5),U(0,4),"t");
 Sequence()
 {
 Boundary("Start base");
 Phase("Pre Chatelperron points)")
 {
 R_F14C("OxA-22564", 0.00892, 0.001)
 {
 Outlier("General", 0.05);
 };
 };
 Boundary("Below/Chatelperron points");
 Phase("Level IX lower (Chatelperron points)")
 {
 R_F14C("OxA-22560", 0.00952, 0.001)
 {
 Outlier("General", 0.05);
 };
 R_F14C("OxA-22561", 0.00878, 0.00099)
 {
 Outlier("General", 0.05);
 };
 R_F14C("OxA-22562", 0.00871, 0.00098)
 {
 Outlier("General", 0.05);
 };
 R_F14C("OxA-22563", 0.00901, 0.00098)
 {
 Outlier("General", 0.05);
 };
 };
 Boundary("IX lower/IX upper");
 Phase("Level IX upper")
 {
 R_Combine("P27311 comb")
 {
 Outlier("General", 0.05);
 R_F14C("OxA-22559", 0.01134, 0.00101)
 {
 Outlier("SSimple", 0.05);
 };
```

```
     R_F14C("OxA-22653", 0.01019, 0.00099)
     {
      Outlier("SSimple", 0.05);
     };
    };
    R_F14C("OxA-23199", 0.00838, 0.00096)
    {
     Outlier("General", 0.05);
    };
    R_F14C("OxA-21777", 0.00919, 0.00101)
    {
     Outlier("General", 0.05);
    };
    R_F14C("OxA-21792", 0.01056, 0.00097)
    {
     Outlier("General", 0.05);
    };
   };
   Boundary("End IX");
  };
 };
};
```

Geißenklösterle

```
Options()
 {
  Resolution=20;
 };
{
  Plot()
  {
   Outlier_Model("General",T(5),U(0,4),"t");
   Sequence()
   {
    Boundary("Start 1");
    Phase("VII")
    {
     R_F14C("OxA-21741", 0.00237, 0.00094)
     {
      Outlier(0.05);
     };
    };
    Boundary("Transition from VII to IV");
    Boundary("Transition V/IV");
    Phase("IV")
    {
     R_F14C("OxA-21720", 0.01202, 0.00096)
     {
      Outlier(0.05);
```

```
 };
 Age("ESR mean", N( 42700, 1300))
 {
  color="red";
  Outlier(0.05);
 };
};
Boundary("Transition IV/Sterile");
Phase("Sterile")
{
 R_F14C("OxA-21657", 0.0074, 0.00097)
 {
  Outlier(0.05);
 };
 R_F14C("OxA-21658", 0.00853, 0.00097)
 {
  Outlier(0.05);
 };
};
Boundary("Transition Sterile/IIIc");
Phase("III")
{
 R_F14C("OxA-21723", 0.009, 0.00095)
 {
  Outlier(1.00);
 };
 R_F14C("OxA-21659**", 0.01274, 0.00099)
 {
  Outlier(0.05);
 };
 R_F14C("OxA-21721**", 0.00967, 0.00098)
 {
  Outlier(0.05);
 };
 R_F14C("OxA-21743**", 0.01117, 0.00097)
 {
  Outlier(0.05);
 };
 R_F14C("OxA-21722", 0.00787, 0.00095)
 {
  Outlier(1.00);
 };
 R_F14C("OxA-21745", 0.01041, 0.00099)
 {
  Outlier(1.00);
 };
 R_F14C("OxA-21746**", 0.01018, 0.00099)
 {
  Outlier(0.05);
 };
```

```
 R_F14C("OxA-21725", 0.00953, 0.00095)
 {
  Outlier(1.00);
 };
 R_F14C("OxA-21744", 0.0102, 0.00098)
 {
  Outlier(1.00);
 };
 R_F14C("OxA-21726**", 0.01414, 0.00097)
 {
  Outlier(0.05);
 };
 Age("TL mean", N( 40200, 1500))
 {
  color="red";
  Outlier(0.05);
 };
 Interval("Interval AHIII");
};
Boundary("Transition III/II");
Phase("II")
{
 R_F14C("OxA-21742", 0.01314, 0.00099)
 {
  Outlier(1.00);
 };
 R_F14C("OxA-21727**", 0.01432, 0.00096)
 {
  Outlier(0.05);
 };
 R_F14C("OxA-21724**", 0.0146, 0.00097)
 {
  Outlier(0.05);
 };
 R_F14C("OxA-21737", 0.01175, 0.00098)
 {
  Outlier(1.00);
 };
 R_F14C("OxA-21738**", 0.01302, 0.00099)
 {
  Outlier(0.05);
 };
 R_F14C("OxA-21661", 0.01661, 0.00098)
 {
  Outlier(0.05);
 };
 R_F14C("OxA-21656", 0.01647, 0.00099)
 {
  Outlier(1.00);
 };
```

```
    Interval("Interval AHII");
   };
   Boundary("End Aurignacian");
   Phase("Gravettian")
   {
    R_Date("OxA-21739", 28600, 290)
    {
     Outlier(0.05);
    };
    R_Date("OxA-21660", 27960, 290)
    {
     Outlier(0.05);
    };
    R_Date("OxA-21740", 26420, 230)
    {
     Outlier(0.05);
    };
   };
   Boundary("End");
   Axis(-52923.5, -26574.5);
  };
  Sequence()
  {
   Boundary("=Transition V/IV");
   Date("Mousterian");
   Boundary("=Transition IV/Sterile");
  };
  Sequence()
  {
   Boundary("=Transition Sterile/IIIc");
   Date("Aurignacian I");
   Boundary("=End Aurignacian");
  };
 };
};
```

Cavallo

```
Options()
 {
  Curve("Marine13","Marine13.14c");
  Delta_R("LocalMarine",58,85);
  Outlier_Model("SSimple",N(0,2),0,"s");
  Outlier_Model("General",T(5),U(0,4),"t");
  Resolution=30;
 };
 Plot()
 {
  Sequence("Cavallo")
  {
```

```
Boundary("F/E");
Phase("E III")
{
 Date("E_III_date");
};
Boundary("EII-I");
Phase("E II-I")
{
 R_Date("OxA-19242", 0.00689, 0.00029)
 {
  Outlier("General", 0.05);
 };
};
Boundary("Transition E II-I/E-D");
Phase("E-D")
{
 R_Combine("Cvl 5")
 {
  Outlier("General", 0.05);
  R_F14C("OxA-19256", 0.00773, 0.0003)
  {
   Outlier("SSimple", 0.05);
  };
  R_F14C("OxA-X-2280-16", 0.00849, 0.00042)
  {
   Outlier("SSimple", 0.05);
  };
 };
};
Boundary("E-D/ DII");
Phase("D II")
{
 R_F14C("OxA-19258", 0.01131, 0.00057)
 {
  Outlier("General", 0.05);
 };
 R_F14C("OxA-19257", 0.00513, 0.00025)
 {
  Outlier("General", 0.20);
 };
};
Boundary("DII/DIb");
Phase("D I")
{
 Sequence("D Ib")
 {
  R_F14C("OxA-20631", 0.01027, 0.00039)
  {
   Outlier("General", 0.05);
  };
```

```
    R_F14C("OxA-19255", 0.01095, 0.00035)
    {
     Outlier("General", 0.05);
    };
    R_F14C("OxA-19254", 0.01269, 0.00036)
    {
     Outlier("General", 0.05);
    };
   };
  };
  Boundary("DI/ CI");
  Phase("CI")
  {
   C_Date("CI", -37330, 110);
  };
  Boundary("CI - B");
 };
};
```

Fumane

```
Options()
 {
  Resolution=20;
  Curve="IntCal09.14c";
 };
 Plot()
 {
  Outlier_Model("General",T(5),U(0,4),"t");
  Sequence("Grotta di Fumane")
  {
   Boundary("A5+A6");
   Phase("A5+A6 Mousterian")
   {
    R_F14C("OxA-21757", 0.00573, 0.00104)
    {
     Outlier(0.05);
    };
    R_F14C("OxA-17566", 0.0065, 0.00029)
    {
     Outlier(0.05);
    };
    R_F14C("OxA-21758", 0.00597, 0.00097)
    {
     Outlier(0.05);
    };
    R_F14C("OxA-21809", 0.00672, 0.00101)
    {
     Outlier(0.05);
```

```
 };
};
Boundary("start A5");
Phase("A5 Mousterian")
{
 R_F14C("OxA-17980", 0.00675, 0.00029)
 {
  Outlier(0.05);
 };
 R_F14C("OxA-21712", 0.00688, 0.00096)
 {
  Outlier(0.05);
 };
 R_F14C("OxA-X-2275-45", 0.00561, 0.00045)
 {
  Outlier(0.05);
 };
};
Boundary("A5-A4");
Phase("A4 Uluzzian")
{
 R_F14C("OxA-21733", 0.00606, 0.00097)
 {
  Outlier(0.05);
 };
 R_F14C("OxA-21734", 0.00536, 0.00095)
 {
  Outlier(0.05);
 };
 R_F14C("OxA-21735", 0.00534, 0.00114)
 {
  Outlier(0.05);
 };
 Interval(A4);
};
Boundary("A4-A3");
Phase("A3 Uluzzian")
{
 R_F14C("OxA-2295-52", 0.00585, 0.00095)
 {
  Outlier(0.05);
 };
 R_F14C("OxA-21736", 0.00774, 0.00096)
 {
  Outlier(0.05);
 };
 Interval(A3);
};
Boundary("A3-A2");
Phase("A2 'Proto Aurignacian")
```

```
  {
   R_F14C("OxA-17569", 0.01184, 0.00033)
   {
    Outlier(0.05);
   };
   R_F14C("OxA-17570", 0.01254, 0.00034)
   {
    Outlier(0.05);
   };
   R_F14C("OxA-19584", 0.01153, 0.00044)
   {
    Outlier(0.05);
   };
   R_F14C("OxA-19414", 0.01419, 0.00048)
   {
    Outlier(0.05);
   };
   R_F14C("OxA-19412", 0.0129, 0.00045)
   {
    Outlier(0.05);
   };
   R_F14C("OxA-21796", 0.0122, 0.00113)
   {
    Outlier(0.05);
   };
  };
  Boundary("A2-A1");
 };
 Sequence()
 {
  Boundary("=A5+A6");
  Date("Mousterian");
  Boundary("=A5-A4");
 };
 Sequence()
 {
  Boundary("=A5-A4");
  Date("Uluzzian");
  Boundary("=A3-A2");
 };
};
```

Ksar Akil (Mousterian only)

```
Options()
 {
  Outlier_Model("General",T(5),U(0,4),"t");
  Resolution=80;
 };
```

```
Plot()
{
 Sequence("Ksar Akil 1")
 {
  Boundary("Start Mousterian");
  Sequence("Mousterian")
  {
   Phase("XXXII")
   {
    Age("G-88177 ", N(51000, 4000))
    {
     Outlier("General", 0.05);
    };
    Age("G-88174", N(47000, 9000))
    {
     Outlier("General", 0.05);
    };
   };
   Boundary("XXII-XXVIII");
   Phase("XXVIII-XXVII")
   {
    Curve("IntCal13","IntCal13.14c");
    R_Date("Gro-2574/75", 44400, 1200)
    {
     Outlier("General", 0.05);
    };
    R_Date("GrN-2579", 43750, 1500)
    {
     Outlier("General", 0.05);
    };
    Curve("Marine13","Marine13.14c");
    Delta_R("LocalMarine",58,85);
    R_F14C("OxA-25656", 0.00729, 0.00030)
    {
     Outlier("General", 0.05);
    };
    R_F14C("OxA-20491", 0.00750, 0.00031)
    {
     Outlier("General", 0.05);
    };
   };
  };
  Boundary("XXVII/S.C. 1");
  Phase("Stone Complex 1")
  {
  };
  Boundary("Start Ksar Akil Phase 1");
 };
};
```

Mezmaiskaya

```
Options()
 {
 Resolution=20;
};
 Plot()
 {
 Outlier_Model("General",T(5),U(0,4),"t");
 Outlier_Model("SSimple",N(0,2),0,"s");
 Sequence()
 {
  Boundary("Transition 2A/2");
  Phase("2")
  {
   R_F14C("OxA-21822", 0.00114, 0.00102)
   {
    Outlier("General", 0.05);
   };
   R_F14C("OxA-21823", 0.0028, 0.00098)
   {
    Outlier("General", 0.05);
   };
   R_F14C("OxA-21824", 0.00672, 0.00099)
   {
    Outlier("General", 0.05);
   };
   R_F14C("OxA-21825", 0.00393, 0.00099)
   {
    Outlier("General", 0.05);
   };
   R_Combine()
   {
    Outlier("General", 0.05);
    R_F14C("OxA-21826 ", 0.00864, 0.001)
    {
     Outlier("SSimple", 0.05);
    };
    R_F14C("OxA-21827", 0.00859, 0.00103)
    {
     Outlier("SSimple", 0.05);
    };
   };
   R_F14C("OxA-21836", 0.01102, 0.00101)
   {
    Outlier("General", 0.05);
   };
   R_F14C("OxA-21839", 0.00716, 0.00095)
   {
    Outlier("General", 0.05);
```

```
  };
 };
 Boundary("End of Middle Palaeolithic");
 Boundary("Transition 2/1C");
};
Sequence()
{
 Boundary("=Transition 2A/2");
 Date("Mousterian");
 Boundary("=End of Middle Palaeolithic");
};
};
```

Acknowledgements

This research was funded by a grant from the UK's Natural Environment Research Council (NERC) (NE/D014077/1: "Dating of the Middle-Upper Palaeolithic transition in western Europe using ultrafiltration AMS radiocarbon"). Rachel Wood was funded by a tied DPhil scholarship to this grant. Other funding (Roger Jacobi (2002-2009) and Katerina Douka (from 2012-13)) was provided by the Ancient Human Occupation of Britain (AHOB) project (of the Leverhulme Trust), the European Research Council (ERC-2012-AdG-324139), the Leventis Foundation and the I.K.Y. Scholarships Foundation (Greece)(KD).

Other dating, at the sites of La Güelga, Esquilleu, Morín and Lezetxiki, has been financed by the ministerial projects (HUM2004-04679 and HAR2010-22013). The SSHRC (Canada) provided funding for some of the Saint-Césaire dates (standard research grant #55-51925, to Eugène Morin).

We are grateful to Prof. C. Stringer at The Natural History Museum of London for his invaluable and continued support of our research (and particularly that of Roger Jacobi), through AHOB, as well as the core AHOB group for funding some AMS determinations over the last few years. In this light we thank Drs N. Ashton (The British Museum, London), A. Currant (The Natural History Museum, London) and Profs. J. Rose and D. Schreeve (Royal Holloway, University of London).

The National Radiocarbon Facility (NRCF) programme of the NERC and AHRC provided funding for the dating of Palaeolithic shell samples (R.E.M. Hedges and K. Douka) as well as charcoal from Castelcivita (R.Wood, K. Douka, T. Higham).

TH, RW and KD acknowledge the support and funding of Keble College, Oxford.

We thank the staff of the Oxford Radiocarbon Accelerator Unit (ORAU) for their contribution to this work, especially C. Tompkins, A. Bowles, M. Humm, B. Emery, P. Leach, J. Davies, P. Ditchfield and J. Graystone. We acknowledge the support of the members of the Research Laboratory for Archaeology and the History of Art (RLAHA).

We thank our many collaborators and their excavation teams who provided archaeological samples for dating for the project and helped in selecting material with us for AMS dating. We acknowledge museum and university curators for their cooperation in providing permission for destructive sampling particularly J-J. Cleyet-Merle, K. Schwab, A. Arellano, M. Gorgonioli, I. Jadin, A. Belen Marin, M. Malina, C. Finlayson and his team in the Gibraltar Museum, and P. Mennecier.

We are grateful to several colleagues for useful discussions, help and advice over the last few years, including P. Mellars, R. White, B. Gravina, D. Arnaud, R.E.M. Hedges, N. Ashton, M. Chapman, F. Wesselingh, A. Sinitsyn, V. Dujardin, P. Ambert, F. Bazile, I. Turq, W. Roebroeks, A. Currant, A. Delagnes, M. Petraglia, N. Barton and W. Davies, as well as all delegates to our 2011 Oxford project conference "*Time for the Palaeolithic*". We thank the many students who helped us during site and institution visits, particularly Ursula Wierer, Filomena Ranaldo, H. Klemperova, Matteo Romandini, Francesca Zeppieri, Aurelie Fort and Enza Spinapolice, and the students and workers from all of the excavation teams involved.

The late Javier Fortea, excavator of La Viña, would have been a co-author on this paper and we acknowledge his seminal contribution to the archaeology of northern Spain.

We dedicate this paper to the memory of our close friend and colleague Roger Jacobi who passed away in 2009, during the course of the project.

Supplementary references

[1] Brock, F., Higham, T.F.G., Ditchfield, P and Bronk Ramsey, C. 2010. Current Pretreatment Methods for AMS Radiocarbon Dating at the Oxford Radiocarbon Accelerator Unit (ORAU). *Radiocarbon* 52(1): 103-112.

[2] Bird M.I., et al. 1999. Radiocarbon dating of 'old' charcoal using a wet oxidation-stepped combustion procedure. *Radiocarbon* 41: 127–140.

[3] Bird, M.I., Levchenko, V., Ascough, P.L., Meredith, W., Wurster, C.M., Williams, A., Tilston, E.L., Snape, C.E. and Apperley, D.C. 2014. The efficiency of charcoal decontamination for radiocarbon dating by three pre-treatments – ABOX, ABA and hypy, *Quaternary Geochronology* 22: 25-32.

[4] Wood, R.E., Douka, K., Boscato, P., Haesaerts, P., Sinitsyn, A and Higham, T.F.G. 2012. Testing the ABOx-SC method: dating known age charcoals associated with the Campanian Ignimbrite. *Quaternary Geochronology* 9: 16—26.

[5] Douka, K., Higham, T. and Sinitsyn, A. 2010. The influence of pretreatment chemistry on the radiocarbon dating of Campanian Ignimbrite-aged charcoal from Kostenki 14 (Russia). *Quaternary Research,* 73 (3): 583-587.

[6] Douka, K., Hedges, R.E.M. and Higham, T.F.G. 2010. Improved AMS ^{14}C dating of shell carbonates using high-precision X-Ray Diffraction (XRD) and a novel density separation protocol (CarDS). *Radiocarbon* 52(2–3): 735–751.

[7] Bronk Ramsey, C., Higham, T.F.G, Bowles, A., Hedges, R. 2004. Improvements to the pretreatment of bone at Oxford. *Radiocarbon*, 46, 155-163.

[8] Higham, T.F.G., Jacobi, R.M. and Bronk Ramsey, C. 2006. AMS radiocarbon dating of ancient bone using ultrafiltration. *Radiocarbon*, 48(2), 179-195.

[9] Wood, R.E., Bronk Ramsey, C. and Higham, T.F.G. 2010. Refining the ultrafiltration bone pretreatment background for radiocarbon dating at ORAU. *Radiocarbon* 52(2–3): 600–611.

[10] Stuiver, M and Polach, H. A. 1977. Discussion: Reporting of ^{14}C Data. *Radiocarbon* 19: 355-363.

[11] Bronk Ramsey, C. 2009. Bayesian analysis of radiocarbon dates. *Radiocarbon* 51(1): 337-360.

[12] Reimer, P.J., Bard, E., Bayliss, A., Beck, J.W., Blackwell, P.G., Bronk Ramsey, C., Grootes, P.M., Guilderson, T.P., Haflidason, H., Hajdas, I., Hatté, C., Heaton, T.J., Hoffmann, D.L., Hogg, A.G., Hughen, K.A., Kaiser, K.F., Kromer, B., Manning, S.W., Mu Niu, Reimer, R.W., Richards, D.A., Scott, E.M., Southon, J.R., Staff, R.A., Turney, C.S.M. and van der Plicht., J. 2013. IntCal13 and Marine13 Radiocarbon Age Calibration Curves 0–50,000 Years cal BP. *Radiocarbon* 55(4): 1869-1887.

[13] Muscheler, R., Adolphi, F. and Svensson, A. 2014. Challenges in ^{14}C dating towards the limit of the method inferred from anchoring a floating tree ring radiocarbon chronology to ice core records around the Laschamp geomagnetic field minimum. *Earth and Planetary Science Letters* 394: 209–215.

[14] Bronk Ramsey, C. 2009b. Dealing with outliers and offsets in radiocarbon dating. *Radiocarbon*, 51(3), 1023-1045.

[15] Galbraith, R.F. and Roberts, R.G. 2012. Statistical aspects of equivalent dose and error calculation and display in OSL dating: An overview and some recommendations. *Quaternary Geochronology* 11:1-27.

[16] Rhodes, E.J., Bronk Ramsey, C., Outram, Z., Batt, C., Willis, L., Dockrill, S. and Bond, J. 2003. Bayesian methods applied to the interpretation of multiple OSL dates: high precision sediment ages from Old Scatness Broch excavations, Shetland Isles. *Quaternary Science Reviews* 22(10-13): 1231-1244.

[17] Douka, K., Grün, R., Jacobs, Z., Lane, C., Farr, L., Hunt, C., Inglis, R.H., Reynolds, T., Albert, P., Aubert, M., Cullen, V., Hill, E., Kinsley, L., Roberts, R.G., Tomlinson, E.L., Wulf, S., Barker, G. 2014. The chronostratigraphy of the Haua Fteah cave (Cyrenaica, northeast Libya). *Journal of Human Evolution* 66: 39-63.
[18] Bar-Yosef, O., Kuhn, S.L., 1999. The big deal about blades: Laminar technologies and human evolution. *American Anthropologist* 101: 322–338.
[19] Bordes, F. 1961. Mousterian cultures in France. *Science* 134: 803–810.
[20] Conard, N. 1990. Laminar lithic assemblages from the last interglacial complex in northwestern Europe. *Journal of Anthropological Research* 46: 243–262.
[21] Révillon S., Tuffreau A. (Eds.) 1994. *Les industries laminaires au Paléolithique Moyen*. CNRS, Paris.
[22] d'Errico F., 2003. The invisible frontier. A multiple species model for the origin of behavioral modernity. *Evolutionary Anthropology* 12: 188–202.
[23] Clark, G. 2007. Putting Transition Research in a Broader Context. In Riel-Salvatore J., Clark, G. (Eds.), *New Approaches to the Study of Early Upper Paleolithic 'Transitional' Industries in Western Eurasia: Transitions Great and Small*. BAR International Series 1620, Oxford: 143–178.
[24] Slimak, L. 2008. Sur un point de vue heuristique concernant la production et la transformation de supports au Paléolithique moyen. *Gallia Préhistoire* 50: 1–22.
[25] Bordes, F. 1950. Principes d'une méthode d'étude des techniques de débitage et de la typologie du Paléolithique ancien et moyen. *L'Anthropologie* 54: 19–34.
[26] Binford, L.R. and Binford, S.R. 1966. A preliminary analysis of functional variability in the Mousterian of Levallois facies. *American Anthropologist* 68 (2): 238–295.
[27] Binford, S.R. and Binford, L.R.1969. Stone tools and human behaviour. *Scientific American* 220 (4): 70–84.
[28] Binford, L. 1989. Isolating the transition to cultural adaptations: An organizational approach. In Trinkaus, E. (Ed.), *The emergence of modern humans: biocultural adaptations in the later Pleistocene.* Cambridge University Press, Cambridge: 18–41.
[29] Mellars, P.A. 1965. Sequence and development of Mousterian traditions in southwestern France. *Nature* 205: 626–627.
[30] Mellars, P.A. 1969. The chronology of Mousterian industries in the Perigord region of south western France. *Proceedings of the Prehistoric Society* 35: 134-71.
[31] Dibble, H.L.1988. The interpretation of Middle Paleolithic scraper reduction patterns. In: Binford, L.R, Rigaud, J.-P. (Eds.), *L'Homme de Neandertal*, Vol. 4, La Technique. ERAUL, Liège: 49–58.
[32] Dibble H.L. and Rolland, N. 1992. On assemblage variability in the Middle Paleolithic of Western Europe: history, perspectives, and a new synthesis. In: Dibble, H.L. and Mellars, P. (Eds.), *The Middle Paleolithic: adaptation, behavior, and variability.* University Museum Monograph 78, University of Pennsylvania: 1–28.
[33] Dibble, H.L. 1983. Variability and change in the Middle Palaeolithic of Western Europe and the Near East. In Trinkaus, E. (Ed.), *The Mousterian legacy: Human biocultural change in the Upper Pleistocene.* BAR International Series 164: 53–71.
[34] Slimak L. (2004) Les dernières expressions du Moustérien entre Loire et Rhône, Phd dissertation, Université de Provence, 864 p.
[35] De Stefani, M., Dini, M., Klempererova, H., Peresani, M., Ranaldo, F., Ronchitelli, A., Ziggiotti, S. 2012. Continuity and replacement in flake production across the Middle-Upper Palaeolithic transition: a view over the Italian Peninsula. In Pastoors, A., Peresani, M. (Eds.), *Flakes not Blades: The Role of Flake Production at the Onset of the Upper Palaeolithic in Europe*. Wissenschaftliche Schriftendes Neanderthal Museums, 5, Mettmann, pp. 135-151.

[36] Jaubert, J., Bordes, J-G., Discamps, E. and Gravina, B. 2011. A new look at the end of the Middle Palaeolithic sequence in southwestern France. In. Derevianko, A.P and Shunkov, M.V. *Characteristc features of the Middle and Upper Palaeolithic transition in Eurasia*. Asian Palaeolithic Association, Novosibirsk, pp 102-115.
[37] Shea, J.J. 2014. Sink the Mousterian? Named stone tool industries (NASTIES) as obstacles to investigating hominin evolutionary relationships in the Later Middle Paleolithic Levant. *Quaternary International* (2014), http://dx.doi.org/10.1016/
j.quaint.2014.01.024.
[38] Basell, L.S. The Middle Stone Age of Eastern Africa. (2013) In Mitchell, P. and Lane, P. (Eds.) *The Oxford Handbook of African Archaeology*. Oxford University Press.
[39] Basell, L.S. (2008) Middle Stone Age (MSA) site distributions in eastern Africa and their relationship to Quaternary environmental change, refugia and the evolution of Homo sapiens *Quaternary Science Reviews* 27. 2484-2498.
[40] Cooper, L.P., Thomas. J.S., Beamish, M.G., Gouldwell, A., Collcutt, S.N., Williams, J., Jacobi, R.M., Currant, A., and Higham, T.F.G. 2011. An Early Upper Palaeolithic Open-air Station and Mid-Devensian Hyaena Den at Grange Farm, Glaston, Rutland, UK. *Proceedings of the Prehistoric Society* 78: 78-93.
[41] Valoch, K. 2008. Brno-Bohunice, eponymous Bohunician site: new data, new ideas. In, Man-Millennia-Environment. Studies in honour of Romuald Schild. (Eds.) Sulgostowska, Z and Tomaszewski, A.J. Institute of Archaeology and Ethnology, Polish Academy of Sciences, Warsaw, Poland. 225-35.
[42] Haesaerts, P., Damblon, F., Nigst, P and Hublin, J-J. 2013. ABA and ABOX radiocarbon cross-dating on charcoal from Middle Pleniglacial loess deposits in Austria, Moravia and western Ukraine. *Radiocarbon* 55(Nr. 2-3): 641-47.
[43] Brock, F., Higham, T.F.G. and Bronk Ramsey, C. 2010. Pre-screening techniques for identification of samples suitable for radiocarbon dating of poorly preserved bones. *Journal of Archaeological Science* 37(4): 855-865.
[44] Marom, A., McCullagh, J.S.O., Higham, T.F.G. and Hedges, R.E.M. 2013. Hydroxyproline dating: experiments on the ^{14}C analysis of contaminated and low-collagen bones. *Radiocarbon* 55, 2-3: 698-708.
[45] Higham, T.F.G., Jacobi, R.M., Julien, M., David, F., Basell, L., Wood, R., Davies, S.W.G. and Bronk Ramsey, C. 2010. The chronology of the Grotte du Renne (France) and implications for the association of ornaments and human remains within the Châtelperronian. *Proceedings of the National Academy of Sciences of the United States of America* 107(47): 20234-20239.
[46] Higham, T. Bronk Ramsey, C., Basell, L., Brock, F., Wood, R. and Davies, S.W.G. 2012. Radiocarbon dating and Bayesian modeling from the Grotte du Renne and a Neanderthal origin for the Châtelperronian. *Before Farming* 2012/3 Article 2.
[47] Valladas, H., Geneste, J-M., Joron, J.-L. and Chadelle, J.P. 1986. Thermoluminescence dating of Le Moustier (Dordogne, France). *Nature,* 322: 452-454.
[48] Mellars, P.A and Grün, R. 1991. A comparison of the Electron Spin Resonance and Thermoluminescence dating methods: the results of ESR dating at Le Moustier (France). Cambridge Archaeological Journal 1(2): 269-276
[49] Bronk Ramsey, C, Higham, T.F.G and Leach, P. 2004. Towards High Precision AMS: Progress and Limitations. *Radiocarbon* 46(1): 17-24.
[50] Coplen TB. 1994. Reporting of stable hydrogen, carbon, and oxygen isotopic abundances. *Pure and Applied Chemistry* 66(2):273–6.
[51] Jelinek, A.J. 2013. Neandertal lithic industries at La Quina. University of Arizona Press. 419 pp.

[52] Higham, T.F.G., Jacobi, R.M., Basell, L., Bronk Ramsey, C., Chiotti, L. and Nespoulet, R. 2011. Precision dating of the Palaeolithic: A new radiocarbon chronology for the Abri Pataud (France), a key Aurignacian sequence. *Journal of Human Evolution* 61(5): 549-563.
[53] Valladas, H., Mercier, N., Falguères, C. and Bahain, J-J. 1999. Contribution des méthodes nucléaires à la chronologie des cultures Paléolithiques entre 300 000 et 35 000 ans BP. *Gallia Préhistoire* 41: 153-166.
[54] Park, S.-J. 2007. Systèmes de production lithique et circulation des matières premières au Paléolithique moyen récent et final. Une approche techno-économique à partir des industries lithiques de La Quina (Charente). Nanterre : Université Paris X, 336 p. Thèse de doctorat.
[55] Lévêque, F., Backer, A.M., Guilbaud, M. (Eds.). 1993. Context of a Late Neandertal: Implications of multidisciplinary research for the transition to Upper Palaeolithic adaptations at Saint-Césaire , Charente-Maritime, France. *Monographs in World Archaeology* 16. Prehistory Press, Madison, 1993.
[56] Lévêque, F and Vandermeersch, B. 1980. Découverte de restes humains dans un niveau castelperronien à Saint-Césaire (Charente-Maritime). *C R Acad Sci Paris* 291:187-189.
[57] Mercier, N., Valladas, H., Joron, J-, Reyss, J.-., Lèvêque, F. and Vandermeersch, B. 1991. Thermoluminescence dating of the late Neanderthal remains from Saint-Césaire. *Nature,* 351 (6329), pp. 737-739.
[58] Soressi, M. 2011. Révision taphonomique et techno-typologique des deux ensembles attribués au Châtelperronien de la Roche-à-Pierrot à Saint-Césaire. *L'Anthropologie* 115(5): 569-584.
[59] Morin, E., Tsanova, T., Sirakov, N., Rendu, W., Mallye, J-B. and Lévêque, F. (2005) Bone refits in stratified deposits: Testing the chronological grain at Saint-Césaire. *Journal of Archaeological Science,* 32 (7), pp. 1083-1098.
[60] Morin, E. 2012. Reassessing Paleolithic subsistence: The Neanderthal and modern human foragers of Saint-Césaire. Cambridge University Press, pp 358.
[61] Bordes, J.-G. and Teyssandier, N., 2011. The Upper Paleolithic nature of the Châtelperronian in South-Western France: Archeostratigraphic and lithic evidence. *Quaternary International* 246: 382-388.
[62] Bocherens, H., Drucker, D.G., Billiou, D., Patou-Mathis, M. and Vandermeersch, B. 2005. Isotopic evidence for diet and subsistence pattern of the Saint-Césaire I Neanderthal: Review and use of a multi-source mixing model. *Journal of Human Evolution,* 49: 71-87.
[63] Hublin, J-J., Talamo, S., Julien, M., David, F., Connet, N., Bodu, P., Vandermeersch, B. and Richards, M.P. 2012. Radiocarbon dates from the Grotte du Renne and Saint-Césaire support a Neandertal origin for the Châtelperronian. *Proceedings of the National Academy of Sciences of the United States of America* 109(46): 18743-48.
[64] Mercier, N., Valladas, H. and Valladas, G. 1995. Flint thermoluminescence dates from the CFR laboratory at Gif: Contributions to the study of the chronology of the Middle Palaeolithic. *Quaternary Science Reviews,* 14 (4), pp. 351-364.
[65] Marom, A., McCullagh, J., Higham, T., Sinitsyn, A. and Hedges, R. 2012. Single amino acid radiocarbon dating of Upper Palaeolithic modern humans. PNAS published ahead of print April 18, 2012, doi:10.1073/pnas.1116328109.
[66] Slimak L., Pesesse D., Giraud Y. 2006. Reconnaissance d'une installation du Protoaurignacien en vallée du Rhône. Implications sur nos connaissances concernant les premiers hommes modernes en France méditerranéenne, *Comptes Rendus Palevol*, 5,7, 909-917
[67] Slimak L. 2007. Le Néronien et la structure historique du basculement du Paléolithique moyen au Paléolithique supérieur en France méditerranéenne, *Comptes Rendus Palevol* 6, 4, 301-309.
[68] Slimak L. 2008. The Neronian and the historical structure of cultural shifts from Middle to Upper Palaeolithic in Mediterranean France, *Journal of Archaeological Science* 35,8, 2204-2214.

[69] Talamo. S., Soressi, M., Roussel, M., Richards, M., and Hublin, J-J. 2012. A radiocarbon chronology for the complete Middle to Upper Palaeolithic transitional sequence of Les Cottés (France). *Journal of Archaeological Science* 39: 175-183.
[70] McPherron, S.P., Talamo, S., Goldberg, P., Niven, L, Sandgath, D., Richards, M.P., Richter, D., Turq, A. and Dibble, H.L. 2012. Radiocarbon dates for the late Middle Palaeolithic at Pech de l'Azé IV, France. *Journal of Archaeological Science* 39: 3436-3442.
[71] Camps, M. 2003. Revisiting the 40,000 BP Crisis in Iberia: A study of selected transitional industries and their significance. Unpublished Ph.D. Dissertation, University of Oxford.
[72] Camps, M., 2006. The Transition to the Upper Palaeolithic in Iberia: Turning data into information. BAR International Series S1517: Archaeopress, Oxford.
[73] Vaquero, M. and Carbonell, E. 2012. Some urgent clarifications on the Middle-Upper Paleolithic transition in Abric Romaní: reply to Camps & Higham (2012). *Journal of Human Evolution* 63(5): 711-717.
[74] Bischoff, J.L., Ludwig, K., Garcia, J.F., Carbonell, E., Vaquero, M., Stafford, T.W. and Jull, A.J.T. 1994. Dating of the Basal Aurignacian Sandwich at Abric Romaní (Catalunya, Spain) by radiocarbon and Uranium-series. *Journal of Archaeological Science,* 21, 541-551.
[75] Camps, M and Higham, T.F.G. 2012. New AMS dates for Abric Romaní's earliest Aurignacian. *Journal of Human Evolution* 62 (2012) 89-103.
[76] Maroto, J., Soler, N. and Fullola, J.M., 1996. Cultural change between Middle and Upper Palaeolithic in Catalonia. In: E. Carbonell and M. Vaquero, eds, *The Last Neandertals the first anatomically modern humans. Cultural change and human evolution: The crisis at 40 ka BP.* Barcelona: Universitat Rovira i Virgili, pp. 219-250.
[77] Soler Subils, J., Soler Masferrer, N. and Maroto, J., 2008. L'Arbreda's archaic Aurignacian dates clarified. *Eurasian Prehistory,* 5(2), pp. 45-55.
[78] Bischoff, J.L., Soler, N., Maroto, J. and Julia, R., 1989. Abrupt Mousterian/Aurignacian boundary at c. 40 ka bp: Accelerator ^{14}C dates from L'Arbreda Cave (Catalunya, Spain). *Journal of Archaeological Science,* 16, pp. 563-576.
[79] Hedges, R.E.M., Housley, R.A., Bronk Ramsey, C. and Van Klinken, G.J., 1994. Radiocarbon dates from the Oxford AMS system: Archaeometry Datelist 18. *Archaeometry* 36(2): 337-374.
[80] D'Errico, F., Zilhão, J., Julien, M., Baffier, D., Pelegrin, J., Conrad, N.J., Demars, P.Y., Hublin, J., Mellars, P., Mussi, M., Svoboda, J., Taborin, Y., Vega Toscano, L.G. and White, R., 1998. Neanderthal Acculturation in Western Europe?: A Critical Review of the Evidence and Its Interpretation [and Comments and Reply]. *Current Anthropology,* 39(2): S1-S44.
[81] Zilhão, J. and D'Errico, F., 2003. The chronology of the Aurignacian and transitional technocomplexes. Where do we stand? In: J. Zilhão and F. D'Errico, eds, *The Chronology of the Aurignacian and of the Transitional Technocomplexes: Dating, Stratigraphies, Cultural Implications.* Lisboa: Instituto Portugues de Arquologia, pp. 313-349.
[82] Zilhão, J., 2006. Chronostratigraphy of the Middle-to-Upper Paleolithic Transition in the Iberian Peninsula. *Pyrenae,* 37(1), pp. 7-84.
[83] Wood, R.E. 2011.The contribution of new radiocarbon dating pre-treatment techniques to understanding the Middle to Upper Palaeolithic transition in Iberia. Unpublished D.Phil dissertation, University of Oxford, 498 p.
[84] Wood, R.E., Arrizabalaga, A., Camps, M., Fallon, S., Iriarte-Chiapusso, M.-J., Jones, R., Maroto, J., de la Rasilla, M., Santamaría, D., Soler, J., Soler, N., Villaluenga, A., Higham, T.F.G. 2014. The chronology of the earliest Upper Palaeolithic in Northern Iberia: New insights from L'Arbreda, Labeko Koba and La Viña. *Journal of Human Evolution.*

[85] Maroto, J., Vaquero, M., Arrizabalaga, A., Baena, J, Baquedano, E., Jordá, J., Julià, R, Montes, R., van der Plicht, J., Rasines, P. and Wood, R., 2012. Current issues in late Middle Palaeolithic chronology: New assessments from Northern Iberia. *Quaternary International* 247: 15-25.
[86] Arrizabalaga, A., Altuna, J. (Eds.), 2000. Munibe (Antropologia-Arkeologia) : Labeko Koba (País Vasco). Hienas y Humanos en los albores del Paleolítico superior. Munibe (Antropologia – Arkeologia), 52.
[87] Arrizabalaga, A., 2000b. Los tecnocomplejos líticos del yacimiento arqueológico de Labeko Koba (Arrasate, País Vasco). In: Arrizabalaga, A., Altuna, J. (Eds.), Labeko Koba (País Vasco). Hienas y Humanos en los Albores del Paleolítico Superior, Munibe (Antropologia-Arkeologia) 52. Sociedad de Ciencias Aranzadi, San Sebastián-Donostia, pp. 193-343.
[88] Mujika, J. 2000. La industria ósea del Paleolítico Superior Inicial de Labeko Koba (Arrasate, País Vasco). *Munibe (Antropologia – Arkeologia)* 52: 355-376.
[89] Villaluenga, A. 2013. Evaluación de los úrsidos en la Cornisa Cantábrica. Estudio tafonómico de conjuntos arqueológicos y paleontológicos del Pleistoceno Superior y Holoceno. Ph.D. Dissertation, University of the Basque Country.
[90] Fortea Pérez, F.J., de la Rasilla Vives, M., Martínez, E., Sànchez-Moral, S., Cañaveras, J.C., Cueza, S., Rosas, A., Soler, V., Juliá̀, R., de Torres, T., Ortiz, J.E., Castro, J., Badal, E., Altuna, J. and Alonso, J., 2003. La Cueva de El Sidron (Borines, Piloña, Asturias); Primeros Resultados. *Estudios Geologicos,* 59(1-4): 159-179.
[91] Rosas, A, Estalrrich, A, García-Vargas, S., García-Tabernero, A., Bastir, M., Huguet, R., Peña-Melián, A., 2011. Los fósiles neandertales de la Cueva de El Sidrón, in *La Cueva de El Sidrón (Borines, Piloña, Asturias). Investigación interdisciplinar de un grupo neandertal* (eds. M. de la Rasilla, A. Rosas and J. C. Cañaveras), Consejería de Cultura y Turismo y Ediciones Trabe SLU, Oviedo, 81-116.
[92] Santamaría, D., Fortea, J., De La Rasilla, M., Martínez, L., Martínez, E., Cañaveras, J.C., Sánchez-Moral, S., Rosas, A., Estalrrich, A., García-Tabernero, A. and Lalueza-Fox, C., 2010. The technological and typological behaviour of a Neanderthal group from El Sidrón (Asturias, Spain). *Oxford Journal of Archaeology,* 29(2): 119-148.
[93] Rosas, A., Martínez-Maza, C., Bastir, M., García-Tabernero, A, Lalueza-Fox, C., Huguet, R., Ortiz, J.E., Julià, R., Soler, V., de Torres, T., Martínez, E., Cañaveras, J.C., Sánchez-Moral, S., Cuezva, S., Lario, J., Santamaría, D., de la Rasilla, M. and Fortea, J., 2006. Paleobiology and comparative morphology of a late Neandertal sample from El Sidrón, Asturias, Spain. *Proceedings of the National Academy of Sciences of the United States of America,* 103(51): 19266-19271.
[94] Tisnérat-Laborde, N., Valladas, H., Kaltnecker, E. and Arnold, M., 2003. AMS radiocarbon dating of bones at LSCE. *Radiocarbon,* 45(3): 409-419.
[95] Torres, T., Ortiz, J. E., Grün, R., Eggins, S., Valladas, H., Mercier, N., Tisnérat-Laborde, N., Juliá, R., Soler, V., Martínex, E., Sánchez-Moral, S., Cañaveras, J.C., Lario, J., Badal, E., Lalueza-Fox, C., Rosas, A., Santamaría, D., de la Rasilla, M. and Fortea, J., 2010. Dating of the hominid (*Homo Neanderthalensis*) remains accumulation from El Sidrón Cave (Piloña, Asturias, North Spain): An example of a multi-methodological approach to the dating of Upper Pleistocene sites. *Archaeometry,* 52(4): 680-705.
[96] Wood, R.E., Higham T.F.G., Torres, T, Tisnerat-Laborde, N., Valladas, H., Ortiz, J.E., Lalueza-Fox, C., Sanchez-Moral, S., Canaveras, J.C., Roses, A., Santamaria, D., de la Rasilla, M. 2013. A new date for the Neanderthals from El Sidron Cave (Asturias, Northern Spain). *Archaeometry* 55(1): 148-158.
[97] Bermudez De Castro, J.M. and Saenz de Buruaga, A. 1999. Preliminary study of the Arrillor Upper Pleistocene hominid site (Basque Country, Spain). *Anthropologie* 103(4): 633-639.

[98] Hoyos Gómez, M., Sáenz De Buruaga, A. and Ormazabal, A. 1999. Cronoestratigrafía y paleoclimatología de los depósitos prehistóricos de la cueva de Arrillor (Araba, País Vasco). *Munibe (Antropologia – Arkeologia)* 51: 137-151.
[99] Hedges, R.E.M., Law, A.I., Bronk, C.R. and Housley, R.A. 1989. The Oxford Accelerator Mass Spectrometry Facility: Technical Developments in Routine Dating. *Archaeometry* 31(2): 99-113.
[100] Castaños Ugarte, P.M., 2005. Revisión actualizada de las faunas de macromamíferos del Würm antiguo en la Región Cantábrica. *Museo de Altamira. Monografías,* 20: 201-207.
[101] Barandiaran, J.M. and Altuna, J. 1970. Excavación de la cueva de Lezetxiki (Campaña de 1968). *Munibe (Antropologia – Arkeologia)* 22, pp. 51-59.
[102] Arrizabalaga, A., Altuna, J., Areso, P., Falgueres, C., Iriarte, M.J., Mariezkurrena, K., Pemán, E., Ruíz-Alonso, M., Tarriño, A., Uriz, A. and Vallverdú, J. 2005. Retorno a Lezetxiki (Arrasate, Pais Vasco): nuevas perspectivas de la investigación. In: M. Santonja, A. Pérez-González and M.J. Machado, eds, *Geoarqueología y Conservación del Patrimonio: Actas de la IVa reunión de geoarqueología.* Madrid: ADEMA, pp. 63-80.
[103] Arrizabalaga, A. 2006. Lezetxiki (Arrasate, País Vasco). Nuevas preguntas acerca de un antiguo yacimiento. In: V. Cabrera Valdés, Bernaldo de Quirós Guidotti, F. and J.M. Maíllo Fernández, eds, *En el centenario de la Cueva de el Castillo: El ocaso de los Neandertales.* Madrid: Centro Asociado a la Univeristat Nacional de Educacion a Distancia en Cantabria, pp. 293-309.
[104] Baldeon, A. 1993. El yacimiento de Lezetxiki (Gipuzkoa, País Vasco). Los niveles musterienses. *Munibe (Antropologia – Arkeologia)* 45, pp. 3-97.
[105] Basabe Prado, J.M. 1970. Dientes humanos del paleolítico de Lezetxiki (Mondragón). *Munibe (Antropologia – Arkeologia),* 22 pp. 113-124.
[106] Esparza, X. 1985. *El Paleolítico superior de la cueva de Lezetxiki (Mondragón, Guipúzcoa).* Memoria de Licenciatura edn. Unpublished: Universidad Complutense de Madrid.
[107] Arrizabalaga, A. 1995. *La industria lítica del Paleolítico Superior Inicial en el oriente Cantábrico.* Tesis Doctoral edn. Unpublished: Universidad del País Vasco, Vitoria.
[108] Arrizabalaga Valbuena, A. and Maíllo Fernández, J.M. 2008. Technology vs Typology? The Cantabrian Archaic Aurignacian/Proto Aurignacian Example. In: T. Aubry, F. Almeida, A.C. Araujo and M. Tiffagom, eds, *Proceedings of the XV World Congress of the International Union for Prehistoric and Protohistoric Sciences. Space and Time: Which Diachronies, Which Synchronies, Which Scales?/ Typology vs. Technology.* Oxford: BAR international series 1831, pp. 133-139.
[109] Altuna, J. 1972. Los Yacimentos Prehistoricos Guipuzcoanos Estudio General de su Fauna de Mamiferos. *Munibe (Antropologia – Arkeologia)* 24: 132-190.
[110] Falgueres, C., Yokoyama, Y. and Arrizabalaga, A. 2005. La Geochronologia del yacimiento Pleistocenico de Lezetxiki (Arrasate, Pais Vasco). Critica de la dataciones existentes y algunas nuevas apotaciones. *Homenaje a Jesus Altuna: Munibe (Antropologia – Arkeologia)* 57: 93-106.
[111] Maíllo Fernández, J.M. 2006. Archaic Aurignacian Lithic Technology in Cueva Morín (Cantabria, Spain). In: O. Bar-Yosef and J. Zilhão, eds, *Towards a Definition of the Aurignacian. Proceedings of the Symposium held in Lisbon, Portugal, June 25-30, 2002.* Instituto Portugues de Arqueologia, pp. 111-130.
[112] González Echegaray, J. and Freeman, L.G. 1971. *Cueva Morin; Vol. 1 Excavaciones 1966-1968.* Santander: Patronato de las Cuevas Prehistóricas de la Provincia de Santander.
[113] González Echegaray, J. and Freeman, L.G., 1973. *Cueva Morín; Vol. 2. Excavaciones 1969*. Santander: Patronato de las Cuevas Prehistóricas de la Provincia de Santander.
[114] Laville, H. and Hoyos, M., 1994. Algunos precisiones sobre a estratigrafía de Cueva Morín (Santander). *El Cuadro geocronologico del Paleolitico Superior inicial.* Madrid: Ministerio de Cultura, pp. 199-209.

[115] Maíllo Fernández, J.M., Valladas, H. and Bernaldo de Quirós, F., Cabrera Valdés, V. 2001. Nuevas dataciones para el Paleolítico Superior de Cueva Morín (Villanueva de Villaescusa, Cantabria). *Espacio, Tiempo y Forma. Serie I, Prehistoria y Arqueología,* 14: 145-150.
[116] Baena, J., Carrión, E., Manzano, I., Velázquez, R., Sanz, E., Sánchez, S., Ruiz, B., Uzquiano, P. and Yravedra, J. 2005. Ocupaciones musterienses en la comarca de Liébana (occidente de Cantabria): La cueva de El Esquilleu. *Geoarqueología y patrimonio en la Península Ibérica y el entorno Mediterráneo,* pp. 113-125.
[117] Baena, J., Carrión, E., Cuartero, F., Fluck, H. 2012. A chronicle of crisis: The Late Mousterian in north Iberia (Cueva del Esquilleu, Cantabria, Spain). *Quaternary International* 247, 199-211.
[118] Menéndez-Fernández, M., García, E. and Quesada, J.M. 2005. La transición Paleolítico Medio-Paleolítico Superior en la Cueva de la Güelga (Cangas de Onís, Asturias). Un avance a su registro. *Museo de Altamira. Monografías* 20(589): 617.
[119] Menéndez-Fernández, M., García-Sánchez, E. and Quesada-López, J.M. 2006. Excavaciones en la Cueva de la Güelga (Cangas de Onís. Asturias). In: V. Cabrera Valdés, Bernaldo de Quirós Guidotti, F. and J.M. Maíllo Fernández, eds, *En el Centenario de la Cueva de El Castillo; El Ocaso de los Neanderthales.* Spain: Centro Asociado a la Universidad Nacional de Educaión a Distancia en Cantabria, pp. 209-229.
[120] Menéndez-Fernández, M., Quesada, J.M., Jordá, J.F., Carral, P., Trancho, G.J., Garcia, E., Álvarez, D., Rojo, J. and Wood, R. 2009. Excavaciones arqueológicas en la cueva de la Güelga (Cangas de Onís). *Excavaciones Arqueológicas en Asturias 2003-2006,* Oviedo: Servicio de Publicaciones de la Consejería de Educación, Cultura, Deportes y Juentud, pp. 209-221.
[121] Wood, R.E, de Quirós, F., Maíllo-Fernández, J.-M., Neira, A.and Higham, T.F.G. in prep. El Castillo, Northern Spain, and the Transitional Aurignacian: the use of radiocarbon dating in understanding early 20th century excavations. *Journal of Human Evolution.*
[122] Jordá Pardo, J.F., 2007. The wild river and the last Neanderthals: A palaeoflood in the geoarchaeological record of the Jarama Canyon (Central Range, Guadalajara province, Spain). *Geodinamica Acta* 20(4): 209-217.
[123] Kehl, M., Burrow, C., Hilgers, A., Navazo, M., Pastoors, A., Weniger, G.-C., Wood, R., Jorda Pardo, J.,F., 2013. Late Neanderthals at Jarama VI (central Iberia)? *Quaternary Research* 80(2): 218-234.
[124] Lorenzo, C, Navazo, M, Díez, J.C, Sesé, C, Arceredillo, D, Jordá Pardo, J.F. 2012. New human fossil to the last Neanderthals in central Spain (Jarama VI, Valdesotos, Guadalajara, Spain). *Journal of Human Evolution*, 62(6): 720-5.
[125] Zilhão, J., 2009. The Ebro Frontier Revisited. In: M. Camps and C. Szmidt, eds, *The Mediterranean from 50 000 to 25 000 BP: Turning points and new directions.* Oxford: Oxbow Books, pp. 293-312.
[126] Wood, R.E., Barroso-Ruiz, C., Caparros, M., Jorda. J.F., Galvan Santos, B., Higham, T.F.G. 2013. Radiocarbon dating casts doubt on the late chronology of the Middle to Upper Palaeolithic transition in southern Iberia, *Proceedings of the National Academy of Sciences of the United States of America*. Published online before print February 4, 2013, doi: 10.1073/pnas.1207656110 PNAS February 4, 2013 201207656.
[127] Barroso, C., Medina, F., Onoratini, G. & Jöris, C., 2003, Las industrias del Paleolítico Superior de la Cueva del Boquete de Zafarraya, in C. Barroso (ed.), *El Pleistoceno Superior de la Cueva del Boquete de Zafarraya*, Junta de Andalucía, Sevilla, 469-495.
[128] Hublin, J.-J., Barroso Ruiz, C., Lara, P.M., Fontugne, M. and Reyss, J., 1995. The Mousterian site of Zafarraya (Andalucia, Spain): dating and implications onmusic: the Palaeolithic peopling processes of Western Europe. *Comptes Rendus - Academie des Sciences, Serie II: Sciences de la Terre et des Planetes,* 321(10): 931-937.

[129] Michel, V., Bard, E., Delanghe, D., El Mansouri, M., Falguères, C., Pettitt, P., Yokoyama, Y. and Barroso, C. 2003. Geocronologia del relleno de la Cueva del Boquete de Zafarraya. C. Barroso (Ed.), El Pleistoceno Superior de la Cueva del Boquete de Zafarraya, Junta de Andalucia, Sevilla, pp. 113–133.
[130] Michel, V., Delanghe, D., Bard, E., Pettitt, P., Yokoyama, Y. and Barroso, C. 2006. Datation C-14, U/Th, ESR des niveaux moustériens de la grotte du Boquete de Zafarraya. C. Barroso Ruiz, H. de Lumley (Eds.), La grotte du Boquete de Zafarraya, Malaga, Andalousie, Tome IDe la edicion: Junta de Andalucia, Consejeria de Cultura (2006), pp. 487–518.
[131] Michel, V., Shen, G., Shen, C.-C., Fornari, M., Vérati, C., Gallet, S. and Sabatier D. 2011. Les derniers Homo heidelbergensis et leurs descendants les néandertaliens: datation des sites d'Orgnac 3, du Lazaret et de Zafarraya. Comptes Rendus Palevol, 10 (2011), pp. 577–587
[132] Michel, V., Delanghe-Sabatier, D., Bard, E. and Barroso Ruiz, C. 2013. U-series, ESR and ^{14}C studies of the fossil remains from the Mousterian levels of Zafarraya Cave (Spain): A revised chronology of Neandertal presence, *Quaternary Geochronology* 15: 20-33.
[133] Zilhão, J., Angelucci, D.E., Badal-García, E., D'Errico, F., Daniel, F., Dayet, L., Douka, K., Higham, T.F.G., Martínez-Sánchez, M.J., Montes-Bernárdez, R., Murcia-Mascarós, S., Pérez-Sirvent, C., Roldán-García, C., Vanhaeren, M., Villaverde, V., Wood, R. and Zapata, J., 2010. Symbolic use of marine shells and mineral pigments by Iberian Neandertals. *Proceedings of the National Academy of Sciences of the United States of America,* 107(3), pp. 1023-1028.
[134] Hahn, J. 1988. Die Geißenklösterle-Höhle im Achtal bei Blaubeuren I. Fundhorizontbildung und Besiedlung im Mittelpalëolithikum und im Aurignacien. Konrad Theiss Verlag, Stuttgart.
[135] Conard, N. J. and M. Bolus. 2006. The Swabian Aurignacian and its place in European prehistory. In *Toward a Definition of the Aurignacian*. Edited by O. Bar-Yosef and J. Zilhão. Trabalhos de Arcqueologia 45: 209-237.
[136] Teyssandier, N., Bolus, M. and Conard, N.J. 2006. The Early Aurignacian in central Europe and its place in a European perspective. In *Towards a Definition of the Aurignacian*. (Eds.) O. Bar-Yosef and J. Zilhão, Lisbon: Trabalhos de Arqueologia, pp. 241-256.
[137] Conard, N.J. and Bolus, M. 2008. Radiocarbon dating the late Middle Paleolithic and the Aurignacian of the Swabian Jura. *Journal of Human Evolution* 55(5): 886-897.
[138] Richter, D., Waiblinger, J., Rink, W.J., Wagner, G.A., 2000. Thermoluminescence, electron spin resonance and ^{14}C-dating of the late Middle and early Upper Palaeolithic site of Geißenklösterle Cave in southern Germany. *Journal of Archaeological Science* 27: 71–89.
[139] Conard, N. J. 2002. The timing of cultural innovations and the dispersal of modern humans in Europe. Proceedings of the DEUQUA-Meeting August 26-28, 2002 Potsdam, Germany, (Eds.) A Brauer, J. F. W. Negendank and M. Bohm. *Terra Nova* 2002/6: 82-94.
[140] Conard, N.J. and Bolus, M. 2003. Radiocarbon dating the appearance of modern humans and timing of cultural innovations in Europe: new results and new challenges. *Journal of Human Evolution* 44(3): 331-371.
[141] Higham, T.F.G., Basell, L., Jacobi, R.M, Wood, R., Bronk Ramsey, C. and Conard, N.J. 2012. Testing models for the beginnings of the Aurignacian and the advent of figurative art and music: the radiocarbon chronology of Geißenklösterle. *Journal of Human Evolution* 62 (6): 664-676.
[142] Palma Di Cesnola, A. (1963) Prima campagna di scavi nella Grotta del Cavallo presso Santa Caterina (Lecce). *Riv. Sc. Preist.* 18: 41-74.
[143] Palma di Cesnola, A. (1964). Seconda campagna di scavo nella grotta del Cavallo. *Riv. Sc. Preist.* 19: 23-39.
[144] Palma di Cesnola, A. (1965a) Notizie preliminari sulla terza campagna di scavi nella Grotta del Cavallo (Lecce). Riv. Sc. Preist. 20: 291-302.

[145] Sarti, L., Boscato, P., Lo Monaco, M. (1998-2000) Il Musteriano finale di Grotta del Cavallo nel Salento, studio preliminare. *Origini* 22: 45-109.
[146] Sarti, L., Boscato, P., Martini, F., Spagnoletti, A.P. (2002) Il Musteriano di Grotta del Cavallo - strati H e I : studio preliminare. *Riv. Sc. Preist*. 52: 21-110.
[147] Moroni, A., Boscato, P., Ronchitelli, A. 2013. What roots for the Uluzzian? Modern behaviour in Central-Southern Italy and hypotheses on AMH dispersal routes. *Quaternary International* 316: 27-44.
[148] Vicino, G. 1984. Lo scavo paleolitico al Riparo Bombrini (Balzi Rossi di Grimaldi, Ventimiglia). *Rivista Ingauna e Intemelia* 39: 1–10.
[149] Holt, B.M., Churchill S.E., Negrino F., Formicola V., Vicino G., Pettit P., Del Lucchese, A., 2003. *New evidence of the Middle-Upper Paleolithic transition from Riparo Bombrini (Grimaldi, Italy)*. Paper presented at the 2003 Annual Meeting of the Paleoanthropology Society.
[150] del Lucchese, A., Formicola, V., Holt, B., Negrino, F., Vicino, G., 2005. Riparo Bombrini, Balzi Rossi (Ventimiglia, Imperia): notizie preliminari degli scavi 2002–2004. *Ligures* 2: 287– 289.
[151] Negrino, F., 2006. Riparo Bombrini, Balzi Rossi (Ventimiglia, Imperia): la campagna 2005. *Ligures* 3: 194–196.
[152] Holt, B.M., Negrino F., Formicola V., Riel-Salvatore J., Churchill S.E., Vicino G., Del Lucchese A., 2006. The Mousterian-Aurignacian transition at the Riparo Bombrini (Liguria, Italy) rock shelter. Paper presented at the 2006 Annual Meeting of the Paleoanthropology Society.
[153] Fiocchi, C., 1998. *Contributo alla conoscenza del comportamento simbolico di* Homo sapiens sapiens *– Le conchiglie marine nei siti del paleolitico superiore europeo: strategie di approvvigionamento, reti di scambio, utilizzo*. Ph.D. dissertation, University of Bologna, Ferrara.
[154] Douka, K., Grimaldi, S., Boschian, G., del Lucchese, A., Higham, T.F.G, 2012. A new chronostratigraphic framework for the Upper Palaeolithic of Riparo Mochi (Italy), *Journal of Human Evolution* 62: 286-299.
[155] Bartolomei, G., Broglio, A., Cassoli, P., Castelletti, L., Cremaschi, M., Giacobini, G., Malerba, G., Maspero, A., Peresani, M., Sartorelli, A., Tagliacozzo, A. 1992. La Grotte-Abri de Fumane. Un site Aurignacien au Sud des Alps. *Preistoria Alpina* 28: 131–179.

[156] Bartolomei, G., Broglio, A., Cassoli, P., Castelletti, L., Cremaschi, M., Giacobini, G., Malerba, G., Maspero, A., Peresani, M., Sartorelli, A., Tagliacozzo, A., 1992. La Grotte-Abri de Fumane. Un site Aurignacien au Sud des Alps. *Preistoria Alpina* 28: 131–179.
[157] Peresani, M., Cremaschi, M., Ferraro, F., Falguères, C., Bahain, J.-J., Gruppioni, G., Sibilia, E., Quarta, G., Calcagnile, L., Dolo, J.-M., 2008. Age of the final Middle Palaeolithic and Uluzzian levels at Fumane Cave, Northern Italy, using 14C, ESR, 234U/230Th and thermoluminescence methods. *Journal of Archaeological Science* 35: 2986–2996.
[158] Martini, M., Sibilia, E., Croci, S., Cremaschi, M., 2001. Thermoluminescence (TL) dating of burnt flints: problems, perspectives and some example of application. *Journal Cultural Heritage* 2: 179-190.

[159] Peresani, M., Chrzavzez, J., Danti, A., De March, M., Duches, R., Gurioli, F., Muratori, S., Romandini, M., Tagliacozzo, A., Trombino, L. 2011. Fire-places, frequentations and the environmental setting of the final Mousterian at Grotta di Fumane: a report from the 2006-2008 research. *Quartär* 58: 131-151.

[160] Peresani, M., 2012. Fifty thousand years of flint knapping and tool shaping across the Mousterian and Uluzzian sequence of Fumane cave. In : Carbonnell E., Gema M., Vaquero M. (Eds.), The Neanderthal Home: Spatial and Social Behaviours. *Quaternary International* 247: 125-150.

[161] Cassoli, P.F., Tagliacozzo, A., 1991. Considerazioni paleontologiche, paleoeconomiche e archeozoologiche sui macromammiferi e gli uccelli dei livelli del Pleistocene superiore del Riparo di Fumane (VR) (Scavi 1988-91). *Bollettino Museo Civico Storia Naturale Verona*, 18: 349-445.
[162] Romandini M., Nannini N., Tagliacozzo A., Peresani M., 2014. The ungulate assemblage from layer A9 at Grotta di Fumane, Italy: a zooarchaeological contribution to the reconstruction of Neanderthal ecology. *Quaternary International* dx.doi.org/10.1016/j.quaint.2014.03.027.

[163] Peresani, M., 2008. A new cultural frontier for the last Neanderthals: the Uluzzian in Northern Italy. *Current Anthropology* 49 (4): 725–731.
[164] Broglio A., 1997. L'estinzione dell'Uomo di Neandertal e la comparsa dell'Uomo moderno in Europa. Le evidenze della Grotta di Fumane nei Monti Lessini. *Atti Istituto Veneto SS.LL.AA 155*: 1–55.
[165] Broglio, A., Giacobini, G., Tagliacozzo, A., Peresani, M., Bertola, S., Cilli, C., se Stefani, M., Gurioli, F., 2005. L'abitato Aurignaziano. In Broglio, A., Dalmeri, G. (Eds.), *Pitture paleolitiche nelle Prealpi Venete: Grotta di Fumane e Riparo Dalmeri*. Memorie Museo Civico Storia Naturale di Verona, vol. 9: 23–37.
[166] Broglio, A., De Stefani, M., Tagliacozzo, A., Gurioli, F., Facciolo, A., 2006. Aurignacian dwelling structures, hunting strategies, and seasonality in the Fumane Cave (Lessini Mountains). In Vasil'ev, S.A., Popov, V.V. Anikovich, M.V., Praslov, N.D., Sinitsyn, A.A., Hoffecker, J.F. (Eds.) *Kostenki and the early Upper Paleolithic of Eurasia: General trends, local developments*. Nestor-Historia Saint Petersburg: 263–268.
[167] Benazzi, S., Douka, K. *et al*. 2011. Early dispersal of modern humans in Europe and implications for Neanderthal behaviour. *Nature* 479, 525–528
[168] Jéquier, C.A., Romandini, M., Peresani, M., 2012. Les retouchoirs en matières dures animales: une comparaison entre Moustérien final et Uluzzien. *Comptes Rendus Palevol* 11 (4): 283-292.

[169] Peresani, M., Fiore, I., Gala, M., Romandini, M., Tagliacozzo, A., 2011. Late Neandertals and the intentional removal of feathers as evidenced from bird bone taphonomy at Fumane cave 44ky BP, Italy. *Proceedings National Academy of Science* 108: 3888-3893.

[170] Peresani, M., Centi, L., Di Taranto, E., 2013. Blades, bladelets and flakes: a case of variability in tool design at the onset of the Middle – Upper Palaeolithic transition in Italy. *Comptes Rendus Palevol* 12 (4): 211-221 (+corrigendum).

[171] Higham, T.F.G, Brock, F., Peresani, M., Broglio, A, Wood, R and Douka, K. 2009. Problems with radiocarbon dating the Middle to Upper Palaeolithic transition in Italy. *Quaternary Science Reviews* 28: 1257-67.
[172] Higham, T.F.G. 2011. European Middle and Upper Palaeolithic radiocarbon dates are often older than they look: problems with previous dates and some remedies. *Antiquity* 85 (327**)**: 235–249.
[173] Giaccio, B., Isaia, R., Fedele, F.F., Di Canzio, E., Hoffecker, J.F., Ronchitelli, A., Sinitsyn, A.A., Anikovich, M.A., Lisitsyn, S.N., Popov, V.V., 2008. The Campanian Ignimbrite and Codola tephra layers: two temporal/stratigraphic markers for the Early Upper Palaeolithic in southern Italy and eastern Europe. *J. Volcanol. Geotherm. Res.* 177: 208-226.
[174] Douka, K., Higham, T.F.G., Wood, R.E., Boscato, P., Gambassini, P., Karkanas, P., Peresani, M. and Ronchitelli, A. 2014. On the chronology of the Uluzzian. *Journal of Human Evolution* http://dx.doi.org/10.1016/j.jhevol.2013.12.007.
[175] Gambassini, P. (Ed.), 1997. Il Paleolitico di Castelcivita, Culture e Ambiente. Electa Napoli, Naples.

[176] Villa, P., Boscato, P., Ranaldo, F., Ronchitelli, A. 2009. Stone tools for the hunt: points with impact scars from a Middle Paleolithic site in southern Italy. *Journal of Archaeological Science* 36: 850-859.
[177] Boscato, P., Gambassini, P., Ranaldo, F., Ronchitelli, A. 2011. Management of Paleoenvironmental Resources and Raw materials Exploitation at the Middle Paleolithic Site of Oscurusciuto (Ginosa, Southern Italy): Units 1 and 4. In Conard N.J., Richter J.(Eds), *Neanderthal Lifeways, Subsistence and Technology - One Hundred Fifty Years of Neanderthal Study.* Springer: 87-98.
[178] Panagopoulou E., Karkanas T., Tsartsidou G., Kotjabopoulou, E., Harvati, K., Ntinou M., 2004. Late Pleistocene archaeological and fossil human evidence from Lakonis Cave, Southern Greece. *Journal of Field Archaeology* 29: 323–349.
[179] Elefanti, E., Panagopoulou, E., Karkanas, P., 2008. The transition from the Middle to Upper Palaeolithic in the southern Balkans: The evidence from the Lakonis I Cave, Greece. *Eurasian Prehistory* 5 (2): 77–87.
[180] Kuhn, S., 2003. In What Sense is the Levantine Initial Upper Paleolithic a ''Transitional'' Industry? In Zilhão, J., d'Errico, F. (Eds.), *The chronology of the Aurignacian and of the Transitional technocomplexes: Dating, Stratigraphies, Cultural Implications*. Trabalhos de Arqueologia 33, Istituto Português de Arqueologia, Lisbon: 61–70.
[181] Rougier, H., Crèvecoeur, I., Fiers, E., Hauzeur, A., Germonpré, M., Maureille, B., Semal, P., 2004. Collections de la Grotte de Spy: (re)découvertes et inventaire anthropologique. *Notae Praehist*. 24: 181-190.
[182] Semal, P., Rougier, H., Crèvecoeur, I., Jungels, C., Flas, D., Hauzeur, A., Maureille, B., Germonpré, M., Bocherens, H., Pirson, S., Cammaert, L., De Clerck, N., Hambucken, A., Higham, T., Toussaint, M., van der Plicht, J., 2009. New data on the Late Neandertals: direct dating of the Belgian spy fossils. *American Journal of Physical Anthropology* 138: 421-428.
[183] Crèvecoeur, I., Bayle, P., Rougier, H., Maureille, B., Higham, T.F.G., van der Plicht, J., de Clerck, N and Semal, P. 2010. The Spy VI child: A newly discovered Neandertal infant. *Journal of Human Evolution* 59: 641-656.
[184] Pirson, S., Flas, D., Abrams, G., Bonjean, D., Court-Picon, M., Di Modica, K., Draily, C., Damblon, F., Haesaerts, P., Miller, R., Rougier, H., Toussaint, M. and Semal. P. 2012. Chronostratigraphic context of the Middle to Upper Palaeolithic transition: Recent data from Belgium. *Quaternary International* 259: 78-94.
[185] Toussaint, M., Pirson, S., 2006. Neandertal studies in Belgium: 2000-2005. *Periodicum Biologorum* 108: 373-387.
[186] Semal, P., Hauzeur, A., Rougier, H., Crèvecoeur, I., Germonpré, M., Pirson, S., Haesaerts, P., Jungels, C., Flas, D., Toussaint, M., Maureille, B., Bocherens, H., Higham, T., Van Der Plicht, J. 2012. Radiocarbon dating of human remains and associated archaeological material. *Anthropologica et Praehistorica* 123 (1): 331-356.
[187] Pirson, S., Draily, C., Toussaint, M., 2011. La grotte Walou à Trooz (Belgique). Fouilles de 1996 à 2004. Volume 1. Les sciences de la terre, Etudes et Documents, Archéologie, 20, Service public de Wallonie, Namur, p. 208.
[188] Draily, C., Pirson, S., Toussaint, M., 2011. La grotte Walou à Trooz (Belgique). Fouilles de 1996 à 2004. Volume 2. Les sciences de la vie et les datations, Etudes et Documents, Archéologie, 21, Service public de Wallonie, Namur, p. 241.
[189] Draily, C., 2011. La grotte Walou à Trooz (Belgique). Fouilles de 1996 à 2004. Volume 3. L'archéologie, Service public de Wallonie, Namur.
[190] Toussaint, M., 2011. Une prémolaire néandertalienne dans la couche CI-8 (anciennement C sup et C8) de la grotte Walou, in: Draily, C., Pirson, S., Toussaint, M. (Eds.), La grotte Walou à Trooz

(Belgique). Fouilles de 1996 à 2004. Volume 2. Les sciences de la vie et les datations, Service public de Wallonie (Etudes et Documents, Archéologie, 21), Namur, pp. 148-163. (OR Toussaint in Draily et al. (ed.), 2011).

[191] Pirson, S., Damblon, F., Haesaerts, P. and Daily, C. 2011. Analyse des dates ^{14}C de la grotte Walou. In, Drailly, C., Pirson, S. and Toussaint, M. (eds) 2011. *La Grotte Walou a Trooz (Belgique). Fouilles de 1996 à 2004. Volume 2 Les sciences de la vie et les datations.* Institut de Patrimoine Wallon, Service public de Wallonie, Namur 2011, pp 198-211.

[192] Jacobi, R.M, Higham, T.F.G.and Bronk Ramsey, C. 2006. AMS radiocarbon dating of Middle and Upper Palaeolithic bone in the British Isles: improved reliability using ultrafiltration. *Journal of Quaternary Science* 21(5): 557-73.

[193] Douka, K. 2013. Exploring "the great wilderness of prehistory": The chronology of the Middle to the Upper Palaeolithic transition in the northern Levant. *Mitteilungen der Gesellschaft für Urgeschichte* 22: 11–40.

[194] Douka, K. 2011. Investigating the Chronology of the Middle to Upper Palaeolithic Transition in Mediterranean Europe by Improved Radiocarbon Dating of Shell Ornaments. Unpublished PhD thesis. Oxford: University of Oxford.

[195] Wright, Jr, H.E. 1951. Ksâr ʾAkil: Its archeological sequence and geological setting. *J. Near East Stud.* 10: 113-122.

[196] Marks, A.E., Volkman, P. 1986. The Mousterian of Ksar Akil: Levels XXVIA through XXVIIIB. *Paléorient* 12:5-20.

[197] Azoury, I. 1986. *Ksar Akil, Lebanon: A technological and typological analysis of the transitional and Early Upper Palaeolithic levels at Ksar Akil and Abu Halka.* Oxford, BAR International Series 289 (i and ii).

[198] Ewing, J.F. 1948. Ksâr 'Akil in 1948. *Biblica* 29: 272-278.

[199] van der Plicht, J., van der Wijk, A., Bartstra, G.J.1989. Uranium and thorium in fossil bones: activity ratios and dating. *Applied Geochemistry* 4: 339–342.

[200] Golovanova LV, Hoffecker JF, Kharitonov VM, Romanova GP. 1999. Mezmaiskaya cave: Neanderthal occupation in the northern Caucasus. *Curr Anthropol* 40: 77–86.

[201] Golovanova LV, et al. 2006. The Early Upper Paleolithic in the Northern Caucasus (new data from Mezmaiskaya cave, 1997). *Eurasian Prehistory* 4: 43–78.

[202] Golovanova LV, Doronichev VB, Cleghorn NE (2010) The emergence of bone-working and ornamental art in the Caucasian Upper Palaeolithic. *Antiquity* 84: 299–320.

[203] Pinhasi, R., Higham, T.F.G., Golovanova, L. Doronichev, V. 2011. Revised age of late Neanderthal occupation and the end of the Middle Paleolithic in the northern Caucasus. *Proceedings of the National Academy of Sciences of the United States of America* 108(21): 8611–8616.

[204] Bailey, S.E. et al. 2014.Taxonomic differences in deciduous upper second molar crown outlines of *Homo sapiens, Homo neanderthalensis* and *Homo erectus*. *Journal of Human Evolution*. Online ISSN 0047-2484, http://dx.doi.org/10.1016/j.jhevol.2014.02.008.

[205] Lee. S. and Bronk Ramsey, C. 2012. Development and application of the trapezoidal model for archaeological chronologies. *Radiocarbon* 54(1): 107–122.